Distribution Agreement

In presenting this thesis or dissertation as a partial fulfillment of the requirements for an advanced degree from Emory University, I hereby grant to Emory University and its agents the non-exclusive license to archive, make accessible, and display my thesis or dissertation in whole or in part in all forms of media, now or hereafter known, including display on the world-wide web. I understand that I may select some access restrictions as part of the online submission of this thesis or dissertation. I retain all ownership rights to the copyright of the thesis or dissertation. I also retain the right to use in future works (such as articles or books) all or part of this thesis or dissertation.

Signature

_____ _____

Brilee Michelle Smith Date

Regulation of Myelin Proteins and Protection Against Demyelination by GPR37 Signaling

By

Brilee Michelle Smith
B.S., Georgia Southern University, 2011

Graduate Division of Biological and Biomedical Sciences
Molecular and Systems Pharmacology

_____
Randy A. Hall, PhD
Advisor

_____
Yue Feng, PhD
Committee Member

_____
John Hepler, PhD
Committee Member

_____
Yoland Smith, PhD
Committee Member

_____
David Weinshenker, PhD
Committee Member

Accepted:

_____
Lisa A. Tedesco, Ph.D.
Dean of the James T. Laney School of Graduate Studies

_____
Date

Regulation of Myelin Proteins and Protection Against Demyelination by GPR37 Signaling

By

Brilee Michelle Smith
B.S., Georgia Southern University, 2011

Advisor: Randy A. Hall, PhD

An abstract of
A dissertation submitted to the Faculty of the
James T. Laney School of Graduate Studies of Emory University
in partial fulfillment of the requirements for the degree of
Doctor of Philosophy
in Molecular and Systems Pharmacology
2017

Abstract

Regulation of Myelin Proteins and Protection Against Demyelination by GPR37 Signaling

By Brilee Michelle Smith

The G protein-coupled receptor (GPCR) superfamily is the largest and most diverse transmembrane receptor family in vertebrates. For this reason, GPCR signaling is involved in numerous biological processes, and GPCRs are major pharmaceutical targets. GPR37 is an orphan GPCR that is predominantly expressed in the brain and found at particularly high levels in oligodendrocytes. GPR37 has been shown to exert effects on oligodendrocyte differentiation and myelination during development, but the molecular basis of these actions is incompletely understood and moreover nothing is known about the potential role(s) of this receptor under demyelinating conditions. To shed light on the fundamental biology of GPR37, we performed proteomic studies comparing protein expression levels in the brains of mice lacking Gpr37 and its close relative Gpr37-like 1 (Gpr37L1). These studies revealed that one of the proteins most sharply decreased in the brains of *Gpr37/Gpr37L1* double knockout mice is the myelin-associated glycoprotein MAG. Follow-up Western blot studies confirmed this finding and demonstrated that genetic deletion of *Gpr37*, but not *Gpr37L1*, results in strikingly decreased brain expression of MAG. Further *in vitro* studies demonstrated that GPR37 and MAG form a complex when expressed together in cells. As loss of MAG has previously been shown to result in increased susceptibility to brain insults, we additionally assessed *Gpr37*-knockout (*Gpr37*$^{-/-}$) vs. wild-type mice in the cuprizone model of demyelination. These studies revealed that *Gpr37*$^{-/-}$ mice exhibit dramatically increased loss of myelin in response to cuprizone, yet do not show any increased loss of oligodendrocyte precursor cells or mature oligodendrocytes. To develop tools to manipulate GPR37 signaling in order to better understand the receptor's physiological functions, we sought to identify compounds and interacting partners that modulate GPR37 signaling. A high-throughput screen of 16,000 compounds revealed that octoclothepin maleate is a nonspecific inhibitor of constitutive GPR37 signaling. The GPR37-interacting proteins regenerating islet-derived family member (REG)2 and REG4 were also found to inhibit GPR37 signaling. The findings presented in this dissertation reveal that loss of Gpr37 alters oligodendrocyte physiology and increases susceptibility to demyelination, indicating that GPR37 could be a potential drug target for the treatment of demyelinating diseases such as multiple sclerosis.

Regulation of Myelin Proteins and Protection Against Demyelination by GPR37 Signaling

By

Brilee Michelle Smith
B.S., Georgia Southern University, 2011

Advisor: Randy A. Hall, PhD

A dissertation submitted to the Faculty of the
James T. Laney School of Graduate Studies of Emory University
in partial fulfillment of the requirements for the degree of
Doctor of Philosophy
in Molecular and Systems Pharmacology
2017

ACKNOWLEDGEMENTS

Over the past five years I have received support and encouragement from a great number of individuals. I would like to acknowledge and thank my advisor Dr. Randy Hall for his guidance and support. I would also like to thank my dissertation committee of Yue Feng, John Hepler, Yoland Smith, and David Weinshenker for their advice as I moved from an idea to a completed dissertation. Pat Marsteller, Gillian Hue, Folashade Alao, and Kristen Frenzel guided me through supplementing my lab work with teaching experiences. I have learned much though our conversations and work together.

During data collection and writing, Michelle Giddens spent countless hours brainstorming, encouraging, and providing feedback on my work. She has been an invaluable colleague and friend during the course of my dissertation research. I would also like to thank other members of the Hall lab for their insights and their friendship. Additionally, I would like to thank my collaborators on the various studies described in this dissertation, including Sharon Owino, Kim Nguyen, Duc Duong, Jessica Neil, Fengqiao Li, Yuhong Du, Haian Fu, and the aforementioned Michelle Giddens, all of whom provided their expertise to help drive the research described in this document.

This work would have been impossible without the support of my classmates and the faculty of the Emory Molecular and Systems Pharmacology program, who helped me to push through the many challenges of graduate school. Finally, thanks to Steven Smith, Rebecca Kennedy, and the rest of my family for pushing me to get started, and for being there daily to support, comfort, and celebrate with me as I completed my studies.

Table of Contents

List of Figures

Abbreviations

7TM……7 Transmembrane

GPCR……..G protein-coupled receptor

GDP……...guanosine diphosphate

GTP……..guanosine-5’-triphosphate

cAMP……...3’,5’-cyclic adenosine monophosphate

PKA……protein kinase A

OPC……...oligodendrocyte precursor cell

G protein……guanine nucleotide binding protein

PDZ……PSD95 Dlg1 zo1

GRK……G protein coupled-receptor kinase

PSD95……...postsynaptic density protein

Dlg1……..drosophila disc large tumor suppressor

zo11……zonula occludens-1 protein

C terminus……..carboxy terminus

N terminus……amino terminus

GAIN domain……GPCR autoproteolysis-inducing

MAPK……mitogen activated protein kinase

PDGFRα……...platelet-derived growth factor receptor

NG2……..neural/glial antigen 2

GSTπ……..glutathione-s-transferase pi

MBP……..myelin basic protein

MOG……...myelin oligodendrocyte glycoprotein

MAG……myelin-associated glycoprotein

CNPase……...2’,3’-cyclic-nucleotide 3’-phosphodiesterase

Na_v channel……voltage-gated sodium channel

MS……..multiple sclerosis

RRMS…….relapsing-remitting multiple sclerosis

M1……muscarinic acetylcholine receptor

ERK……..extracellular signal-regulated kinase

pERK……phosphorylated ERK

KOR……...κ-opioid receptor

EAE……experimental autoimmune encephalomyelitis

4-PBA…….4-phenylbutarate

UPR……..unfolded protein response

ARJP……..autosomal recessive juvenile parkinsonism

Gpr37$^{-/-}$……GPR37-knockout

cGMP……cyclic guanosine monophosphate

PIP2……...phosphatidylinositol 4,5-bisphosphate

IP3……..inositol 1,4,5-trisphosphate

DAG……diacylglycerol

PLC……..phospholipase C

PKC……..protein kinase C

T1R……taste receptor type 1

VLGR1……...very large G protein-coupled receptor 1

ADAM…….....A disintegrin and metalloproteinase

C18…….(5HD[1,2,4]triazino[5,6Db]indolD3Dylthio)acetamide

LOPAC……..Sigma-Aldrich Library of Pharmacologically Active Compounds

PFA……paraformaldehyde

Chapter I: Introduction to G protein-coupled receptors and their role in myelination

1.1 Background and history of the study of GPCRs

Since the emergence of the first multicellular organisms around 600 million years ago, communication between individual cells in the same organism has been critical to survival (Yuan et al., 2011). Cells use chemical transmitters to send messages about their status to neighboring cells. Eukaryotic cells are bound by a selectively permeable lipid bilayer membrane; any highly polar or large molecules are unable to enter the cell without facilitation. Messages from outside the cell are transduced into useful intracellular information by receptor proteins expressed at the cell surface. The G protein-coupled receptor (GPCR) superfamily is the largest and most diverse set of transmembrane receptors in vertebrates, and it constitutes an estimated 1-2% of the human genome (Bockaert and Pin, 1999; Fredriksson and Schioth, 2005)

Receptor theory originated as a way to explain cellular responses to external stimuli and was developed in large part based on laws of mass action applied to pharmacological dose-response curves (Clark, 1933). The discovery of second messengers and G proteins allowed for more direct measurement of receptor activation, reducing the need to rely on complex physiological responses to understand signaling pathways (Gilman, 1987). Until the 1970s, a widely-held belief was that receptors did not exist as discrete molecular entities, but rather served as a theoretical framework on which to base cellular responses to external stimuli or a binding site on already-identified signaling effectors such as adenylyl cyclase (Robison et al., 1967).

In the 1970s, advances in radioligand binding allowed for the identification of glucagon receptors (Rodbell et al., 1971), opioid receptors (Pert and Snyder, 1973), muscarinic cholinergic receptors (Yamamura and Snyder, 1974), and adenylyl cyclase-coupled adrenergic receptors (Mukherjee et al., 1975). Radioligand binding also allowed for the purification and subsequent reconstitution of receptors; these studies validated the identity of isolated proteins as receptors and resulted in a better understanding of the necessary components of receptor activation (Cerione et al., 1984; Cerione et al., 1983).

Cloning of the adrenergic receptors, a muscarinic acetylcholine receptor, and a substance K receptor, along with the purification and cloning of the sensory receptor rhodopsin, revealed that GPCRs contain seven α-helical transmembrane (7TM) domains with a conserved structural architecture (Dixon et al., 1986; Kobilka et al., 1987; Kubo et al., 1986; Masu et al., 1987; Nathans and Hogness, 1983). These key reports laid the groundwork for the cloning of many more GPCRs using homology models and the rapid expansion of the study of GPCR pharmacology (Dohlman et al., 1991).

1.2 GPCR classification

GPCRs do not have any unifying overall sequence homology (Kolakowski, 1994; Probst et al., 1992). The only structural feature in all GPCRs is the 7TM region. However, considerable sequence homology is found when GPCRs are subdivided into families. Several accepted classification systems for GPCRs are actively used today (Bjarnadottir et al., 2006; Fredriksson and Schioth, 2005). The earliest and still widely used system separates GPCRs into six classes or clans, A, B, C, D, E, and F (Attwood

and Findlay, 1994; Kolakowski, 1994). This class system encompasses GPCRs expressed in both vertebrates and invertebrates.

A more recent classification system based on phylogenetic analysis of human GPCR sequences identified five families, named for notable receptors within the family. The families are glutamate (G), rhodopsin (R), adhesion (A), frizzled/taste2 (F), and secretin (S) (Fredriksson et al., 2003). Major differences between these two systems include the fact that class D and E of the A-F system contain no human homologs, and therefore do not have a GRAFS system equivalent. Furthermore, the adhesion and secretin families of the GRAFS system are combined into class B of the A-F system. Conversely, several key similarities unite the two systems, most notably that both systems have large families with similarity to rhodopsin, classified as family A in the A-F system and as R in the GRAFS system.

The glutamate or class C family includes 22 receptors in humans and is broken down into four subgroups in vertebrates (Bjarnadottir et al., 2005). Group I is further subdivided into four branches: sweet and amino acid taste 1 receptors, L-α-amino acid binding GPCRs, calcium binding receptors, and pheromone receptors. While pheromone receptors are found in high numbers in other vertebrates, they are only found as pseudogenes in the human genome. Group II contains the metabotropic glutamate receptors, and group III contains GABA receptors. Several orphan receptors are found in group IV. Receptors in this class are characterized by long N-termini containing ligand-binding sites.

The rhodopsin or class A family is the by far the largest and most well characterized in both classification systems described above, and it includes receptors for a variety of neurotransmitters, hormones, cytokines, peptides, fatty acids, purines, and light (Joost and Methner, 2002). Unlike the other families in the GRAFS system, receptors in the rhodopsin family do not have notably long N-termini. Many ligands in this family bind their receptors within the TM regions (Baldwin, 1994).

Adhesion family GPCRs form the second-largest GPCR family in humans and are characterized by long N-termini that are cleaved from the 7TM region of the receptor but remain covalently associated at the cell surface (Langenhan et al., 2013). Almost all adhesion GPCRs have a GPCR autoproteolysis-inducing (GAIN) domain, at which the N-termini are cleaved (Arac et al., 2012). All adhesion receptors are currently considered orphans, although a growing body of evidence shows that removal of the non-covalently associated N-terminus activates G protein-mediated signaling (Kishore et al., 2016; Paavola et al., 2011; Stephenson et al., 2013). Recent work suggests that after removal of the long N-terminus, the remaining N-terminal stalk of at least some adhesion GPCRs can act as a tethered cryptic agonist (Liebscher et al., 2014; Petersen et al., 2015; Stoveken et al., 2015). Many adhesion GPCRs are known to be heavily involved in development, and several mutations in adhesion GPCRs have been associated with neurological disorders in humans (Langenhan et al., 2016).

The frizzled/taste2 receptor family is subdivided into two branches. The frizzled receptors mediate signaling of Wnt glycoproteins, which direct cell fate, proliferation, and polarity during development (Logan and Nusse, 2004). The taste2 branch of this family contains bitter taste receptors (Hoon et al., 1999). They are characterized by a short N-terminus and are expressed in the tongue and palate. Taste2 receptors of this family show no clear similarities to the taste1 receptors of the glutamate family (class C) (Adler et al., 2000; Matsunami et al., 2000).

Secretin family receptors (class B) are activated by large peptides (Fredriksson et al., 2003). The N-termini of secretin-like receptors contain conserved cysteine bridges (Lagerstrom and Schioth, 2008). Much of the variation between members of the secretin family results from differences in the N-terminus, and ligand binding creates a bridge connecting the N terminus to the extracellular loops and TM segments, thereby leading to activation of the receptor (Dong et al., 2004).

The variability in GPCR structure and functions allows for remarkable specificity of function based on cell-type specific expression patterns. This diversity of function is achieved by the activation of a variety of downstream effectors and subsequent generation of second messengers that occurs upon activation of a GPCR.

1.3 GPCR signaling

1.3.1 Diversity of GPCR signaling

As described in the preceding section, GPCRs are 7 transmembrane (7TM) proteins that are expressed on the cell surface. These receptors are so-named because they couple to guanine nucleotide binding proteins, or G proteins. G proteins are heterotrimeric complexes consisting of a guanine nucleotide-binding α subunit and β γ subunit dimer. At baseline, the α subunit of the G protein is bound to guanosine diphosphate (GDP). Upon agonist binding, the 7TM receptor undergoes a conformational change such that the GDP bound to the G protein is exchanged for guanosine-5'-triphosphate (GTP). Following the exchange of GTP for GDP, the α subunit dissociates from the βγ subunit of the G protein. Both freed subunits are then able to act on downstream effectors to begin a wide variety of signaling cascades. G proteins have intrinsic GTPase activity, and GPCR signaling is terminated when GTP is cleaved to GDP and the α and βγ subunits reassociate, returning the G protein to its inactive state (Bourne et al., 1990).

This model of activation is described by the ternary complex model, which is based on the concept that at baseline a GPCR is inactive, and that GPCRs become activated upon ligand binding and form complexes consisting of the activated receptor, the ligand, and another membrane component (the G protein) (De Lean et al., 1980). In this model, the ligand stabilizes the active conformation of the receptor, and without ligand stimulation, GPCRs favor the inactive conformation. This view of GPCR activation was expanded in 1993 to account for the existence of intermediate states in between the inactive and active conformation of a GPCR (Samama et al., 1993).

The extended ternary complex model considers the fact that GPCR conformation can be affected by factors in addition to binding of the ligand, such as membrane composition and presence of interacting partners. This model is also reconcilable with the observation of constitutively active GPCRs, which have some level of baseline activity in the absence of ligand stimulation. GPCR ligands are categorized broadly into three categories: agonists, inverse agonists, and antagonists. Agonists induce G protein-mediated signaling by stabilizing an active conformation of the receptor. Conversely, inverse agonists inhibit constitutive GPCR signaling by stabilizing the receptor in its inactive conformation (Costa and Herz, 1989). Finally, neutral antagonists do not shift the equilibrium toward either active or inactive states, but prevent the activity of agonists and inverse agonists.

In the heterotrimeric G protein complex, the Gα subunit contains the GTP binding site, while the Gβγ subunit is membrane-anchored via lipid modifications. The number of different G proteins available to mediate intracellular signaling is relatively small compared to the incredibly large and diverse GPCR superfamily. Gα subunits have 21 different isoforms, and they are classified broadly into four families: $G\alpha_s$, $G\alpha_i$, $G\alpha_q$, and $G\alpha_{12}$ (Oldham and Hamm, 2008; Syrovatkina et al., 2016). A schematic detailing the signaling pathways downstream of different G proteins is outlined in figure I-1. The $G\alpha_s$ family is made up of $G\alpha_s$ and $G\alpha_{olf.}$ The s in this family stands for stimulatory, as $G\alpha_s$ subunits stimulate adenylyl cyclase, resulting in increasing levels of 3',5'-cyclic adenosine monophosphate (cAMP). This cAMP second messenger serves to activate

protein kinase A (PKA). Similarly, $G\alpha_{olf}$ stimulates adenylyl cyclase activity in olfactory sensory neurons.

Conversely, $G\alpha_i$ subunits inhibit adenylyl cyclase activity. The $G\alpha_i$ family is the most diverse of the G protein families, including $G\alpha_{i1}$, $G\alpha_{i2}$, $G\alpha_{i3}$, $G\alpha_o$, $G\alpha_t$, $G\alpha_g$, and $G\alpha_z$. $G\alpha_{i1-3}$ are widely expressed throughout the body. $G\alpha_o$ proteins are highly expressed in neurons, and are further subdivided into two splice variants: $G\alpha_{oA}$ and $G\alpha_{oB}$. Transducin, or $G\alpha_T$, is expressed in rods and cones. Upon light-induced activation of rhodopsin, transducin removes inhibition on phosphodiesterases that break down cyclic guanosine monophosphate (cGMP), leading to a decrease in intracellular cGMP. Gustducin, or $G\alpha_g$, is expressed in ~25% of taste receptor cells (Margolskee, 2002). Analogous to transducin, gustducin activation binds the inhibitory unit of taste cell cAMP phosphodiesterase, resulting in decreased intracellular cAMP. $G\alpha_z$ is expressed in neurons and platelets (Ho and Wong, 2001).

The $G\alpha_q$ family activates phospholipase C (PLC), which cleaves phosphatidylinositol 4,5-bisphosphate (PIP2) into the second messengers inositol 1,4,5-trisphosphate (IP3) and diacylglycerol (DAG). IP3 mobilizes intracellular calcium stores by activating ligand-gated calcium channels in the endoplasmic reticulum. DAG remains membrane-associated and activates protein kinase C (PKC), resulting in downstream phosphorylation of target proteins. This family includes $G\alpha_q$ and $G\alpha_{11}$, which are expressed ubiquitously, $G\alpha_{14}$ with expression in liver, kidney, and lung, and $G\alpha_{15}$ and $G\alpha_{16}$ in hematopoetic stem cells.

The $G\alpha_{12}$ subgroup contains $G\alpha_{12}$ and $G\alpha_{13}$ proteins. Both family members regulate the activity of small GTPase Rho through guanine nucleotide exchange factor (RhoGEF). This modulation of RhoGEF results in activation of Rho and subsequent reorganization of the actin cytoskeleton (Kristiansen, 2004; Neves et al., 2002).

The β and γ subunits of the heterotrimeric G protein complex form a single functional unit. This unit can be composed of one of five β isoforms and one of twelve γ isoforms. Except for $G\beta_5$, which is expressed mainly in the brain, Gβ isoforms are widely expressed. Gγ isoforms are more diverse; isoforms of show restricted expression in the olfactory epithelium (Gγ8), the brain (Gγ3, Gγ4), retinal rods and brain (Gγ1), and taste receptor cells and brain (Gγ13) (Syrovatkina et al., 2016).

Figure I-1. Representation of various G protein-mediated signaling pathways. Schematic representation of GPCR signaling via Gα and Gβγ subunits. $G\alpha_s$ stimulates adenylyl cyclase (AC) to increase cytosolic cAMP, while $G\alpha_i$ inhibits AC, resulting in decreased cAMP. $G\alpha_q$ activates phospholipase C (PLC), which leads to subsequent activation of protein kinase C (PKC) and increases in intracellular calcium. $G\alpha_{12}$-family subunits activate RhoGEF, increasing GTP-Rho. Gβγ subunits can act by activating PLC, inhibiting calcium ion channels, activating potassium ion channels, activating mitogen-activated protein kinases (MAPK), and activating the phosphatidylinositide-3 kinase (PI3K) signaling pathway.

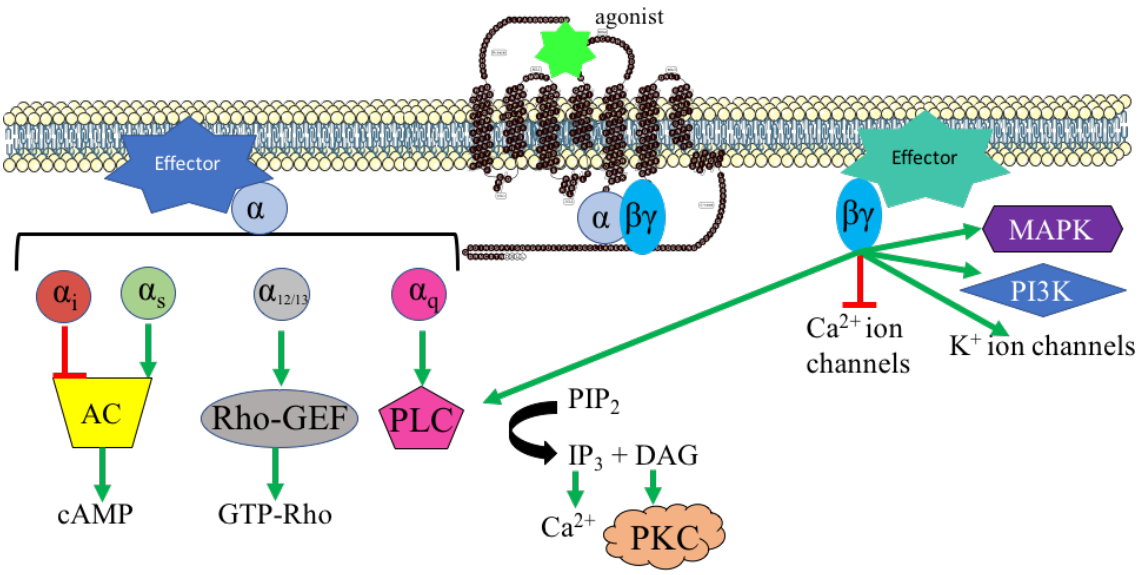
agonist
Effector
α
α
βγ
Effector
βγ
MAPK
PI3K
Ca^{2+} ion channels
K^+ ion channels
α_i
α_s
$\alpha_{12/13}$
α_q
AC
Rho-GEF
PLC
cAMP
GTP-Rho
PIP_2
IP_3 + DAG
Ca^{2+}
PKC

1.3.2 Termination and modulation of GPCR signaling

The maintenance of cellular homeostasis requires that cells have mechanisms for terminating and regulating signals once they are received. Upon activation, most GPCRs are internalized from the cell surface, then either recycled to the surface after dissociating from the agonist or targeted to the lysosome for degradation (Ferguson et al., 1996). When exposed to a stimulus for an extended amount of time, desensitization occurs, wherein cells become decreasingly responsive to the continued presence of a ligand (Breer et al., 1990; Schleicher et al., 1993). Receptor desensitization is associated with phosphorylation of the receptor and is known to be mediated by the interaction of two protein families: β-arrestins and G protein coupled-receptor kinases (GRKs) (Attramadal et al., 1992; Stadel et al., 1983). Kinases activated downstream of GPCRs, such as PKA and PKC, can also phosphorylate GPCRs, usually at sites distinct from GRK phosphoryaltion. Phosphorylated receptors are less capable of stimulating G proteins, leading to general, or heterologous, desensitization (Benovic et al., 1985; Pitcher et al., 1992).

Homologous desensitization occurs when GRKs are activated, which phosphorylate only activated receptors (Lohse et al., 1992). There are seven known GRK family members. GRK1 and 7 regulate rhodopsin and the color opsins, and thus are only expressed in retinal rods and cones, respectively (Weiss et al., 2001). GRK4 is expressed in the testes, cerebellum, and kidneys (Virlon et al., 1998). GRK2, 3, 5, and 6 are ubiquitously expressed (Willets et al., 2003). Receptor phosphorylation by GRKs leads to recruitment of arrestin proteins, which prevent coupling to G proteins and promote

internalization of receptors. The retinal-specific arrestin deactivates rhodopsin, whereas the ubiquitously expressed β-arrestin proteins 1 and 2 (also called arrestins 2 and 3) interact with a wider variety of receptors (Kuhn and Wilden, 1987). β-arrestins facilitate clathrin-mediated endocytosis of receptors, and ubiquitination of β-arrestin proteins bound to activated receptors results in the targeting of the activated receptor to the lysosome for degradation (Shenoy et al., 2001).

In addition to facilitating the termination of receptor signaling, β-arrestins can transduce G protein-independent signals by activating their own complement of downstream effectors. For example, β-arrestins act as scaffolds linking activated GPCRs to signaling pathways such as the mitogen activated protein kinase (MAPK) signaling cascade (Lefkowitz and Shenoy, 2005). Furthermore, β-arrestin1 can translocate to the nucleus and promote gene transcription by recruiting cofactors and enhancing histone acetylation (Kang et al., 2005). Interestingly, β-arrestin signaling predominantly acts on pro-survival and anti-apoptotic pathways.

β-arrestin-mediated signaling does not occur in a 1:1 fashion with G protein activation. Signaling bias toward the β-arrestin pathway was discovered when different agonists of the muscarinic acetycholine receptor M1 (M1) demonstrated differing efficacies for distinct second messenger systems (Fisher et al., 1993; Gurwitz et al., 1994). Since then, biased agonism has been demonstrated for dopamine, opioid, and chemokine receptors (Kohout et al., 2004; Lewis et al., 1998; Whistler and von Zastrow, 1998).

Direct interacting partners of GPCRs have been shown to be critical signaling regulators. These interacting partners can be other GPCRs, as is the case with GPCR dimerization. In some cases, dimerization is critical for receptor function. For example, the sweet and umami taste receptors are obligate heterodimers of the taste receptor type 1 member 3 (T1R3) with T1R2 and T1R1 respectively (Nelson et al., 2002; Nelson et al., 2001). In other cases, dimerization modulates receptor responsivity to agonists, as is the case for the δ and κ opioid receptors (Jordan and Devi, 1999). Other interacting partners bind GPCRs at PSD95-Dlg1-ZO1 (PDZ) domains located on their distal carboxy (C)-termini. PDZ proteins regulate subcellular localization and modulate signaling pathways by maintaining cellular scaffolds (Fanning and Anderson, 1999; Ritter and Hall, 2011).

The signaling of GPCRs through various subtypes of G proteins and β-arrestins presents a complex signaling landscape for each receptor. Modulation of GPCR signaling by interaction with various partners adds a further layer of regulation on cellular responses to external stimuli. Because of the broad expression of GPCRs throughout the body, such versatility in function contributes to a staggeringly diverse array of downstream physiological responses.

1.4 Clinical relevance of GPCRs

1.4.1 Advantages of pharmacologically targeting GPCRs

Mutations in GPCRs are known contributors to the development of human disease. Mechanistically, diseases associated with GPCR mutations can occur due to *i)* loss of receptor function through misfolding, *ii)* decreased receptor signaling activity, or *iii)* increased constitutive signaling. Mutations in GPCRs are implicated in disorders ranging from color blindness and retinitis to familial glucocorticoid deficiency (Spiegel, 1996; Thompson et al., 2014). Defects in G protein function can also contribute to the development of disease.

Given that GPCRs are involved in many critical signaling systems throughout the body, it is unsurprising that GPCRs are the targets of ~30% of small molecule drugs currently on the market (Santos et al., 2017). Restricted expression patterns allow for selective activation of desired signaling pathways in target organs (Tobin et al., 2008), and GPCRs are expressed in all tissue types (Regard et al., 2008). The localization of most GPCRs to the cell surface simplifies drug design, as many small molecule drugs do not easily cross cell membranes. Looking forward, GPCRs still have great potential as targets for novel therapeutics. Although the human genome contains 390 nonodorant GPCRs, only about 10% of them have been successfully pharmacologically targeted so far (Alexander et al., 2015; Congreve et al., 2011; Hopkins and Groom, 2002; Overington et al., 2006).

1.4.2 Orphan GPCRs

Of the nearly 800 identified human GPCRs, ~120 remain orphans, without an identified endogenous ligand (Alexander et al., 2015). Orphan receptors have been

implicated in many neurological diseases, and many orphan GPCRs are abundantly expressed in the brain (Ahmad et al., 2015). Understanding the signaling of orphan GPCRs will provide greater insight into the mechanisms of neurological diseases.

Although a large percentage of FDA-approved drugs target GPCRs, current GPCR drugs only act on about 10% of known receptors (Alexander et al., 2015). Consequently, orphan GPCRs represent a largely unexploited group of potential pharmacological targets. Efforts have been made to deorphanize (identify the endogenous ligands of) various orphan GPCRs, with some success. High-throughput screening for small molecule agonists has shed light on the pharmacology of some orphan receptors for which ligands have not yet been identified (Ahmad et al., 2015). Lacking an endogenous ligand, many efforts toward understanding the pharmacology of orphan GCPRs focus on the regulation of GPCR expression and signaling by small molecules (when available) and interacting partners.

1.5 GPR37 and GPR37L1

1.5.1 Identification

GPR37 and GPR37L1 are class A (rhodopsin family) orphan receptors that are highly expressed in the brain. GPR37 was originally cloned as a putative 7TM receptor by two separate groups in 1997 (Marazziti et al., 1997; Zeng et al., 1997). It was identified both as GPR37 and as the human endothelin B receptor-like protein hET(B)R-LP because of its close homology to the endothelin B (ET_B) receptor (Zeng et al., 1997). Subsequent efforts to identify homologs of the bombesin family, ET_B, or both endothelin

and bombesin receptor families also resulted in identification of GPR37 (Donohue et al., 1998; Leng et al., 1999; Valdenaire et al., 1998). GPR37L1 was identified a year after GPR37, and it was originally named ET(B)R-LP-2 (Valdenaire et al., 1998). It has 68% similarity and 48% identity to GPR37. Despite their similarity to the ET_B receptor, GPR37 and GPR37L1 are not activated by endothelins or related peptides (Donohue et al., 1998; Leng et al., 1999; Valdenaire et al., 1998; Zeng et al., 1997).

1.5.2 Expression pattern

GPR37 and GPR37L1 are both widely expressed in the brain. GPR37 is particularly highly expressed in the corpus callosum and substantia nigra (Donohue et al., 1998; Marazziti et al., 1997; Zeng et al., 1997). Lower levels of GPR37 expression are found in the spinal cord, placenta, liver, stomach, and testes (La Sala et al., 2015). Some groups have reported low levels of GPR37 expression in heart, liver, kidney, pancreas, and skeletal muscle (Leng et al., 1999; Zeng et al., 1997), although others failed to detected GPR37 in these other peripheral tissues (Marazziti et al., 1997). Within the brain, GPR37 is most highly expressed in myelinating oligodendrocytes, dopaminergic neurons, and hippocampal neurons, with lower expression in oligodendrocyte precursor cells (Cahoy et al., 2008; Imai et al., 2001; Yang et al., 2016).

GPR37L1 is expressed in the heart and gastrointestinal system in addition to the brain (Ito et al., 2009; Leng et al., 1999; Min et al., 2010; Valdenaire et al., 1998). Low levels of GPR37L1 transcripts have also been identified in rodent pituitary, stomach, lung, liver, and kidney (Leng et al., 1999). However, this expression pattern has not been

observed in human tissue. In the brain, GPR37L1 is most highly expressed in Bergmann glia in the cerebellum (Valdenaire et al., 1998). Expression of GPR37L1 is also observed in astrocytes, oligodendrocyte precursor cells and certain neuronal populations (Cahoy et al., 2008; Meyer et al., 2013).

1.5.3 Putative ligands

Several peptides have been reported to bind to GPR37 and/or GPR37L1, although there is not presently a consensus as to whether any of these peptides represents endogenous ligands for these receptors. For example, head activator (HA) peptide, which was originally identified in *Hydra* and reported to have a human homolog (Bodenmuller and Schaller, 1981), was reported to promote GPR37-mediated signaling (Rezgaoui et al., 2006). In this study, HA was found to induce internalization of GPR37 and provoke GPR37-mediated calcium signaling in transfected human embryonic kidney (HEK)293 cells. Another study reported that HA stimulated calcium-mediated nuclear factor of activated T cells (NFAT) reporter gene expression in a GPR37-dependent manner and also induced internalization of GPR37 (Gandia et al., 2013). However, another study found no effect of HA on GPR37 surface expression or signaling (Dunham et al., 2009). Furthermore, no human analogue of HA has been definitively identified.

The secreted glycoprotein prosaposin, and a peptide fragment known as prosaptide, were found to induce internalization of GPR37 and GPR37L1, increase phosphorylation of the extracellular signal-regulated kinase (ERK), and decrease accumulation of cAMP in a manner dependent on expression of GPR37 or GPR37L1

(Meyer et al., 2013). This evidence led to the conclusion that prosaposin and its peptide analog prosaptide might be agonists for GPR37 and GPR37L1. The interaction of prosaptide with GPR37 was confirmed in subsequent work utilizing fluorescence correlation spectroscopy and other approaches (Lundius et al., 2014), but subsequent functional studies have not provided evidence that prosaptide significantly stimulates the signaling activity of GPR37 or GPR37L1 (Coleman et al., 2016; Yang et al., 2016). Although the lack of a widely-accepted endogenous ligand has represented a stumbling block in studies on GPR37 and GPR37L1, other work over the past decade has focused on the study of regulators and interacting partners of GPR37 and GPR37L1 that regulate the receptors' trafficking and/or constitutive signaling activity.

Figure I-2. Reported GPR37 and GPR37L1 signaling pathways. A) HA was reported to increase intracellular calcium via GPR37 by activation of transient receptor potential family (TRP) calcium channels (Rezgaoui et al., 2006). This observed signaling was sensitive to pertussis toxin, indicating that HA signals through $G\alpha_i$. B) Our lab reported that PSAP activates GPR37 and GPR37L1, resulting in activation of $G\alpha_i$ and decreased intracellular cAMP (Meyer et al., 2013). Furthermore, increased ERK phosphorylation was observed upon PSAP treatment of cells expression GPR37 or GPR37L1. Finally, PSAP treatment resulted in internalization of GPR37 and GPR37L1. C) GPR37L1 was reported to have constitutive $G\alpha_s$-coupled activity in a cAMP response element (CRE) reporter gene assay (Coleman et al., 2016). Truncation of the N-terminus of GPR37L1 attenuates its constitutive signaling to CRE.

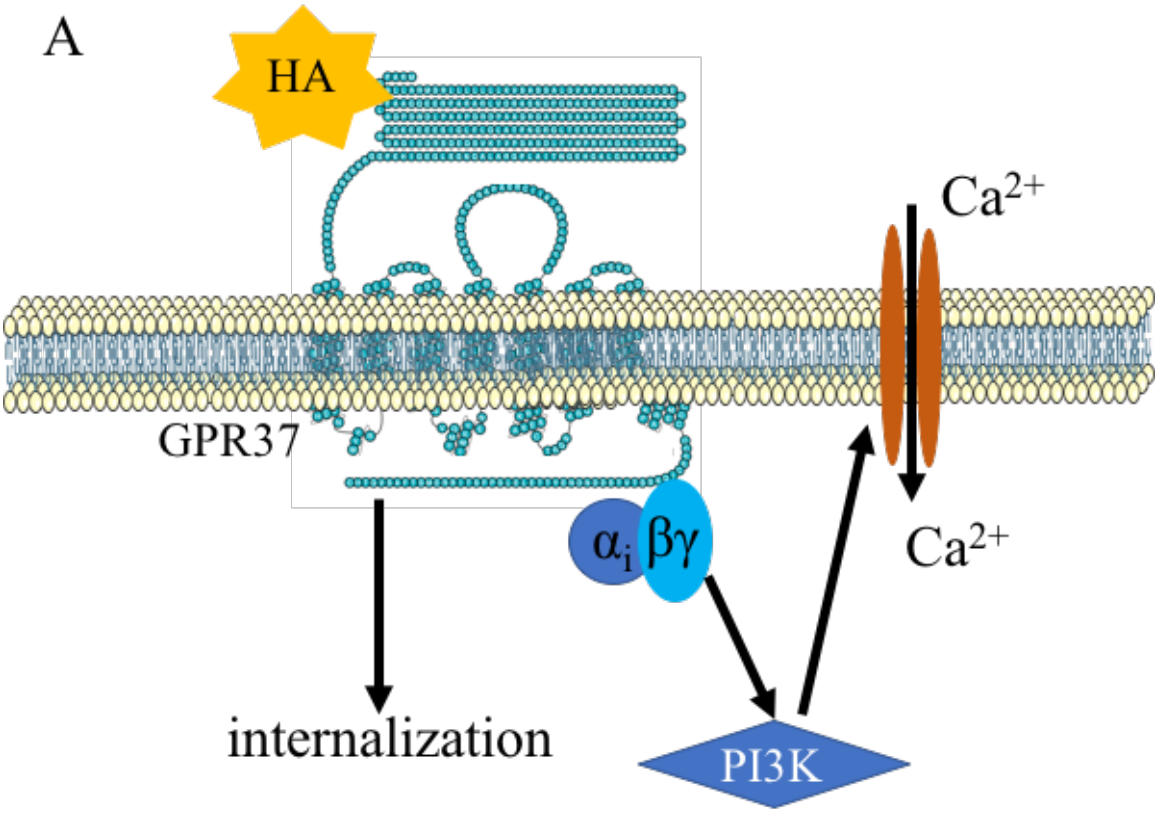
A
HA
Ca2+
GPR37
αi βγ
Ca2+
internalization
PI3K

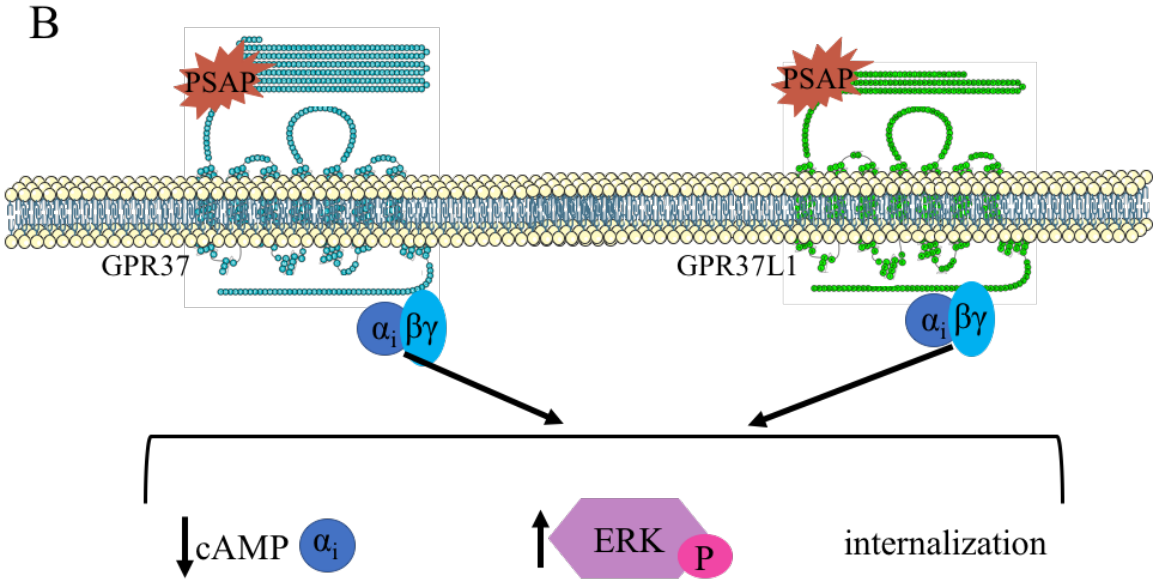
B
PSAP
PSAP
GPR37
GPR37L1
αi βγ
αi βγ
cAMP αi
ERK P
internalization

C

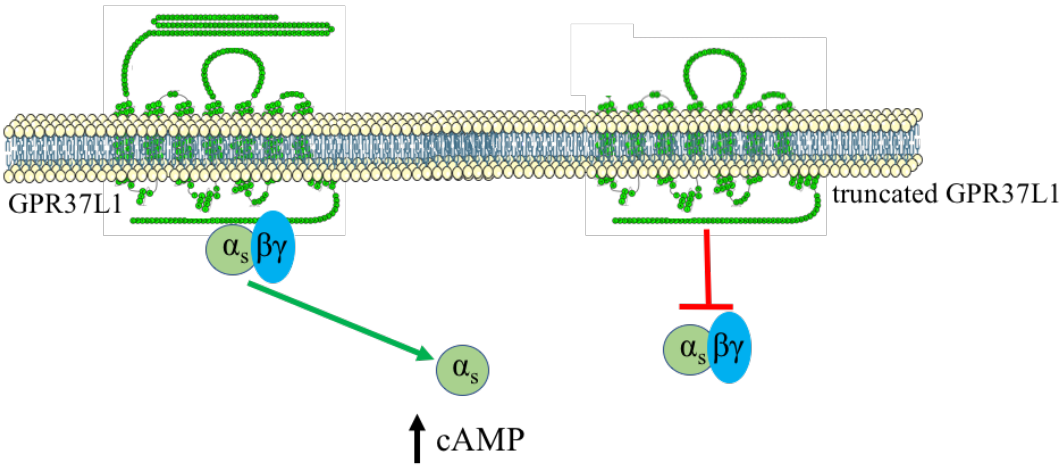

1.5.4 Regulation and interacting partners

GPR37 is infamous for its aggregation and poor trafficking to the cell surface upon expression in heterologous cells (Dunham et al., 2009; Imai et al., 2001; Zeng et al., 1997). Because GPR37 in implicated in various neurological diseases (see section 1.5.6), extensive efforts have been made to promote surface expression of the receptor *in vitro* to facilitate examination of the receptor's pharmacology. For example, GPR37 surface expression can be increased by treatment with the chemical chaperone, 4-phenylbutarate (4-PBA) (Kubota et al., 2006). Truncation of the long-unstructured N-terminus (Dunham et al., 2009) or a six-cysteine motif in the C-terminus (Gandia et al., 2013) also results in enhanced GPR37 surface expression. Finally, co-expression of GPR37 with the PDZ protein syntenin-1 substantially enhances receptor surface expression (Dunham et al., 2009).

As discussed in section 1.3.2, the regulation of GPCR signaling is critical for the maintenance of homeostasis, and heterodimerization is one method through which GPCR signaling is modulated. GPR37 has been reported to interact with the D_2 dopamine receptor and the A2 adenosine receptor (Dunham et al., 2009; Gandia et al., 2015). Moreover, GPR37L1 undergoes truncation at its amino (N)-terminus by members of the disintegrin and metalloproteinases (ADAM) family, which reduces receptor constitutive signaling activity *in vitro* (Coleman et al., 2016). In separate work, the long NT of GPR37 was also shown to be cleaved and released in heterologous cells (Mattila et al., 2016). Whether and how these truncations and interacting partners affect receptor signaling *in vivo* are questions that drive active areas of research.

1.5.5 Cytotoxicity and cytoprotection

Overexpression of GPR37 in heterologous cell lines can cause cytotoxicity, an effect that has been observed since the infancy of the GPR37 field (Imai et al., 2001; Zeng et al., 1997). In 2001, GPR37 was identified as a novel interacting partner of the E3 ubiquitin ligase parkin, and thus was named the parkin-associated endothelin receptor-like receptor (PaelR) (Imai et al., 2001). GPR37 is prone to misfolding, and under normal conditions, misfolded GPR37 is bound to Hsp70, a molecular chaperone that promotes correction of misfolded proteins (Imai et al., 2002; Imai et al., 2001). However, following cell stress, carboxyl terminus of the Hsc70-interacting protein (CHIP) is upregulated and promotes dissociation of Hsp70 from GPR37. Parkin associates with the GPR37-CHIP complex to polyubiquitinate GPR37, thus targeting the receptor for proteasomal degradation. When parkin activity is lost, misfolded GPR37 aggregates and triggers the unfolded protein response (UPR) and subsequent cell death (Yang et al., 2003). Mutations in parkin are linked to autosomal recessive juvenile parkinsonism (ARJP), and so the identification of GPR37 as a parkin substrate inspired extensive work focused on the role of GPR37 in dopaminergic neuotoxicity and parkinsonism.

Evidence for GPR37-induced cytotoxicity is mainly linked to misfolding and aggregation of the receptor upon overexpression. However, recent work suggests that GPR37, when appropriately folded and trafficked to the cell surface, can protect cells from insults (Lundius et al., 2013; Lundius et al., 2014; Meyer et al., 2013). A better understanding of the signaling pathways activated by GPR37 and GPR37L1 will be necessary to tease apart the cytoprotective and cytotoxic effects of these two receptors.

1.5.6 Disease association and animal models

There have been a number of studies on mice lacking GPR37 or GPR37L1, with this body of work laying the foundation for understanding the roles of these receptors *in vivo* (reviewed in (Smith, 2015)).These reports span a variety of biochemical and behavioral readouts, including altered dopaminergic tone (Imai et al., 2007; Marazziti et al., 2004; Marazziti et al., 2007), increased anxiety- and depression-like behavior (Mandillo et al., 2013), and altered behavioral responses to cocaine and methamphetamine in *Gpr37*$^{-/-}$ mice (Marazziti et al., 2011). Only one study to date has examined the phenotype of *Gpr37L1*$^{-/-}$ mice, which showed precocious development of the cerebellum, again resulting in a mild phenotype (Marazziti et al., 2013).

Despite the high expression of GPR37 in myelinating oligodendrocytes, little is known about the contribution of GPR37 signaling to oligodendrocyte and myelin physiology. A study of *Gpr37*$^{-/-}$ mice during development revealed that they display precocious myelination and slightly increased thickness of the myelin sheath (Yang et al., 2016). However, no published studies have yet explored the effect of GPR37 signaling on demyelination.

1.6 Oligodendroglia and myelination

1.6.1 Role of oligodendrocytes and myelin in brain function

Oligodendrocytes are the myelinating cells of the central nervous system. Neuronal signaling depends on action potentials, wherein a chemical signal is received by

the neuron and converted into an electrical signal. This electrical signal travels the length of the axon and is converted back into a chemical signal via the release of neurotransmitters from the axon terminal (Bean, 2007). The electrical signal is propagated by opening of voltage-gated sodium (Na_v) channels expressed along the length of the axon, with the resulting influx of sodium causing depolarization of the membrane. Oligodendrocytes produce myelin that is wrapped around axons in multilayered segments (Bunge, 1968). Myelin is a fatty sheath that is highly structured by organization of specific myelin proteins.

Myelin prevents ions from entering or leaving the axon by reducing membrane capacitance and increasing membrane resistance in myelinated segments, and it confers two major advantages in neuronal signaling: rapid conduction velocity and energy efficiency (Baumann and Pham-Dinh, 2001). In between myelin segments, unmyelinated regions of the axon form nodes of Ranvier containing Na_v channels. The current of the action potential is carried by the cytoplasm through myelinated segments to the next node, where it causes depolarization and a fresh influx of sodium ions (Tasaki, 1939). This "jumping" conduction from node to node is termed saltatory conduction, from the Latin *saltare,* meaning to hop or leap (Huxley and Stampfli, 1949). In unmyelinated axons, on the other hand, action potentials propagate in a way more analogous to a wave; depolarization of one axon membrane segment results in depolarization of the membrane directly next to it. Thus, an action potential is more rapidly propagated along a myelinated axon than an unmyelinated axon.

In addition to the rapid conduction of electrical signals, myelin prevents the loss of ions through membrane "leaking" (Hartline and Colman, 2007). Thus, less current is needed to successfully fire an action potential in myelinated axons because the density of Na_v channels along the axon is lower, and the overall ionic imbalance that needs restoration following depolarization is smaller. This setup decreases the metabolic demand of neuronal signaling. Given that myelin is what allows neuronal signals to travel long distances with high fidelity, understanding the signaling pathways underlying the development of myelin are critical to understanding the function of the brain.

1.6.2 Oligodendrocyte development

Oligodendrocyte differentiation is a terminal process. Thus, the timing of differentiation and axon ensheathment is tightly regulated by the upregulation of a series of positive regulators of myelination and removal of negative regulators of myelination (Bercury and Macklin, 2015). Oligodendrocyte precursor cells (OPCs) differentiate from neural stem cells following the gliogenic switch during development (Shimazaki, 2016). OPCs migrate along the nascent vasculature to populate the entire developing brain (Tsai et al., 2016). After migration, an intrinsic internal clock and pro-differentiation external signaling factors promote the differentiation of OPCs into mature oligodendrocytes. Differentiation of oligodendrocytes is a multistep process characterized by changes in expression of molecular markers and morphological changes. Mature oligodendrocytes have a complex morphology, with branched processes. Following differentiation, oligodendrocytes extend processes in search of an axon to myelinate (Hughes et al.,

2013; Kirby et al., 2006). Once an axon has been selected for myelination, the oligodendrocyte process wraps around the axon to form a multilamellar myelin sheath.

1.6.3 Myelination

Mature oligodendrocytes can contribute myelin segments on about 20-60 axons (Chong et al., 2012; Hildebrand et al., 1993; Matthews and Duncan, 1971). The process of myelination is thought to involve actin disassembly, wherein filamentous actin (f-actin) is stimulated to depolymerize into globular actin (g-actin) (Zuchero et al., 2015). G-actin is then free to re-polymerize on the leading edge of the myelin sheath, pushing the inner tongue forward around the axon. Myelin basic protein (MBP) is the most abundant protein present in myelin, and its expression is critical for myelin wrapping and compaction (Rosenbluth, 1980; Shine et al., 1992). When MBP is knocked down in cultured oligodendrocytes using siRNA, the density of actin filaments in oligodendrocytes is increased, suggesting that MBP is necessary to promote the depolymerization of actin that allows the myelin sheath to wrap around the axon (Zuchero et al., 2015).

To serve one of its main functions as an insulator that prevents the leakage of ions, myelin must be compacted (Hartline and Colman, 2007). Compaction results in tightly wrapped layers with very little cytoplasm in between. Myelin proteins can serve as structural support for the myelin sheath, and they are differentially expressed throughout the myelin depending on their function (Han et al., 2013). For example, the myelin-

associated glycoprotein MAG stabilizes the axon-myelin connection, and is therefore enriched on the innermost layer of the myelin sheath (Trapp et al., 1989).

Organization of the nodes of Ranvier depends on appropriate subcellular localization of adhesion proteins in the process of the myelinating oligodendrocyte and the axon (Arroyo and Scherer, 2000). Each nodal unit consists of the node, which lacks myelin, the paranode, which is the segment of the myelin sheath that is immediately next to the node and is uncompacted, and the juxtaparanode, which acts as the compacted separator between the myelin and the node (Rasband and Peles, 2015). All other sections of the myelin sheath are considered internodal myelin. One reported GPR37 interacting partner, CASPR2, is known to be involved in compaction of myelin in the juxtaparanode (Arroyo and Scherer, 2000; Tanabe et al., 2015).

Myelination begins in late embryonic development, but mostly occurs postnatally. During development, myelination contributes to the generation of functional circuits. However, the brain maintains myelin plasticity throughout adulthood (Boulanger and Messier, 2014). One way in which this is mediated is via neuronal activity-dependent myelination. Oligodendrocytes express glutamate receptors, and activation of these receptors has been shown to promote an increase in myelin sheath thickness (Fields, 2015). There is also evidence that direct electrical stimulation from active neurons can induce thickening of myelin at specialized axon-oligodendrocyte synapses. In addition to receiving functional inputs from neurons, myelin and oligodendrocytes also provide trophic support for myelinated axons (Nave, 2010).

Myelin turnover is common in the healthy adult brain, and a pool of OPCs is maintained into adulthood, which can migrate to sites lacking myelin and differentiate into mature myelinating oligodendrocytes (Boulanger and Messier, 2014). Disruptions in regular myelin maintenance and turnover, either through direct insults to myelin, failure of differentiation of oligodendrocytes, or exhaustion of the pool of adult OPCs, results in demyelination and neurological deficits.

Figure I-3. Schematic representing the differentiation pathway of oligodendroglia. OPCs differentiate into mature oligodendrocytes and extend processes to ensheath axons (shown in cross section in green) in a multilamellar myelin sheath. A subpopulation of OPCs capable of migrating to sites of demyelination and differentiating into myelinating oligodendrocytes is maintained into adulthood.

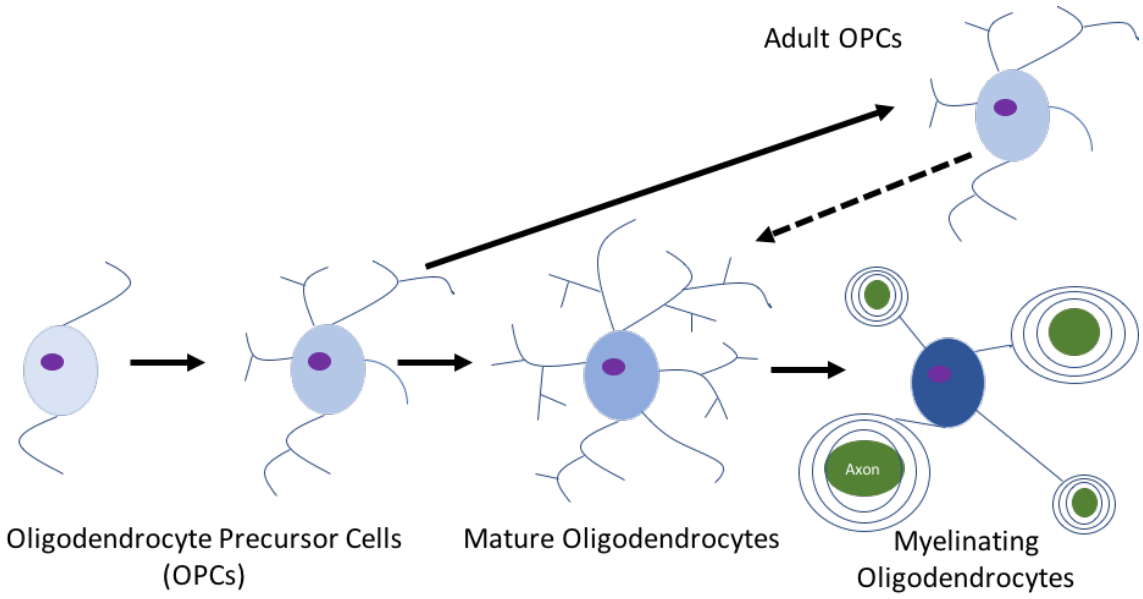
Adult OPCs
Axon
Oligodendrocyte Precursor Cells (OPCs)
Mature Oligodendrocytes
Myelinating Oligodendrocytes

1.6.4 Demyelination and remyelination

The causes of pathological demyelination are incompletely understood and variable. Demyelination has been linked to blood-brain barrier disruption and subsequent peripheral immune cell infiltration (Aube et al., 2014), apoptosis of oligodendrocytes (Traka et al., 2016), viral infection (Trandem et al., 2010), and environmental factors (Ebers, 2013). Demyelinated axons are, at least initially, spontaneously remyelinated (Barnabe-Heider et al., 2010). However, almost invariably, remyelination fails as demyelinating diseases progress.

One of the most common demyelinating disorders is multiple sclerosis (MS), an autoimmune inflammatory disorder that leads to progressive demyelination in the central nervous system (Steinman, 1996). The exact causes of MS are unknown. Patients with MS experience a wide variety of neurological deficits because of the loss of rapid signal conduction in demyelinated lesions (Compston and Coles, 2008). Some of the most common symptoms include vision impairment, numbness or tingling of the extremities, difficulty walking, fatigue, and depression. The median age of onset of MS is 29, while the median time to death is around 30 years from disease onset (Bronnum-Hansen et al., 2004). In addition to complications from demyelination, patients with MS have an increased risk of suicide, with an increase in lifetime frequency of depression around 50% (Minden and Schiffer, 1990). MS preferentially affects females, with a 3:1 female to male ratio in MS patients (Orton et al., 2006).

All currently FDA-approved therapies for MS suppress the immune system. When used early and aggressively, these drugs can reduce frequency of relapses in patients with relapsing-remitting forms of MS. Unfortunately, long-term use of immunosuppressants is associated with undesired side effects (Wingerchuk and Carter, 2014). Furthermore, patient compliance with MS drugs is frequently low, because they require daily or weekly injections (Wingerchuk and Carter, 2014). The current MS treatment landscape has two great unmet needs: myelin-protective therapies that can slow or halt progressive MS and regenerative therapies that can restore lost myelin and axons. GPCRs selectively expressed in myelinating cells present attractive targets for both the understanding of the molecular underpinnings of demyelinating disease and for developing novel treatments that do not solely rely on suppressing the immune system. Further understanding of the mechanisms underlying prolonged demyelination and failure of remyelination will open the door for the development of therapeutics that could contribute to improved quality of life for patients with demyelinating disorders and overall improved patient outcomes.

1.6.5 Animal models of demyelination and remyelination

Preclinical studies on mechanisms of and treatments for demyelination disorders rely on animal models. MS is a complex disease and can affect a variety of brain regions to different degrees in different patients. Given the heterogeneity of symptoms and clinical features of MS, no one animal model can completely recapitulate the human disease. However, several different well-established classes of demyelination models exist and feature many similarities with human disease (Procaccini et al., 2015). One of

the most well characterized models is experimental autoimmune encephalomyelitis (EAE), in which autoimmunity to myelin is induced by immunization of mice with self-antigens derived from myelin proteins such as myelin basic protein (MBP), myelin oligodendrocyte glycoprotein (MOG), and proteolipid protein (PLP) (Batoulis et al., 2011). Animals in the EAE paradigm experience ascending paralysis and cyclic disease course reminiscent of the relapsing-remitting pattern typical early in many cases of MS (Tuohy et al., 1989). However, EAE is limited in that demyelinated lesions occur stochastically, making it difficult to reliably study mechanisms of remyelination in this model. Furthermore, EAE mainly affects myelination in the spinal cord, whereas MS and other demyelination disorders show prominent demyelination in the brain.

In addition to provoking autoimmunity, demyelination can be induced in animals through treatment with toxins. One of the most common toxic demyelinating agents is bis-cyclohexanone-oxaldihydrazone, or cuprizone. Cuprizone is a copper chelator that causes oligodendrocyte cell death and demyelination (Matsushima and Morell, 2001). Maintenance of myelin places an extensive metabolic demand on mature oligodendrocytes, and copper deficiency due to the chelation activity of cuprizone is thought to be the reason behind cuprizone-induced oligodendrocyte apoptosis. However, the reason(s) that cuprizone-induced apoptosis is selective for oligodendrocytes remain unclear (Liu et al., 2010; Lucchinetti et al., 2000). While cuprizone is not suitable for studying autoimmune-mediated demyelination, a strength of this model is that demyelination can be followed by reliable remyelination after removal of cuprizone

treatment. Thus, the cuprizone model is well suited for exploring mechanisms of myelination and remyelination.

1.7 GPCRs in myelin health and disease

1.7.1 GPCRs regulating oligodendrocyte development and myelination

Several well-established GPCR signaling pathways contribute to the development of oligodendrocytes and myelination. Canonical Wnt signaling through frizzled GPCRs inhibits OPC differentiation and myelination (Fancy et al., 2009; Fancy et al., 2014) and plays a key role in interactions between migrating OPCs and the vascular endothelium (Tsai et al., 2016). GPR17 is a rhodopsin-family orphan receptor that is highly enriched in OPCs and pre-myelinating oligodendrocytes, but not myelinating oligodendrocytes (Chen et al., 2009; Fumagalli et al., 2011). The endogenous ligand of GPR17 is unknown, but *in vitro* work with small molecule agonists demonstrates that GPR17 has the capacity to couple to $G\alpha_s$, $G\alpha_{i/o}$, and $G\alpha_q$ proteins (Hennen et al., 2013; Simon et al., 2016). This work also shows that activation of GPR17 inhibits differentiation of oligodendrocytes *in vitro*, which complements reports that loss of GPR17 *in vivo* results in precocious myelination, while overexpression of GPR17 results in impaired oligodendrocyte development and hypomyelination (Chen et al., 2009).

As mentioned above, it was recently shown that loss of GPR37 results in precocious myelination in the brains of developing mice (Yang et al., 2016). While GPR17 expression decreases upon oligodendrocyte differentiation, GPR37 expression

remains high in mature myelinating oligodendrocytes. However, the role that GPR37 might play in myelination beyond development is incompletely understood at present.

1.7.2 GPCRs regulating demyelination and remyelination

While the exact mechanisms of demyelination are unknown, several oligodendrocyte-enriched GPCRs are emerging as key regulators of the stability of myelin and differentiation of oligodendrocytes. The κ-opioid receptor (KOR) was identified as a target in a high-throughput screen for compounds that affect oligodendrocyte differentiation (Mei et al., 2016). The authors reported that KOR agonists promote differentiation and KOR antagonists inhibit differentiation of OPCs. This work was further validated *in vivo* when it was reported that KOR agonists relieved the clinical features of experimental autoimmune encephalomyelitis (EAE), an animal model of demyelination, while genetic deletion of KOR exacerbates EAE (Du et al., 2016).

An *in vitro* high-throughput screen for compounds regulating OPC differentiation revealed that benztropine, an antagonist of the muscarinic acetylcholine receptor subtypes M1 and M3, promotes remyelination *in vitro* (Deshmukh et al., 2013). As discussed previously, the high expression of GPR37 in oligodendrocytes (Cahoy et al., 2008; Imai et al., 2001; Yang et al., 2016) and the recent report about the effect of GPR37 deletion on myelination during development (Yang et al., 2016) mark GPR37 as a myelin-regulating GPCR. However, the potential regulation of demyelination or remyelination by GPR37 has not yet been explored. Further understanding the signaling of various

GPCRs that are highly expressed in myelinating cells will prove enlightening in the understanding of myelin development and demyelination while also providing new therapeutic targets for the treatment of demyelination disorders.

1.8 Aim of dissertation research

The goal of these dissertation studies has been to expand our understanding of the role of GPR37 signaling in oligodendroglial biology and demyelination. My colleagues and I approached this goal by using knockout models to identify differentially regulated proteins in *Gpr37*$^{-/-}$ mice (Chapter 2), utilizing a model of demyelination to investigate a potential role for GPR37 in demyelinating disease (Chapter 3), and identifying synthetic compounds and interacting partners that modulate GPR37 signaling (Chapter 4). Findings from my dissertation research show that GPR37 regulates the expression of the myelin-associated glycoprotein MAG and protects against cuprizone-induced demyelination. Furthermore, octoclothepin maleate and regenerating islet-derived family member (REG) proteins are identified as novel inhibitors of GPR37 signaling *in vitro*.

CHAPTER II: GPR37 Regulates Expression of the Myelin-associated Glycoprotein MAG

This chapter is adapted in part from: Smith, B.M.; Giddens, M.M.; Neil, J.; Owino, S.; Nguyen, T.T.; Duong, D.; Li, F.; and Hall, R.A. Mice lacking *Gpr37* exhibit decreased expression of the myelin-associated glycoprotein MAG and increased susceptibility to demyelination. Manuscript submitted.

Author contributions: Samples for proteomic analyses were prepared by M. Giddens. Mass spectrometry was performed by D. Duong. Proteomic data were analyzed by D. Duong, M. Giddens, and B. Smith. T. Nguyen contributed to the mRNA quantification in Fig. II-1C, and M. Giddens provided replicates for the coimmunoprecipitation studies in Fig. II-3B. All other experiments described in this chapter were designed and performed by B. Smith.

2.1 Abstract

Given the high expression of GPR37 and GPR37L1 in oligodendroglia and the identified role for GPR37 in myelination, we sought to identify differentially expressed proteins in mice lacking Gpr37 and/or Gpr37L1 and potential interacting partners of the two receptors. We utilized proteomic analysis of differentially expressed proteins in Gpr37/Gpr37L1 double knockout (DKO) mice compared to wild type (WT) mice. One of the most significantly decreased proteins identified was the myelin-associated glycoprotein Mag. Conversely, other proteins expressed in oligodendroglia identified by the proteomic analysis were not differentially expressed between WT and DKO mice. Decreased Mag expression in DKO mice was confirmed at the protein level using western blot analysis, and Mag protein expression was also found to be decreased in mice lacking Gpr37 (*Gpr37*$^{-/-}$) but not Gpr37L1 (*Gpr37L1*$^{-/-}$). *Mag* mRNA expression levels in WT and *Gpr37*$^{-/-}$ mice were assessed using reverse transcription and quantitative polymerase chain reaction (qPCR). These studies found that there was not a significant difference between *Mag* mRNA expression levels in WT and *Gpr37*$^{-/-}$ mice, indicating that loss of Gpr37 regulates Mag expression at the protein level. MAG and GPR37 were co-expressed in HEK293T/17 cells to further study GPR37-mediated regulation of MAG expression *in vitro*. No significant differences in MAG protein expression were observed in the presence or absence of GPR37, and thus the *in vivo* regulation of MAG expression by GPR37 was not recapitulated in our *in* vitro system. However, coimmunoprecipitation studies indicated that GPR37 coimmunoprecipitates with MAG *in vitro*. Future work will seek to identify the structural determinants and functional significance of the MAG/GPR37 interaction.

2.2 Introduction

GPR37 and GPR37L1 are highly expressed in oligodendrocytes (Cahoy et al., 2008; Imai et al., 2001; Yang et al., 2016) and known to be protective in certain cellular contexts (Lundius et al., 2013; Lundius et al., 2014; Meyer et al., 2013). Furthermore, GPR37 has recently been shown to be a regulator of oligodendrocyte differentiation (Yang et al., 2016). Although evidence exists for several different ligands that bind to GPR37 and GPR37L1 (Gandia et al., 2013; Lundius et al., 2014; Meyer et al., 2013; Rezgaoui et al., 2006), the standards for deorphanization of this receptor have not been met (Alexander et al., 2015). Furthermore, the signaling effects observed with either prosaposin or HA are modest, reducing the dynamic range of any assay attempting to examine factors that cause changes in the GPR37 or GPR37L1 signaling system. The lack of a widely-accepted endogenous agonist or small molecule ligands presents a challenge in understanding the mechanism of GPR37 and GPR37L1 signaling.

Even in the absence of efficacious agonists, there are still many avenues available for understanding the physiological importance of a given receptor (Ahmad et al., 2015). For example, much can be learned from phenotypically characterizing knockout animals. The exploration of the phenotypes of *Gpr37*$^{-/-}$ and *Gpr37L1*$^{-/-}$ mice has provided valuable information on GPR37 and GPR37L1 signaling based on what pathways seem to be deficient when the receptors are lost (Mandillo et al., 2013; Marazziti et al., 2013; Marazziti et al., 2011; Wang et al., 2008; Yang et al., 2016). In addition to animal models, orphan GPCR activity can be assessed by measuring constitutive signaling, identifying interacting partners with which the receptors form heteromeric complexes,

and developing synthetic surrogate ligands, all of which are discussed in detail in chapter 4. In the studies described in this chapter, we utilized *Gpr37/Gpr37L1* double knockout (DKO) mice to assess which proteins and/or signaling pathway components may be up- or down-regulated in the absence of Gpr37 and/or Gpr37L1. We found that the myelin-associated glycoprotein Mag is one of the most significantly decreased proteins in DKO mice compared to wild type (WT) mice. Furthermore, we observed that Mag protein levels are sharply reduced in the brains of *Gpr37*$^{-/-}$ mice and that GPR37 coimmunoprecipitates with MAG when both are overexpressed in HEK-293T cells.

2.3 Experimental procedures

Tissue preparation for mass spectrometry: Brain tissue was collected from three-month-old wild-type (WT) and GPR37/GPR37L1 double knockout (DK) mice and then vortexed in urea lysis buffer (8M urea, 100 mM NaHPO4, pH 8.5), including HALT protease and phosphatase inhibitor cocktail (Pierce). All homogenization was performed using a Bullet Blender (Next Advance) per manufacturer protocols. Protein supernatants were transferred to 1.5 ml Eppendorf tubes, subjected to centrifugation at 14,000 rpm for 1 min and sonicated (Sonic Dismembrator, Fisher Scientific) 3 times for 5 s with 15 s intervals of rest at 30% amplitude to disrupt nucleic acids. Samples were subsequently vortexed. Protein concentrations were determined by the bicinchoninic acid (BCA) method, and samples frozen in aliquots at −80°C. Protein homogenates (100 µg) were then treated with 1 mM dithiothreitol (DTT) at 25°C for 30 minutes, followed by 5 mM iodoacetimide (IAA) at 25°C for 30 minutes in the dark. Protein was digested with 1:100 (w/w) lysyl endopeptidase (Wako) at 25°C overnight. Samples were then diluted with 50 mM NH_4HCO_3 to a final concentration of less than 2M urea and further digested overnight with 1:50 (w/w) trypsin (Promega) at 25°C. Resulting peptides were desalted with a Sep-Pak C18 column (Waters) and dried under vacuum.

LC-MS/MS analysis*:* Derived peptides were resuspended in loading buffer (0.1% formic acid, 0.03% trifluoroacetic acid, 1% acetonitrile). Peptide mixtures were separated on a self-packed C18 (1.9 um Dr. Maisch, Germany) fused silica column (25 cm x 75 uM internal diameter (ID); New Objective, Woburn, MA) by a Dionex

Ultimate 3000 RSLCNano and monitored on a Fusion mass spectrometer (ThermoFisher Scientific, San Jose, CA). Elution was performed over a 120-minute gradient at a rate of 300 nl/min with buffer B ranging from 3% to 80% (buffer A: 0.1% formic acid in water, buffer B: 0.1 % formic in acetonitrile). The mass spectrometer cycle was programmed to collect at the top speed for 3 second cycles. The MS scans (400-1500 m/z range, 200,000 AGC, 50 ms maximum ion time) were collected at a resolution of 120,000 at m/z 200 in profile mode, and the HCD MS/MS spectra (1.6 m/z isolation width, 32% collision energy, 10,000 AGC target, 35 ms maximum ion time) were detected in the ion trap. Dynamic exclusion was set to exclude previous sequenced precursor ions for 20 seconds within a 10 ppm window. Precursor ions with +1 and +8 or higher charge states were excluded from sequencing.

Data Analysis for LC-MS/MS*:* RAW data for the samples was analyzed using MaxQuant v1.5.4.1 with Thermo Foundation 2.0 for RAW file reading capability. The search engine Andromeda, integrated into MaxQuant, was used to build and search a concatenated target-decoy Uniprot mouse reference protein database (retrieved April 20, 2015; 53,289 target sequences), plus 245 contaminant proteins from the common repository of adventitious proteins (cRAP) built into MaxQuant. Methionine oxidation (+15.9949 Da), asparagine and glutamine deamidation (+0.9840 Da), and protein N-terminal acetylation (+42.0106 Da) were variable modifications (up to 5 allowed per peptide); cysteine was assigned a fixed carbamidomethyl modification (+57.0215 Da). Only fully tryptic peptides were considered with up to 2 miscleavages in the database search. A precursor mass tolerance of ±20 ppm was applied prior to mass accuracy

calibration and ±4.5 ppm after internal MaxQuant calibration. Other search settings included a maximum peptide mass of 6,000 Da, a minimum peptide length of 6 residues, 0.50 Da tolerance for low resolution MS/MS scans. Co-fragmented peptide search was enabled to deconvolute multiplex spectra. The false discovery rate (FDR) for peptide spectral matches, proteins, and site decoy fraction were all set to 1 percent. Quantification settings were as follows: requantify with a second peak finding attempt after protein identification has completed; match MS1 peaks between runs; a 0.7 min retention time match window was used after an alignment function was found with a 20 minute RT search space. Quantification of proteins was performed using summed peptide intensities given by MaxQuant. The quantification method only considered razor plus unique peptides for protein level quantification.

Western blotting: Protein samples were reduced and denatured in Laemmli buffer, loaded into 4-20% Tris-Glycine gels (Bio-Rad) for SDS-PAGE, and then were run at 120V for 20 minutes followed by 180V for 40 minutes. Proteins were transferred to nitrocellulose membranes for 10 minutes using the Trans-Blot Turbo transfer system (Bio-Rad). Blots were blocked for 30 minutes at room temperature with 2% milk (in 50mM NaCl, 10mM HEPES, pH 7.3 with 0.1% Tween-20 (Sigma)) and then incubated in milk with primary antibodies for Mag (Abcam ab89780), Gstπ (Abcam ab53943), Mog (Abcam ab32760), Mbp (Cell Signaling Technology D8X4Q), actin (Abcam ab8227), Gpr37 (MAb Technologies GPR37-3), or FLAG (Sigma-Aldrich A8592) overnight at 4°C. The following day, blots were washed with milk three times for five minutes. Blots were then incubated in milk with secondary antibody at a 1:20,000 dilution for 30

minutes at room temperature. Secondary antibody incubation was followed by three seven-minute washes. Blots were developed using SuperSignal West Pico, West Dura, or West Femto chemiluminescent substrate (Thermo) and visualized using a LiCor imaging platform. Proteins were quantified using densitometry, performed with Image Studio Lite software.

cDNA conversion and RT-PCR for Mag mRNA quantification*:* RNA was isolated from the brains of 3 WT and 3 *Gpr37*$^{-/-}$ adult mice using TriZOL (Life technologies). cDNA was prepared using random hexamers and reverse transcription. Real-time RT-PCR (qPCR) was performed using DyNaMo Sybr Green qPCR kit (Thermo-Scientific). Changes in gene expression between WT and *Gpr37*$^{-/-}$ mice were assessed by ΔCt relative to *Gapdh* expression and fold change ($2^{\wedge-\Delta\Delta Ct}$) of *Mag* expression in *Gpr37*$^{-/-}$ compared to WT mice. *Gapdh* primers (forward: ACCACAGTCCATGCCATCAC; reverse: TCCACCACCCTGTTGCTGTA; ordered from IDT) were used as an internal control and *Mag* primers (forward: AAAGGTGCCAGCAGCCCAGC; reverse: CTTGACTCGGATTTCTGCATAC; ordered from IDT) were used to amplify MAG cDNA.

Cell culture*:* HEK-293T/17 cells were acquired from ATCC (Manassas, VA) and maintained in DMEM (Life Technologies) supplemented with 10% fetal bovine serum and 1% penicillin/streptomycin in a humid, 5% CO_2, 37°C incubator. Cells were

transfected using Mirus (Madison, WI) TransIT-LT1 according to the manufacturer's protocol.

Coimmunoprecipitation: HEK-293T/17 cells were transfected in 10 cm dishes with 2µg of either empty vector plasmid, GFP-tagged GPR37, or FLAG-tagged M1 and 1µg of MAG (Origene) DNA at 50% confluency. After a 72-hour incubation, cells were harvested in 500 µl of lysis buffer (1% Triton X-100, 25 mM HEPES, 150 mM NaCl, 10 mM $MgCl_2$, 1 mM EDTA, HALT protease inhibitor mix, and 2% glycerol) and lysed by slowly rotating for 60 min at 4 °C. Cells were subjected to centrifugation to clear cellular debris, and soluble cell lysates were incubated with 60µl of protein A/G beads and 3uL of MAG antibody for 1 h at 4 °C. Following five washes with lysis buffer, beads were resuspended in 60 µl of 2X Laemmli buffer.

Generation of Knockout Mice and Maintenance of Mouse Colony: We obtained GPR37-knockout (*Gpr37*$^{-/-}$) mice from Jackson Laboratory (strain Gpr37^{tm1Dgen}, stock number 005806) and GPR37L1-knockout (*Gpr37L1*$^{-/-}$) mice from the NIH Mutant Mouse Regional Resource Centers (strain Gpr37l1^{tm1Lex}, stock number 011709-UCD). Following 10 backcrosses each with wild-type C57BLl/6 mice (Jackson Laboratory), the *Gpr37*$^{-/-}$ and *Gpr37L1*$^{-/-}$ mice were crossed to develop the DKO line of mice. Genetic deletion of GPR37 and/or GPR37L1 was confirmed by DNA sequencing, and loss of GPR37 and/or GPR37L1 protein expression was confirmed by Western blotting of brain tissue samples with specific anti-GPR37 and anti-GPR37L1 antibodies (MAb Technologies). All mice were maintained on a C57BL/6J background and housed on a 12-h light/dark cycle, with

food and water available *ad libitum.* All experiments were performed in accordance with the guidelines of the Institutional Animal Care and Use Committee of Emory University. Age-matched WT controls were used in all experiments.

2.4 Results

2.4.1 Mag protein expression, but not mRNA expression, is decreased in brains of *Gpr37*$^{-/-}$ mice

To gain molecular insight into the roles of GPR37 and GPR37L1 in the CNS, brain tissue samples from double knockout (DKO) mice lacking both Gpr37 and Gpr37L1 were subjected to LC/MS, and the expression levels of brain proteins were evaluated. One of the most significantly decreased proteins identified in this screen was the myelin-associated glycoprotein Mag, which exhibited almost 70% lower expression in DKO vs. WT brain tissue (Table II-1). Given this striking difference, in addition to the fact that GPR37 is found at its highest levels in oligodendrocytes (Cahoy et al., 2008; Imai et al., 2001; Yang et al., 2016), we focused further analyses of the proteomic data on other oligodendroglia-expressed proteins. However, none of the other oligodendroglia-expressed proteins assessed were found at significantly different levels between WT and DKO mice (Table II-1).

Western blot studies were performed next to provide a second independent measure of oligodendroglia-expressed proteins in DKO brain tissue. Moreover, brain tissue samples from GPR37-knockout (*Gpr37*$^{-/-}$) and GPR37L1-knockout (*Gpr37L1*$^{-/-}$) mice were also included in these studies to determine whether one receptor or the other might be more responsible for any observed alterations in the levels of oligodendroglia-expressed proteins. A one-way ANOVA comparing Mag expression between WT, *Gpr37*$^{-/-}$, *Gpr37L1*$^{-/-}$, and DKO mice resulted in a significant difference [$F(3,28)=4.964$,

p=0.0069]. Post-hoc analysis using Sidak's multiple comparisons test revealed that, as in the proteomic analyses, Mag expression in the Western blot studies was significantly decreased in DKO mice compared to WT (Figure II-1A-B). Expression of Mag was decreased to a similar extent in brain tissue from *Gpr37*$^{-/-}$ mice. In contrast, Mag levels in brain tissue from *Gpr37L1*$^{-/-}$ mice were not significantly different from WT. Quantitative PCR of whole RNA extracted from WT and *Gpr37*$^{-/-}$ mouse brains revealed no difference in *Mag* mRNA expression (Figure II-1C-D). These results indicate that GPR37 regulates expression of MAG at the protein level but not at the level of mRNA. Expression levels of a handful of other oligodendroglia-expressed proteins (Gstπ, Mog, and Mbp) were also assessed via Western blot and found to not be significantly different between WT, *Gpr37*$^{-/-}$, *Gpr37L1*$^{-/-}$ or DKO brain tissue (Figure II-2).

Table II-1 Differentially expressed myelin-associated proteins in brain of mice lacking Gpr37 and Gpr37L1

Protein	P value	Percent Change DKO/WT	Significant (p<0.01)
Myelin-associated glycoprotein (MAG)	0.0004	-69%	Yes
Myelin proteolipid protein (PLP)	0.072	21%	No
2,3-cyclic-nucleotide 3-phosphodiesterase (CNPase)	0.53	6%	No
Glutathione S-transferase P 1 (GSTπ)	0.037	7%	No
Myelin basic protein (MBP)	0.17	24%	No
Myelin-associated oligodendrocyte basic protein (MOBP)	0.73	8%	No
Myelin-oligodendrocyte glycoprotein (MOG)	0.99	0%	No

Figure II-1. Expression of Mag protein, but not Mag mRNA, is decreased with loss of Gpr37. Representative Western blot images (A) and quantification (B) for total MAG protein in whole brain tissue samples from WT and *Gpr37*$^{-/-}$ mice showed significantly decreased MAG protein expression in *Gpr37*$^{-/-}$ and DKO mice, but not *Gpr37L1*$^{-/-}$ mice. (n=8 per genotype, data analyzed using one-way ANOVA *$p<0.01$, **$p<0.001$). Molecular mass markers (in kDa) are shown on the left side of the blots. C) Relative *Mag* mRNA expression was not significantly different between whole brain samples from WT and *Gpr37*$^{-/-}$ mice, as assessed via qPCR (n=3).

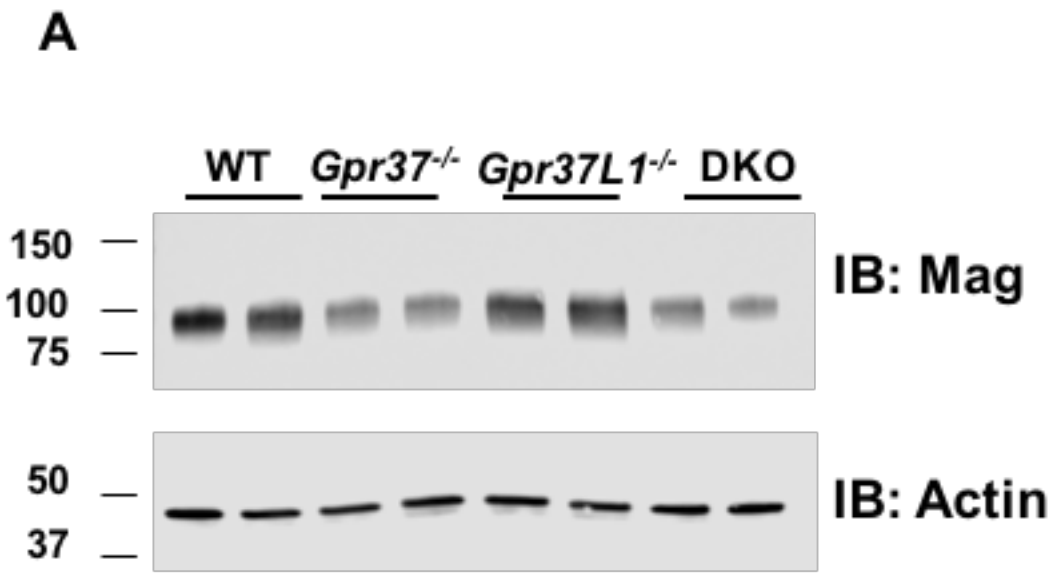
A
WT
Gpr37-/-
Gpr37L1-/-
DKO
150
100
75
IB: Mag
50
37
IB: Actin

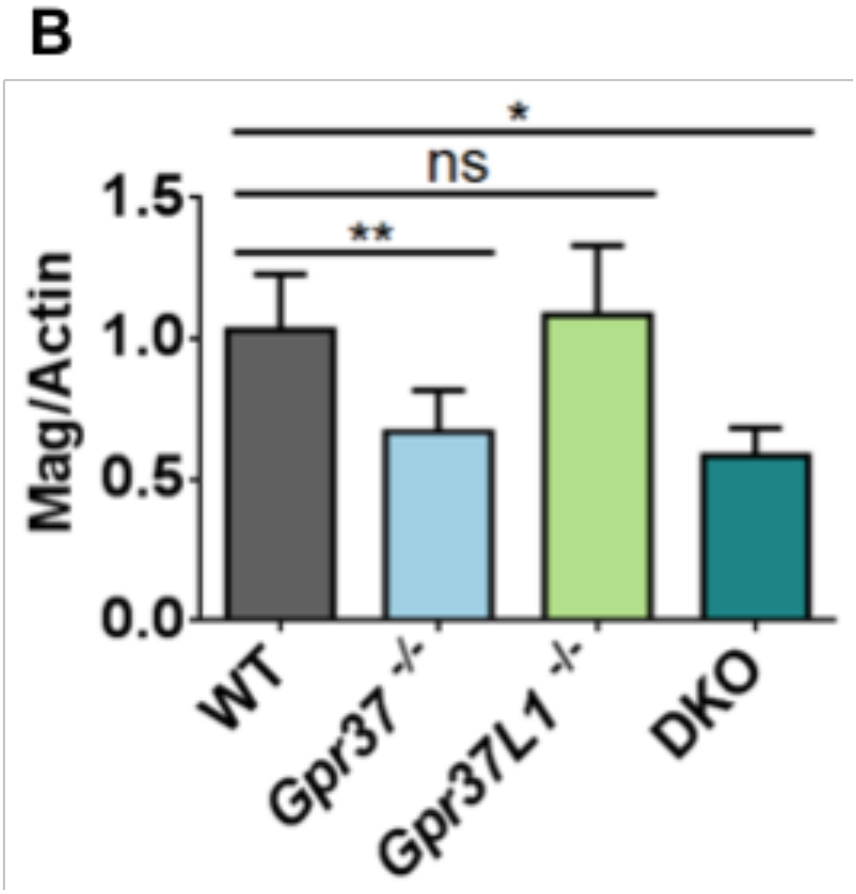
B
*
ns
**
1.5
1.0
0.5
0.0
Mag/Actin
WT
Gpr37 -/-
Gpr37L1 -/-
DKO

C

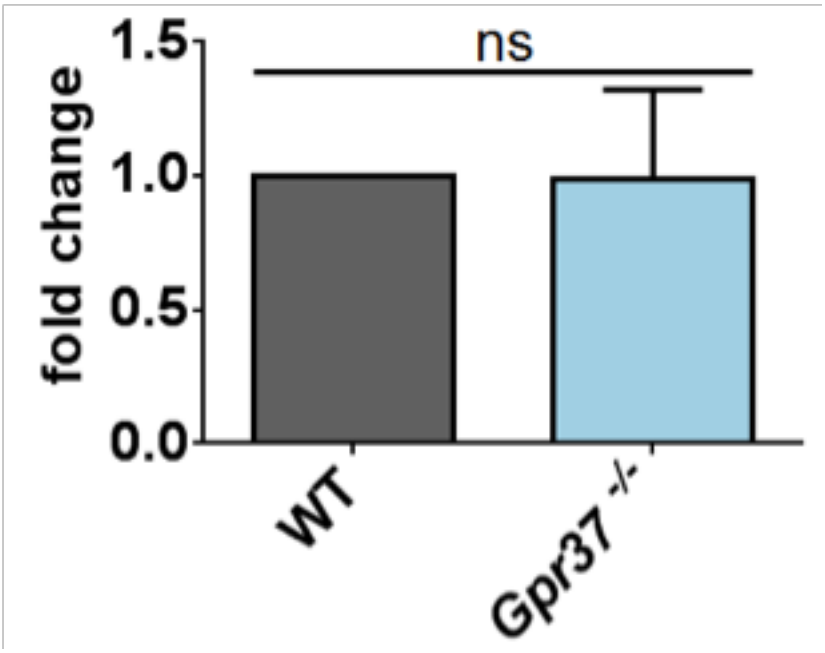

Figure II-2. Expression of other oligodendrocyte and myelin proteins is unaffected by loss of GPR37. Representative Western blot images (A) and quantification of expression of the myelin-associated proteins Mbp (B), Mog (C), and Gstπ (D) in whole brain tissue samples from WT and *Gpr37*$^{-/-}$ mice revealed no significant differences in protein expression. All protein levels were normalized to actin expression (n=8 per genotype). Molecular mass markers (in kDa) are shown on the left side of each immunoblot (IB).

A

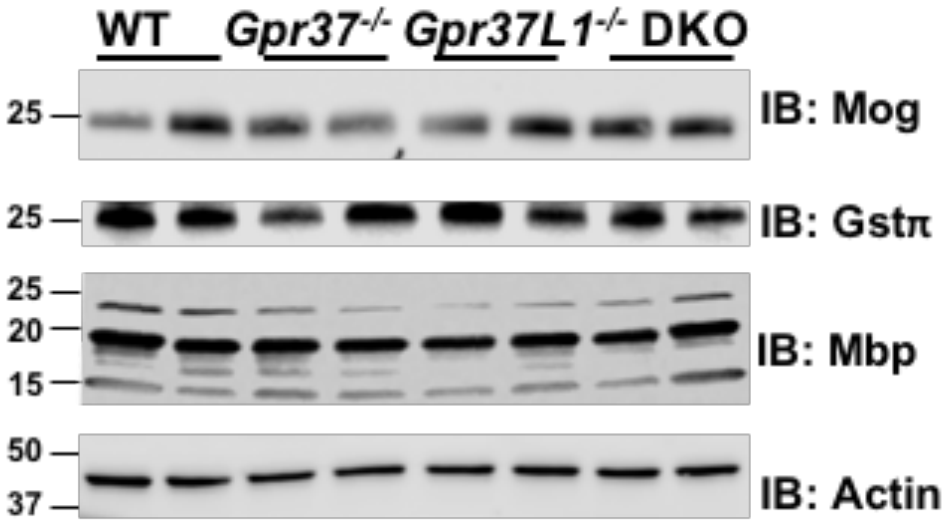
WT
Gpr37-/-
Gpr37L1-/-
DKO
25
IB: Mog
25
IB: Gstπ
25
20
15
IB: Mbp
50
37
IB: Actin

B

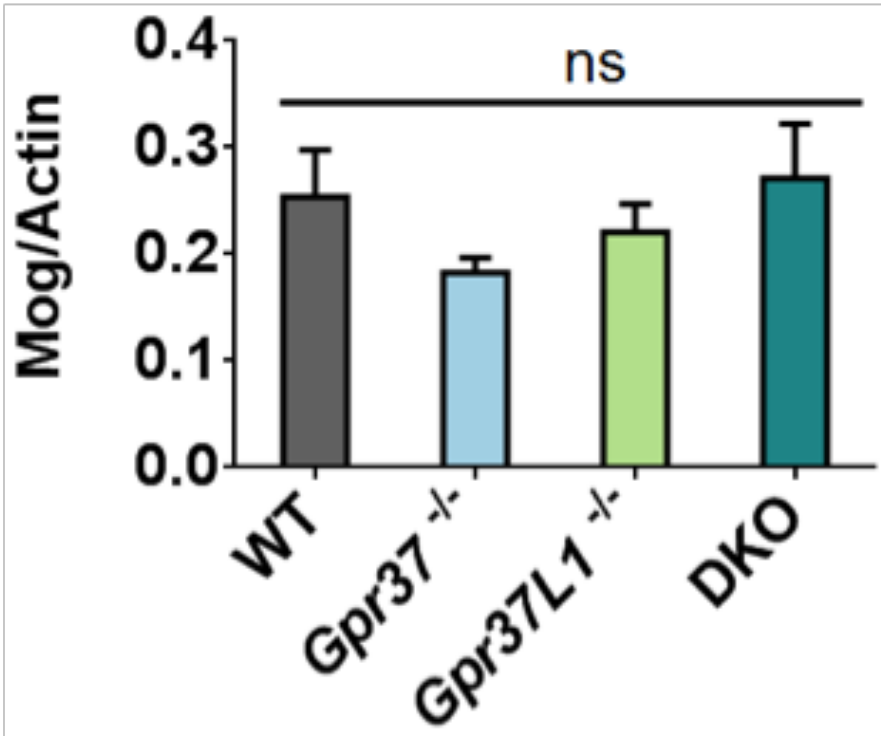
Mog/Actin
0.4
0.3
0.2
0.1
0.0
ns
WT
Gpr37 -/-
Gpr37L1 -/-
DKO

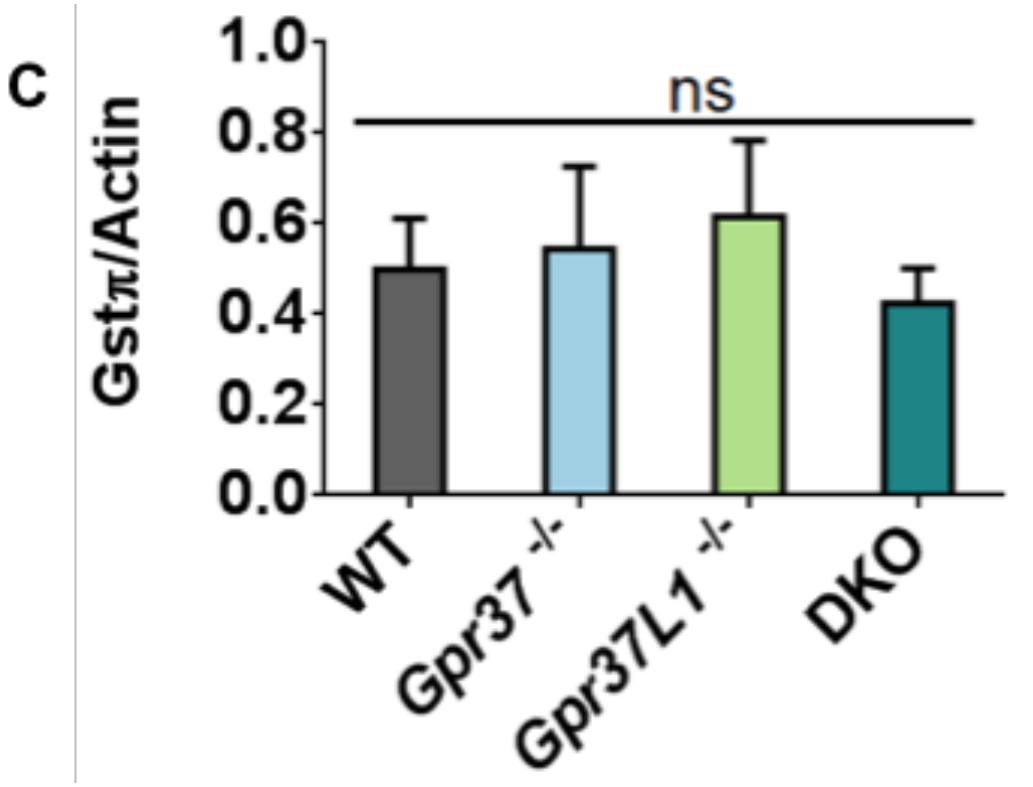
C
Gstπ/Actin
1.0
0.8
0.6
0.4
0.2
0.0
ns
WT
Gpr37 -/-
Gpr37L1 -/-
DKO

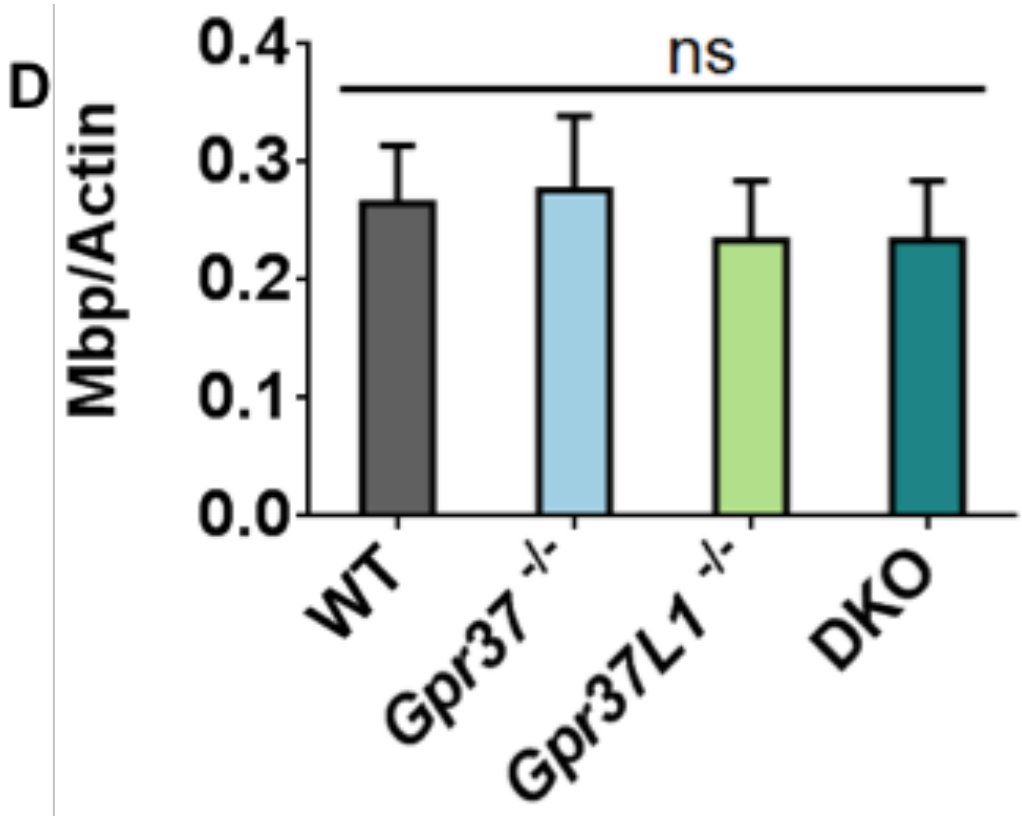
D
Mbp/Actin
0.4
0.3
0.2
0.1
0.0
ns
WT
Gpr37 -/-
Gpr37L1 -/-
DKO

2.4.2 MAG interacts with GPR37

Given the specific regulation of MAG expression by GPR37 in brain tissue, we explored whether these two proteins might be found in complex together. Co-immunoprecipitation assays revealed that GPR37 robustly interacts with MAG in lysates derived from co-transfected HEK-293 cells (Figure II-3). The M1 muscarinic acetylcholine receptor (M1), another receptor known to be highly expressed in oligodendrocytes (Deshmukh et al., 2013), was also assessed for potential co-immunoprecipitation with MAG. However, no M1 co-immunoprecipitation with MAG was observed, suggesting a specific interaction between GPR37 and MAG rather than a general capacity of MAG to interact with GPCRs. We also assessed whether the effect of GPR37 on MAG expression *in vivo* could be recapitulated via co-expression of the two proteins in heterologous cells. However, transfection of MAG into HEK-293 cells in the absence and presence of GPR37 co-transfection resulted in no significant differences in MAG expression (Figure II-4). Thus, GPR37-mediated regulation of MAG expression *in vivo* may be dependent on cellular context or other factors not easily recapitulated in cultured cells.

Figure II-3. GPR37 coimmunoprecipitates with MAG. GFP-tagged GPR37, but not Flag-tagged M1 muscarinic acetylcholine receptor, coimmunoprecipitates with MAG. Molecular mass markers are shown (in kDa) on the left side of the blots. IP=immunoprecipitation IB=immunoblot 37=GFP-tagged GPR37 M1=Flag-tagged M1 muscarinic acetylcholine receptor

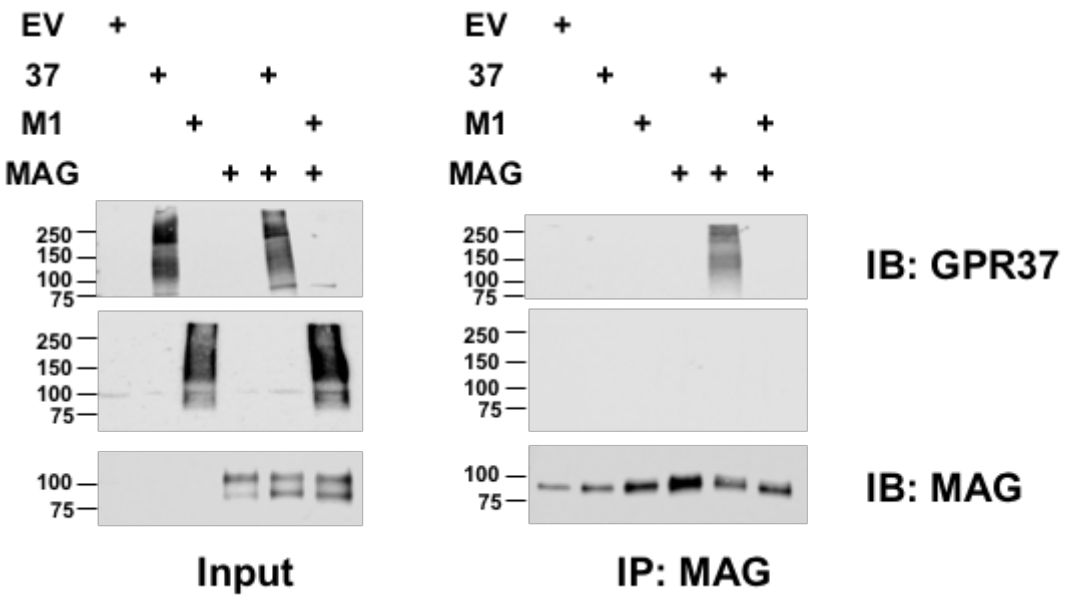
EV +
37 + +
M1 + +
MAG + + +
250
150
100
75
250
150
100
75
100
75
Input
EV +
37 + +
M1 + +
MAG + + +
250
150
100
75
250
150
100
75
100
75
IP: MAG
IB: GPR37
IB: MAG

Figure II-4. GPR37 does not increase MAG expression upon co-transfection *in vitro.* A) Representative immunoblots (IB) and B) Quantification of MAG protein revealed that co-transfection of GFP-tagged GPR37 (GFP37) with MAG did not increase MAG expression in HEK293 cells. All protein levels were normalized to actin expression (n=7 per genotype). Molecular mass markers are shown in kDa on the left side of each blot.

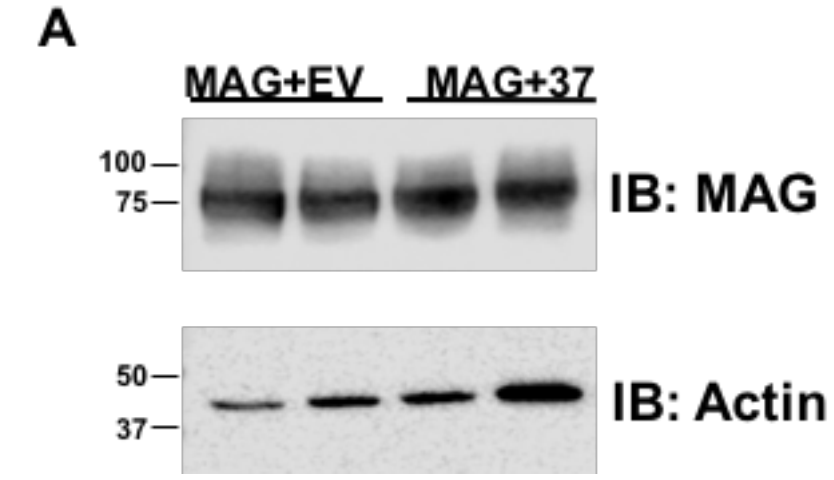
A
MAG+EV
MAG+37
100
75
IB: MAG
50
37
IB: Actin

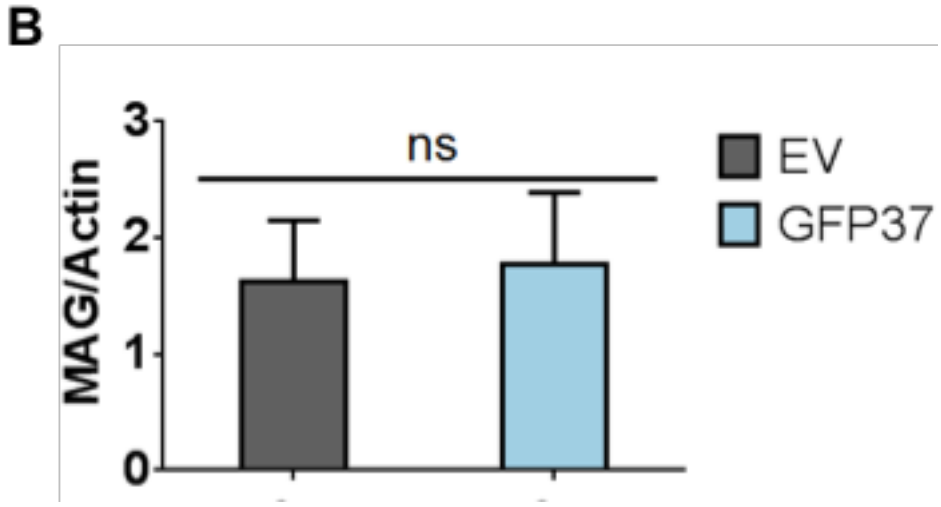
B
MAG/Actin
3
2
1
0
ns
EV
GFP37

2.5 Discussion

The studies described in this chapter reveal that loss of GPR37 expression sharply reduces MAG expression *in vivo*. MAG, or siglec4a, is a member of the siglec subgroup of the Ig superfamily and is notable for being the only siglec family member not involved in the immune system (Lehmann et al., 2004). Two RNA splice variants of MAG are produced at roughly equal levels in adult animals: L-MAG and S-MAG, for long and short MAG, respectively. MAG is a sialic-acid binding glycoprotein that is perhaps best known for its ability to inhibit neurite outgrowth (Kelm et al., 1994; Quarles, 2009; Tang et al., 1997). In this respect, MAG is seen as a negative factor in the CNS, preventing regeneration after injury. MAG is also known to promote the stability of myelinated axons (Pan et al., 2005) and maintain myelin-axon spacing (Lopez, 2014; Trapp and Quarles, 1982; Trapp et al., 1984). However, the mechanisms through which MAG mediates its effects are incompletely understood.

MAG is part of a bidirectional signaling complex wherein it acts as a ligand of axonal receptors as well as a receptor in myelinating oligodendrocytes. Because MAG can bind to sialic acid groups on both gangliosides and glycoproteins, it is likely to have many different binding partners on the axonal membrane (Kelm et al., 1994; Strenge et al., 1998; Strenge et al., 1999; Vyas and Schnaar, 2001). It is known to act via the axonal Nogo receptor to inhibit neurite outgrowth through both sialic acid-dependent and sialic acid-independent mechanisms (Domeniconi et al., 2002; Liu et al., 2002; McKerracher and Winton, 2002; Robak et al., 2009).

MAG transduces signals into myelinating oligodendrocytes, possibly through the phosphorylation of MAG and subsequent activation of Fyn kinase (Marta et al., 2004; Umemori et al., 1994). These signals promote the survival of myelinating oligodendrocytes (Gard et al., 1996), stabilize the axo-glial interface (Fruttiger et al., 1995; Pronker et al., 2016), and facilitate organization of nodes of Ranvier (Marcus et al., 2002). While both L-MAG and S-MAG bind Fyn, the L-MAG isoform seems to be responsible for Fyn activation (Jaramillo et al., 1994; Umemori et al., 1994). L-MAG and S-MAG have identical extracellular domains but differing C termini, and the C terminus of L-MAG appears to be critical for the activity of MAG in the CNS (Fujita et al., 1998; Quarles, 2007). It cannot be determined from our studies whether loss of Gpr37 preferentially decreases the expression of one MAG isoform over the other, so further work would be required to address this question.

The data presented in this chapter reveal that GPR37 can interact with MAG. However, it is unclear whether this interaction is related to the mechanism by which GPR37 regulates MAG expression, which is a topic that will require further investigation. A previous report of a GPCR regulating MAG expression showed that co-transfection of MAG with the adhesion GPCR VLGR1 resulted in enhanced MAG levels, thereby recapitulating in cultured cells the MAG-stabilizing effect of VLGR1 observed *in vivo* (Shin et al., 2013). In contrast, no significant increases in MAG expression were observed in the present study upon co-transfection of MAG with GPR37 in HEK-293 cells *in vitro*. The regulation MAG expression by GPR37 could possibly be dependent on cellular context and/or factors *in vivo* that are not present *in vitro*.

Although GPR37 is most highly expressed in oligodendrocytes (Cahoy et al., 2008; Imai et al., 2001; Yang et al., 2016), it is also expressed in some neuronal populations. It is therefore possible that GPR37 could interact with MAG either in cis or in trans, if the interaction we observed *in vitro* also occurs *in vivo*. Future studies will be needed to dissect the structural determinants of the GPR37/MAG interaction and determine its functional significance. However, the observation that MAG levels are dramatically decreased in *Gpr37*$^{-/-}$ mice suggests that these mice may exhibit phenotypic similarities to *Mag*$^{-/-}$ mice. This idea was explored in the studies described in the next chapter.

Chapter III: Loss of Gpr37 results in increased susceptibility to cuprizone-induced demyelination

This chapter is adapted in part from: Smith, B.M.; Giddens, M.M.; Neil, J.; Owino, S.; Nguyen, T.T.; Duong, D.; Li, F.; and Hall, R.A. Mice lacking *Gpr37* exhibit decreased expression of the myelin-associated glycoprotein MAG and increased susceptibility to demyelination. Manuscript submitted.

Author contributions: Cuprizone studies were designed by B. Smith, R.A. Hall and F. Li and performed by F. Li and J. Neil. Results were analyzed and interpreted by B. Smith, R.A. Hall and F. Li.

3.1 Abstract

The cuprizone model of demyelination was used to determine the susceptibility of *Gpr37*$^{-/-}$ mice to induced demyelination. We found that *Gpr37*$^{-/-}$ mice exhibit more extensive demyelination than their WT counterparts. Density of mature oligodendrocytes was not significantly altered in *Gpr37*$^{-/-}$ mice at any time point during cuprizone administration, indicating that increased demyelination in *Gpr37*$^{-/-}$ mice was not the result of increased oligodendrocyte cell death. Similarly, *Gpr37*$^{-/-}$ mice did not display decreased density of NG2+ oligodendrocyte precursor cells (OPCs), from which we concluded that increased demyelination in *Gpr37*$^{-/-}$ mice was not the result of impaired recruitment of OPCs to the corpus callosum. Analysis of g ratio using electron microscopy indicated significantly thinner myelin sheaths and decreased density of myelinated axons in the corpus callosum of *Gpr37*$^{-/-}$ mice compared to their WT counterparts. From these results, we conclude that loss of Gpr37 leads to increased susceptibility to demyelinating insults, independently of trophic effects on mature oligodendrocytes or OPCs. Future work will seek to identify the mechanism through which Gpr37 regulates resistance to demyelination.

3.2 Introduction

Myelinated axons exhibit a high degree of structural organization, to which MAG contributes significantly. Mice lacking Mag develop sufficient myelin, but display long-term axonal degeneration, changes in axonal cytoskeletal structure, and disorganization of ion channels and adhesions proteins at nodes of Ranvier (Fruttiger et al., 1995; Marcus et al., 2002; Schnaar and Lopez, 2009; Yin et al., 1998). Mag deficient mice also display mild myelination phenotypes (Li et al., 1994; Montag et al., 1994), but these phenotypes are more severe when mice are exposed to insults such as toxins, age, or demyelinating agents (Jones et al., 2013; Lassmann et al., 1997; Lopez, 2014; Weiss et al., 2000). MAG loss and accompanying periaxonal oligodendrocyte pathology has been reported in cuprizone-induced demyelination (Ludwin and Johnson, 1981) and lipopolysaccharide-induced demyelination in the spinal cord (Felts et al., 2005). Furthermore, MAG has been implicated in demyelinating diseases in humans, with many demyelinating lesions first presenting with selective loss of MAG (Itoyama et al., 1980; Johnson et al., 1986; Quarles, 2007).

The data shown in the previous chapter reveal that *Gpr37*$^{-/-}$ mice exhibit a dramatic decrease in Mag expression. This observation raises the question of whether these mice might share phenotypic similarities to mice lacking Mag. The developmental myelination phenotype of *Gpr37*$^{-/-}$ mice has been characterized in a previous report (Yang et al., 2016). *Gpr37*$^{-/-}$ mice display precocious myelination, which is mediated by increased phospho-ERK signaling in oligodendrocytes of *Gpr37*$^{-/-}$ mice. Adult mice display slight but significant increases in myelin sheath thickness. Thus, similar to mice

deficient in Mag, *Gpr37*$^{-/-}$ mice exhibit a fairly modest myelination phenotype under normal conditions. Given that *Gpr37*$^{-/-}$ mice are deficient in Mag, and that dramatic phenotypes are only observed in Mag-deficient mice following brain insults, we explored the possibility that brain insults might also reveal a more dramatic myelination phenotype in the *Gpr37*$^{-/-}$ mice. In the studies described in this chapter, we assessed the responses of WT vs. *Gpr37*$^{-/-}$ mice to demyelination induced by cuprizone.

3.3 Experimental Procedures

Cuprizone administration: A total of 90 WT mice and 91 *Gpr37*$^{-/-}$ mice between two and three months of age were used for the experiment, in which 80 WT mice and 81 *Gpr37*$^{-/-}$ mice were fed 0.2% cuprizone diet and 10 control animals from both groups received normal diet. A cohort of animals (10) from each group was sacrificed to evaluate demyelination at 0, 3, 4 and 6 weeks after cuprizone feeding. Remaining mice were removed from the cuprizone diet, returned to normal chow alone, and were sacrificed at week 9 (3 weeks into the remyelination phase) and week 12 (6 weeks into the remyelination phase) for luxol fast blue (LFB) staining and immunohistochemical (IHC) staining with NG2 or GSTπ antibodies to visualize OPCs or oligodendrocytes, respectively.

Tissue collection: To harvest tissue for histological analysis, mice were perfused with buffered 4% PFA (paraformaldehyde). All mice were anaesthetized with 100ml ketamine/xylazine mix. A lack of response to a toe pinch was used to ensure a sufficient depth of anesthetization. The thoracic cavity was opened surgically, the diaphragm was cleared from ribs, and a flap including sternum was cut and pinned back. Pericardium was cleared from the heart and a needle (with fixative and pump attached) was inserted into the left ventricle of the heart, the right atrium was cut, and 4% PFA was pumped through the circulatory system. The animals were checked for stiffness during and after perfusion. Brains were then removed from the cranial cavity.

Brain slicing: Brains were placed (dorsal side down) on a brain slicing mold. Two single edge knives were placed at an angle on groove #4 and #5. One edge of the knife was held with one finger and the knives were slowly pushed down on the brain using the other hand. The slice was then transferred to a glass vial containing 2.5% glutaraldehyde/4% PFA fixative in Sorenson's buffer and post-fixed overnight. To dissect out the corpus callosum, the slice was placed in a petri dish containing Sorenson's buffer and two cuts were made along the edge of the corpus callosum. The curvature of the cortex served as a landmark for the orientation. A third cut was made along the midline of the corpus callosum. The two halves of the corpus callosum were then stored in glutaraldehyde/PFA for three to five days before embedding in Epon or mounting in paraffin blocks.

Processing for electron microscopy: Brain samples were washed for three times for 10 minutes in 0.08M Sorenson's buffer. Tissues were placed in 2% osmium tetroxide (OsO_4) in Sorenson's buffer for 2 hours at room temperature to preserve lipid. The tissues were washed twice in 0.08M Sorenson's buffer and dehydrated through graded alchohols (as shown below) at room temperature in a fume hood on a rotator:

- 70% EtOH 2X 10 minutes
- 80% EtOH 2X 10 minutes
- 95% EtOH 2X 10 minutes
- 100% EtOH 3X 15 minutes

The tissues were then washed twice with polypropylene oxide (10 min each wash) and then embedded in epoxy resin. The resin blocks were trimmed with a razor blade to

expose the tissue region of interest. Then, sections are cut with a diamond tip blade for fixation onto grids for placement into the transmission electron microscope. A counterstain of uranyl acetate and lead citrate was performed. For each animal, five images were taken at the center of corpus callosum. G ratios were calculated by dividing the inner diameter by the outer diameter of each myelinated axon.

Paraffin mounting of tissue: Tissue was first dehydrated through graded alcohol as shown below:

- 5ml 70% EtOH 2X 30 minutes
- 5ml 95% EthOH 2X 30 minutes
- 5ml 100% EthOH 4X 1 hour
- 5ml SafeClear 2X 1 hour

Tissue was then placed in cassettes and incubated in 60℃ paraffin for 4 hours. Paraffin blocks were allowed to harden overnight and stored at room temperature for further processing. When ready for processing, paraffin blocks were sliced into 8 μm sections and mounted on glass slides.

Luxol fast blue staining: Rehydrated tissue was incubated in LFB solution overnight at 60°C. After rinsing, tissue was incubated in 0.05% lithium carbonate and differentiated in 70% EtOH until grey and white matter could be distinguished. Samples were dehydrated

in 95% EtOH, 100% EtOH, and xylene, then mounted on glass slides. Myelination of the corpus callosum was visualized using a Nikon Eclipse Ti microscope.

Immunohistochemistry*:* Rehydrated tissue was incubated in antigen retrieval buffer (10mM sodium citrate, 0.05% Tween 20), quenched in H_2O_2, and blocked at room temperature. The tissue was then incubated with primary antibodies [anti-NG2 (Abcam AB101807) or anti-GST-π (MBL International #311)] overnight at 4°C. Tissue was incubated with biotinylated secondary antibody followed by Vectastain ABC reagent. DAB (3,3'-diaminobenzidine) was used to develop the tissue, after which it was dehydrated through graded alcohols and xylene and then mounted on a glass coverslip. Microscopy was performed on a Nikon Eclipse Ti microscope. To quantify positively stained cells, boxes were drawn to capture the center of the corpus callosum. The area of the box was measured, and positively stained cells were quantified using BR Elements software. Data shown as number of positive cells per square millimeter in the center of the corpus callosum.

3.4 Results

3.4.1 Loss of Gpr37 increases susceptibility to cuprizone-induced administration

Given the striking decrease in MAG expression that we observed in mice lacking Gpr37, we assessed the susceptibility of these mice to demyelination induced by cuprizone. In these studies, *Gpr37*$^{-/-}$ vs. WT mice were fed chow with cuprizone for 6 weeks to induce demyelination, and then fed normal chow for 6 additional weeks to assess remyelination (Figure III-1). Luxol fast blue (LFB) staining of myelin revealed a marked and progressive decrease in myelination for both WT and *Gpr37*$^{-/-}$ mice from week 0 to week 4 of cuprizone treatment (Figure III-2). However, by week 6, the *Gpr37*$^{-/-}$ mice further progressed to nearly full demyelination, whereas demyelination in the WT mice was significantly less dramatic. Significant differences in myelination between WT and *Gpr37*$^{-/-}$ were exhibited at weeks 4, 6 and 9, with *Gpr37*$^{-/-}$ mice showing more extensive demyelination than WT animals in all cases. By week 12, remyelination had occurred in both WT and *Gpr37*$^{-/-}$ mice and no significant differences were observed between the two groups at the final time point examined (Figure III-2).

Myelin sheath thickness and density of myelinated axons were assessed by electron microscopy. Sheath thickness was determined by calculation of the g ratio, which is the ratio of the diameter axon to the outer diameter of the myelin sheath. A higher g ratio is indicative of a thinner myelin sheath if axon caliber is consistent. No baseline difference in g ratio was observed between WT mice and *Gpr37*$^{-/-}$ mice (figure III-3A), although WT mice at week four displayed a modestly higher average g ratio than

Gpr37$^{-/-}$ mice. Conversely, at weeks six and nine, *Gpr37*$^{-/-}$ mice had slightly higher average g ratios, with no significant difference in g ratio was observed at week 12. The only significant difference in density of myelinated axons was observed at week nine, the first part of the remyelination phase, when *Gpr37*$^{-/-}$ mice averaged slightly fewer myelinated axons per square millimeter of corpus callosum tissue sampled (figure III-3B).

Figure III-1. Schematic representation of cuprizone administration for induction of demyelination. Cuprizone was ground into animal chow for six weeks to induce demyelination. At week six, cuprizone was withdrawn and a normal diet was resumed for six additional weeks to allow for remyelination. Ten mice per genotype were sacrificed at each time point (represented by vertical lines) to assess myelination.

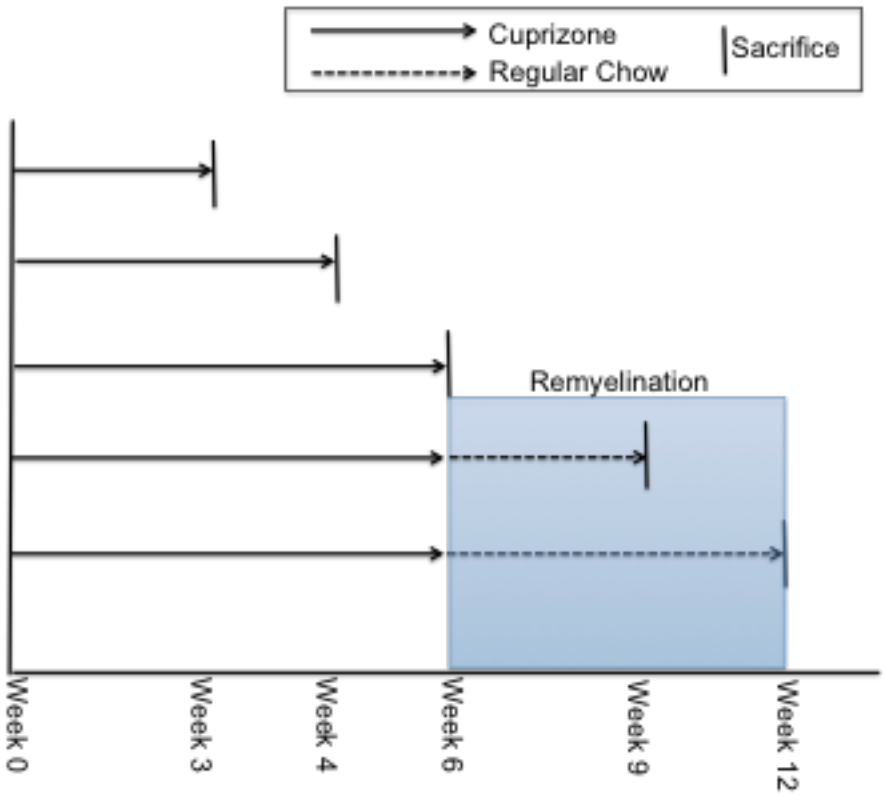
Cuprizone
Regular Chow
Sacrifice
Remyelination
Week 0
Week 3
Week 4
Week 6
Week 9
Week 12

Figure III-2. Loss of Gpr37 increases susceptibility to demyelination.

Representative images (A) and quantification (B) of luxol fast blue (LFB)-stained corpus callosum from cuprizone-treated mice. *Gpr37*$^{-/-}$ mice displayed significantly more demyelination than WT mice at weeks 4, 6, and 9 of cuprizone administration. LFB analysis of myelination was done by objective, blinded scoring on a scale of 0-4: 0=completely demyelinated, 1=25% myelinated, 2=50% myelinated, 3=75% myelinated, 4=100% myelinated. WT=wildtype, Data analyzed using two-way ANOVA [$F(5,113)=2.763$, $p=0.0215$] with Sidak post-hoc analysis **$p<0.01$, ***$p<0.001$, ****$p<0.0001$.

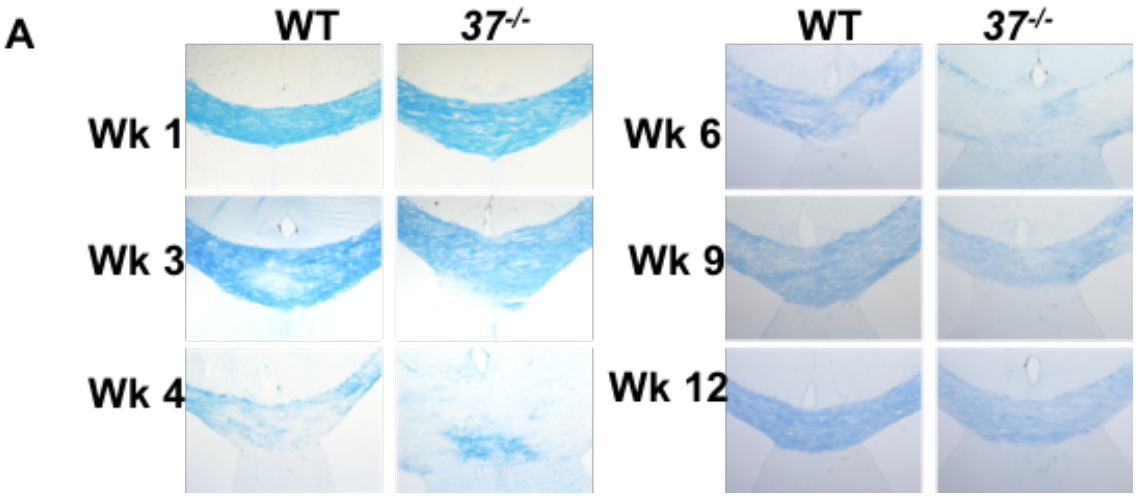
A
WT
37-/-
WT
37-/-
Wk 1
Wk 3
Wk 4
Wk 6
Wk 9
Wk 12

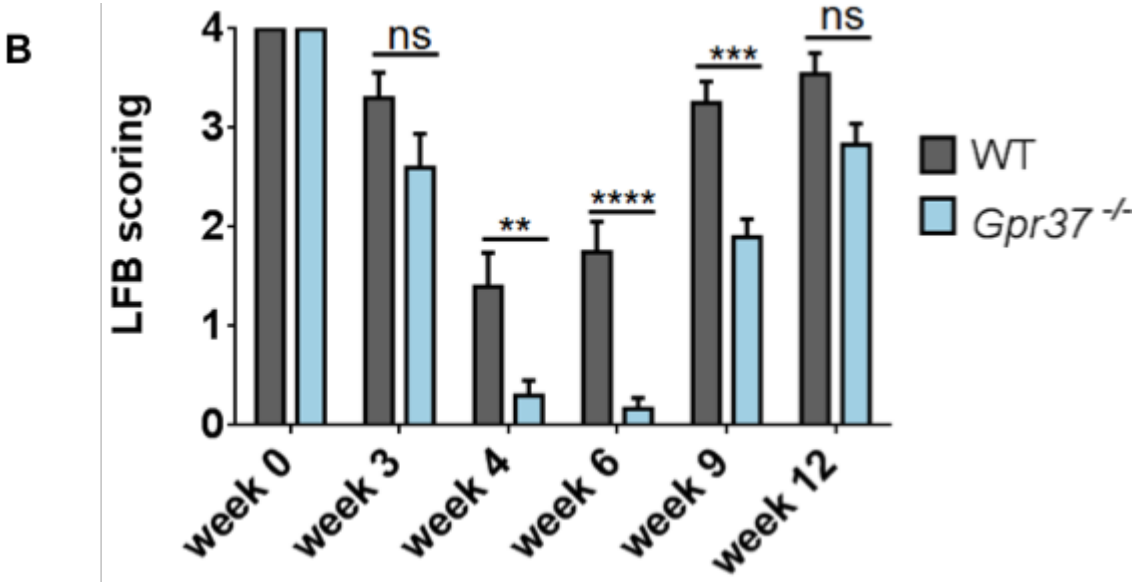
B
LFB scoring
0
1
2
3
4
ns
**
****
***
ns
week 0
week 3
week 4
week 6
week 9
week 12
WT
Gpr37 -/-

Figure III-3. Altered g-ratios in *Gpr37*$^{-/-}$ mice subjected to cuprizone-induced demyelination. A) g ratios of WT and *Gpr37*$^{-/-}$ mice during cuprizone administration revealed differences in myelin thickness at weeks 4, 6, and 9. B) The density of myelinated axons in the corpus callosum was significantly lower in *Gpr37*$^{-/-}$ mice at week 9 of the cuprizone paradigm. C) Representative electron micrographs of quantified data, WT= wildtype, Data analyzed using two-way ANOVA [$F(5,1068)=15.72$, $p<0.0001$] *$p<0.05$, ****$p<0.0001$.

A

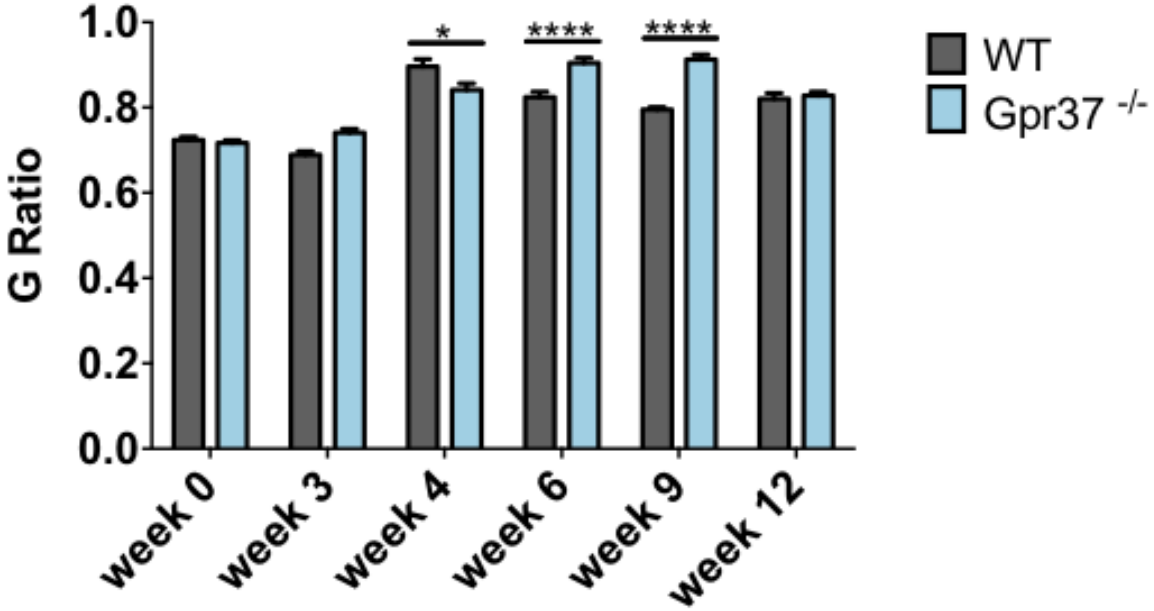
G Ratio
1.0
0.8
0.6
0.4
0.2
0.0
*
****
****
WT
Gpr37 -/-
week 0
week 3
week 4
week 6
week 9
week 12

B

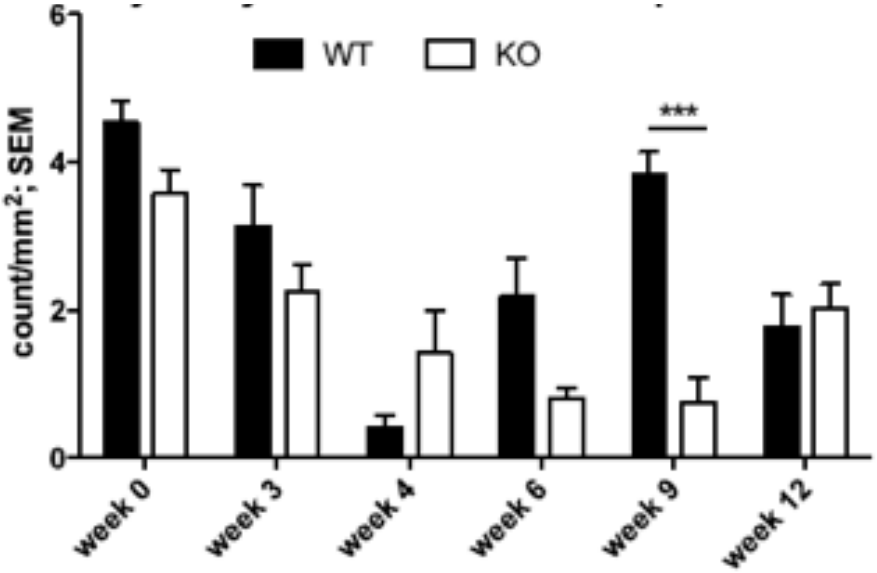
count/mm²; SEM
6
4
2
0
WT
KO
***
week 0
week 3
week 4
week 6
week 9
week 12

Figure III-4. Representative electron micrographs of myelinated axons in the corpus callosum during the cuprizone paradigm. WT=wild type

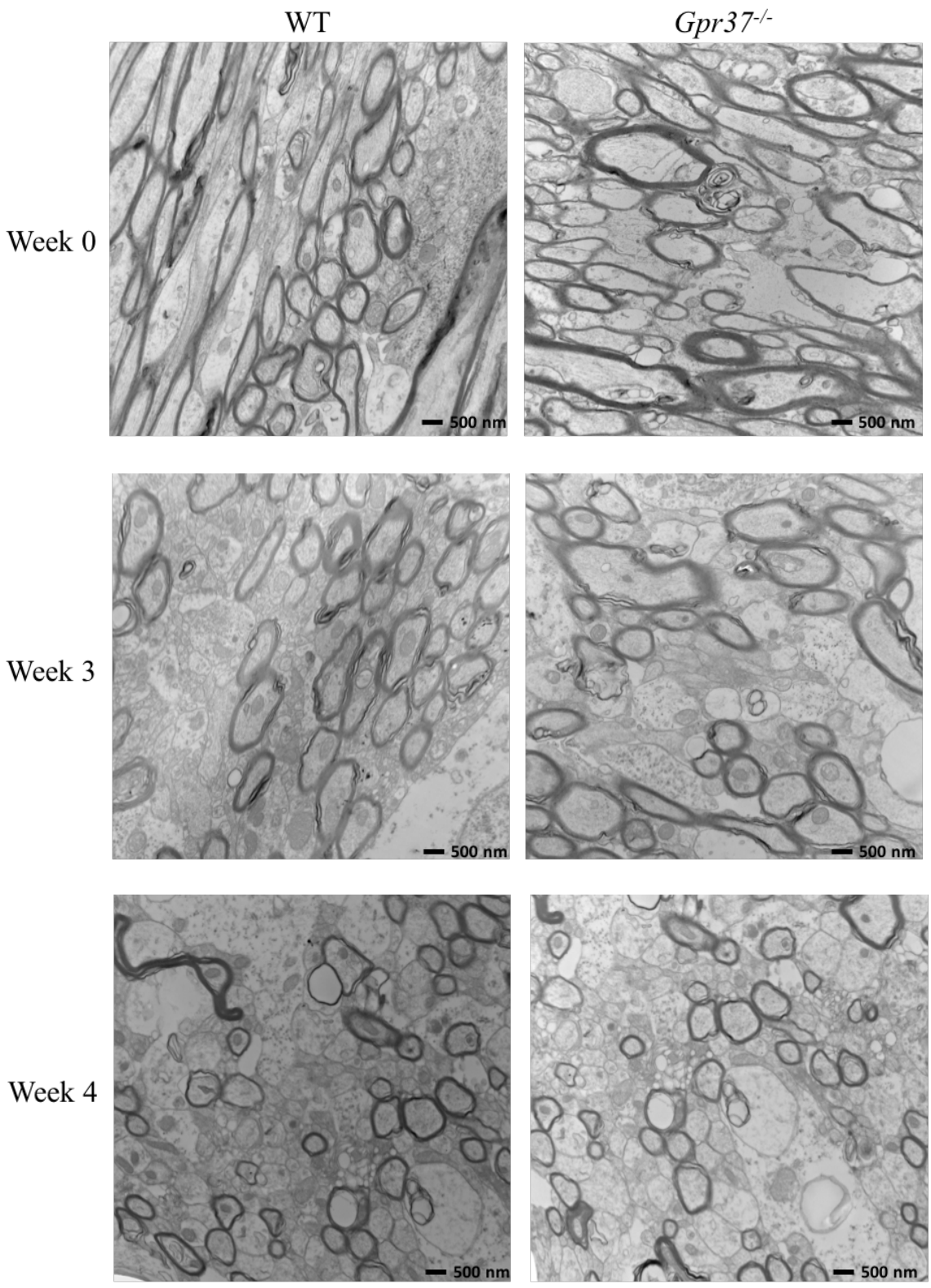
WT
Gpr37-/-
Week 0
Week 3
Week 4
500 nm
500 nm
500 nm
500 nm
500 nm
500 nm

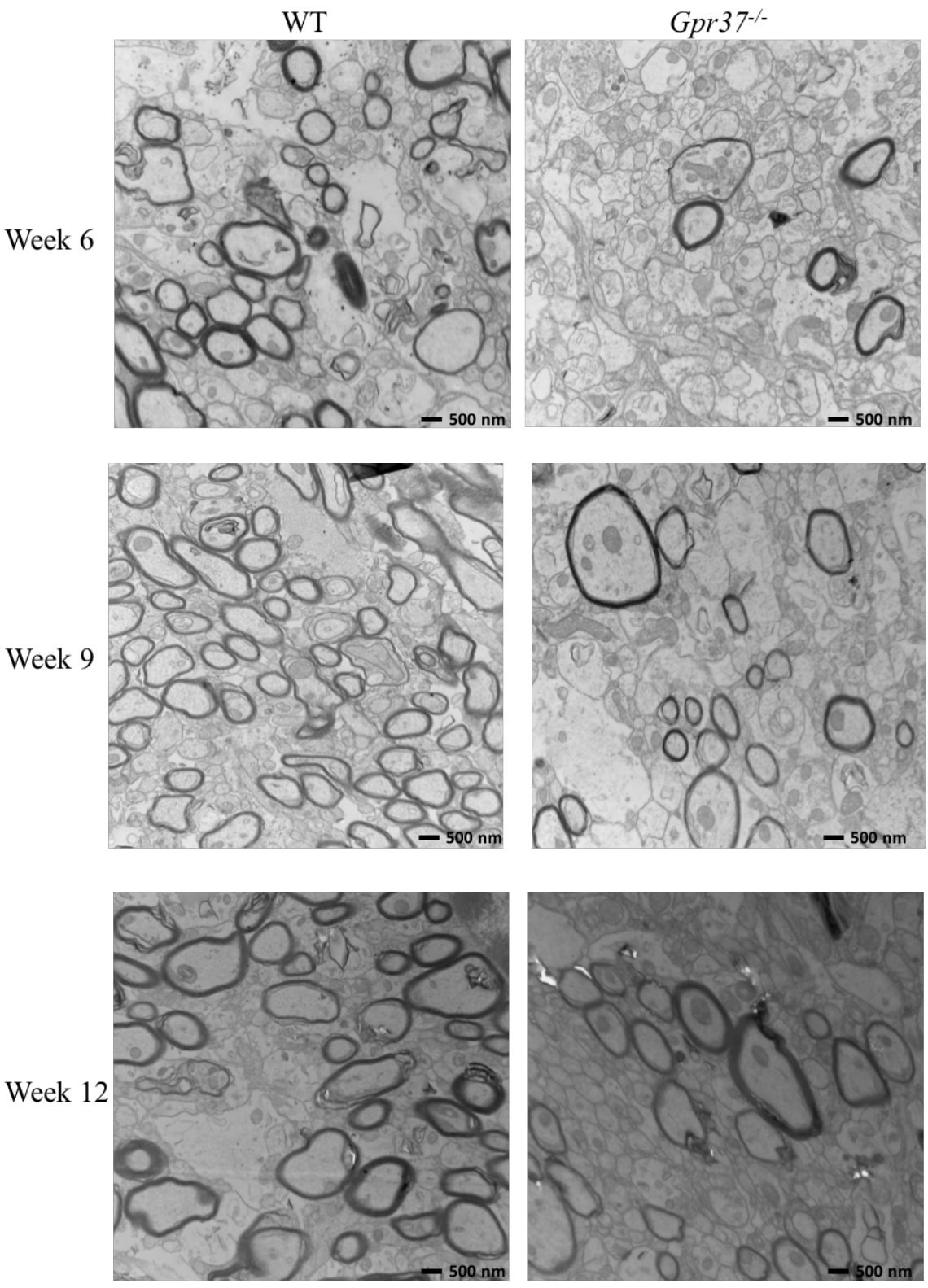
WT
Gpr37-/-
Week 6
Week 9
Week 12
500 nm
500 nm
500 nm
500 nm
500 nm
500 nm

3.4.2 Loss of Gpr37 does not affect density of OPCs or mature oligodendrocytes during cuprizone-induced demyelination

Differential responses to demyelinating insults can be accounted for by a variety of factors, including differences in oligodendrocyte survival, differences in OPC recruitment to damaged regions and/or differences in myelin stability (Franklin and Ffrench-Constant, 2008; Stangel and Trebst, 2006). To help distinguish between these possibilities, we evaluated whether *Gpr37*$^{-/-}$ mice displayed lesser recruitment of OPCs and/or greater loss of mature oligodendrocytes upon cuprizone-induced demyelination. During cuprizone administration, NG2-positive OPCs proliferate and migrate to sites of demyelination to replace lost oligodendrocytes (Matsushima and Morell, 2001; Stangel and Hartung, 2002). Indeed, analyses of NG2 immunostaining revealed substantial recruitment of OPCs in both WT and *Gpr37*$^{-/-}$ mice during cuprizone administration (Figure III-5A). However, no significant differences in NG2 staining between WT and *Gpr37*$^{-/-}$ mice was observed at any time point, indicating that loss of GPR37 did not affect overall OPC number (Figure III-5B).

In parallel analyses, mature oligodendrocytes were assessed by immunohistochemical staining for Gstπ (Figure III-6A). Staining for mature oligodendrocytes decreased from week 0 to week 6, as expected, as oligodendrocytes were lost to cuprizone-induced apoptosis. However, no significant differences in Gstπ staining were observed between WT and *Gpr37*$^{-/-}$ mice at any time point (Figure III-6B). The lack of difference in either OPC or oligodendrocyte cell number between WT and *Gpr37*$^{-/-}$ mice during cuprizone-induced demyelination suggests that GPR37 specifically

alters the process of myelination and/or the stability of myelin, rather than modulating OPC recruitment or exerting cytoprotective effects on mature oligodendrocytes.

Figure III-5. Loss of Gpr37 does not affect numbers of OPCs. Representative images (A) and quantification (B) of NG2+ oligodendrocyte precursor cells (OPCs) in the corpus callosum of mice treated with cuprizone. No significant differences between WT and *Gpr37*$^{-/-}$ mice were observed at any time point.

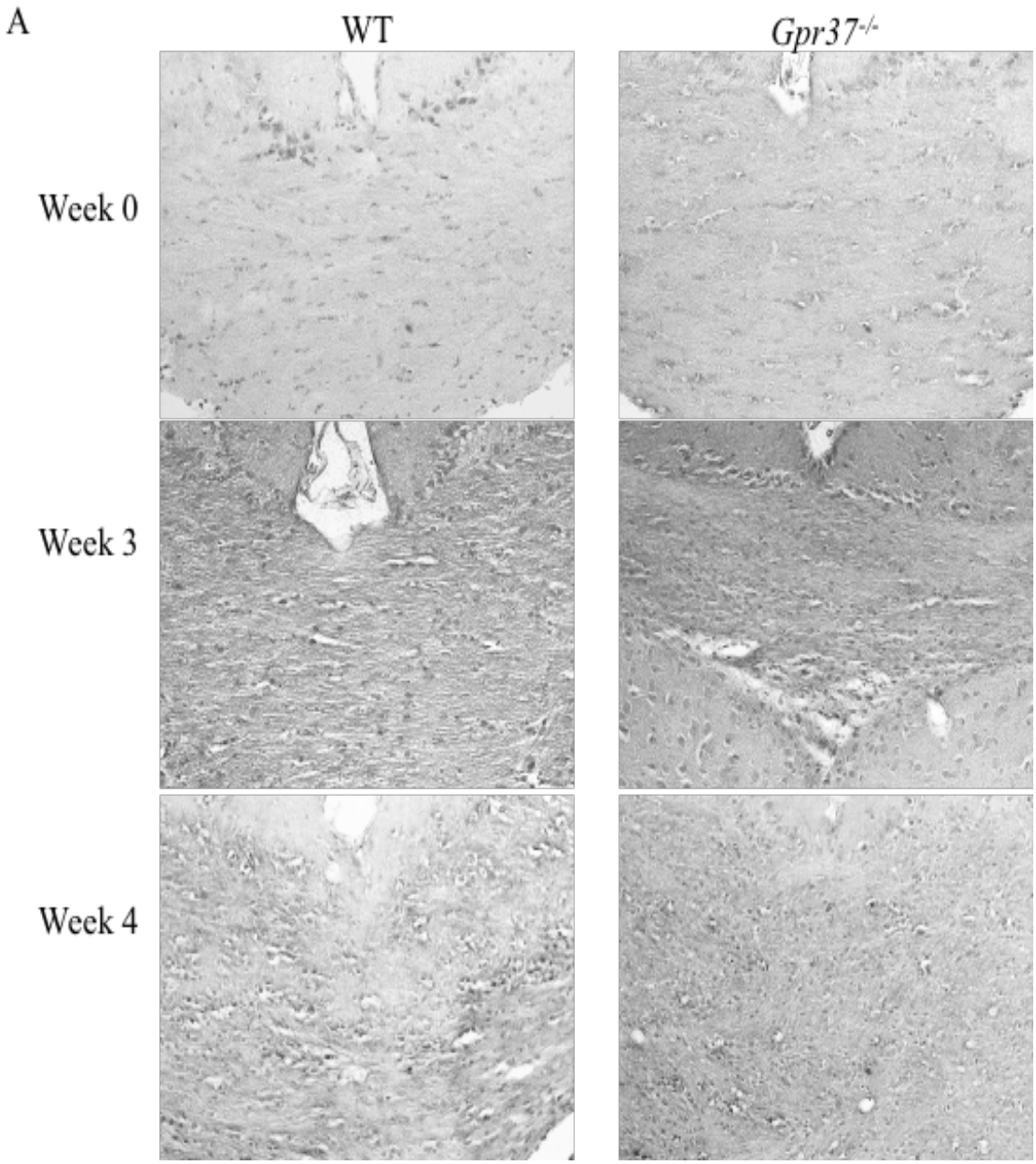
A
WT
Gpr37-/-
Week 0
Week 3
Week 4

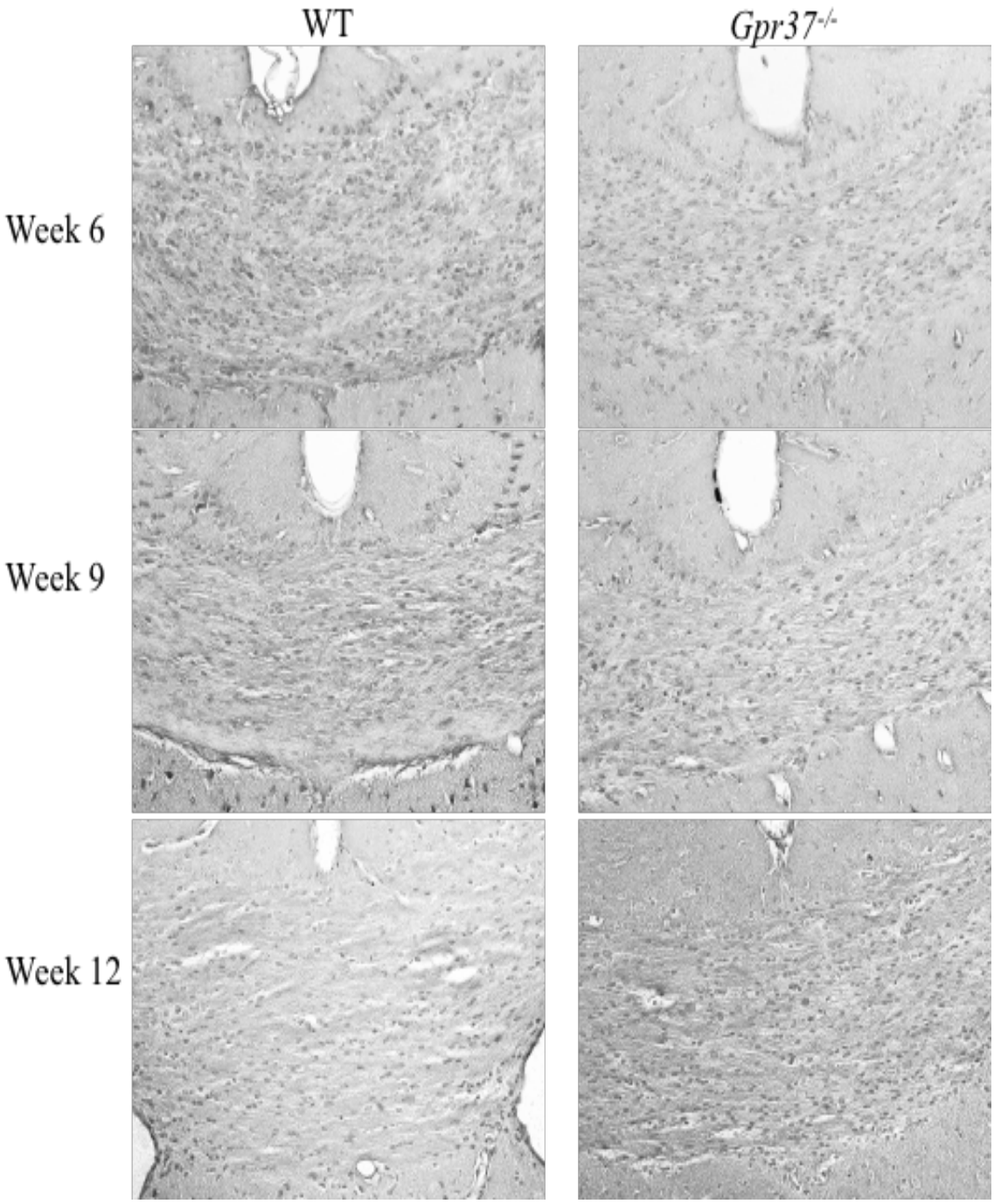
WT
Gpr37-/-
Week 6
Week 9
Week 12

B

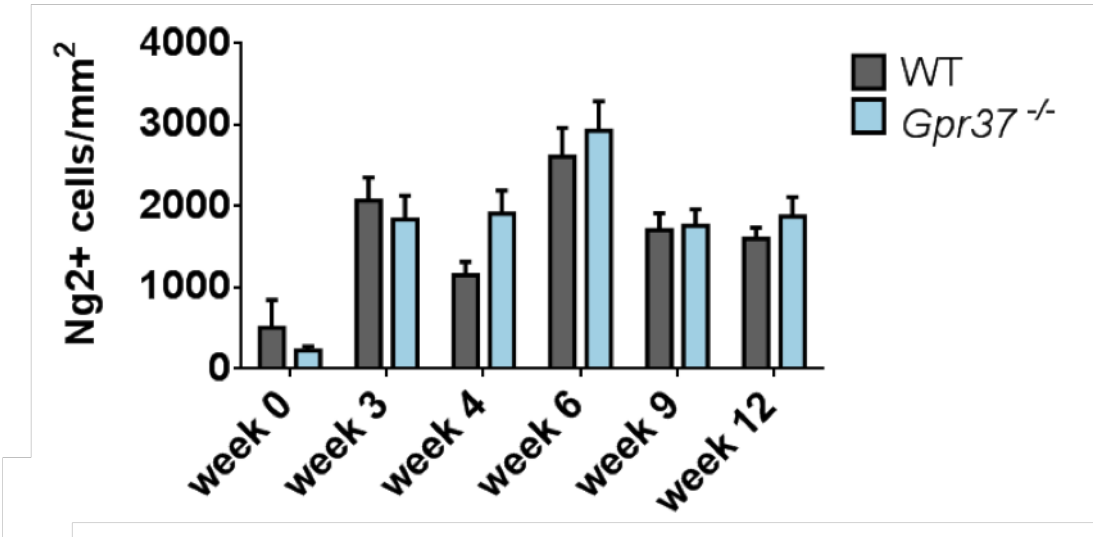
Ng2+ cells/mm2
4000
3000
2000
1000
0
WT
Gpr37 -/-
week 0
week 3
week 4
week 6
week 9
week 12

Figure III-6. Loss of Gpr37 does not affect numbers of mature oligodendrocytes. Representative images (A) and quantification (B) of GSTπ+ mature oligodendrocytes in the corpus callosum of mice treated with cuprizone. No significant differences between WT and *Gpr37*$^{-/-}$ mice were observed at any time point.

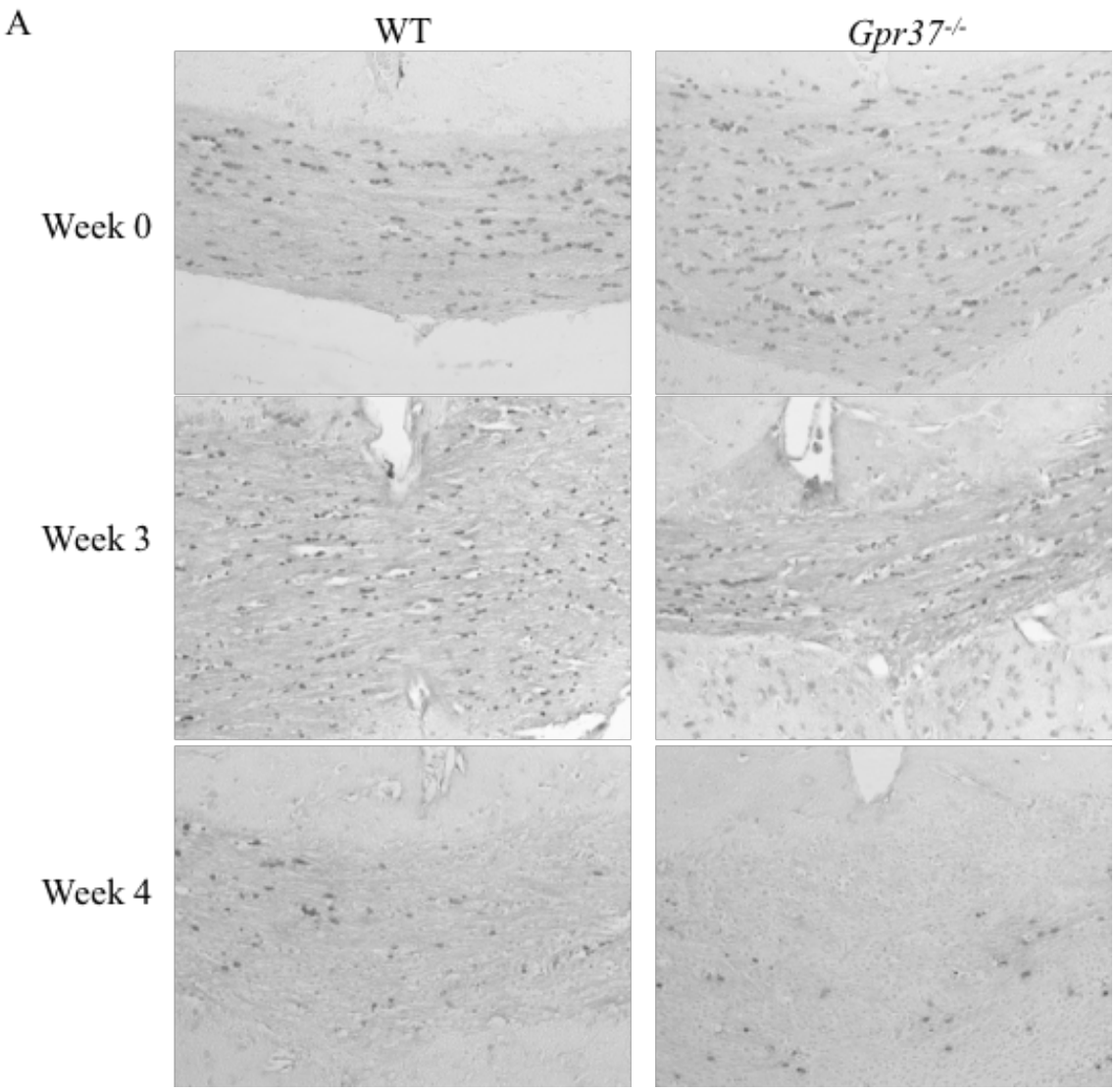
A
WT
Gpr37-/-
Week 0
Week 3
Week 4

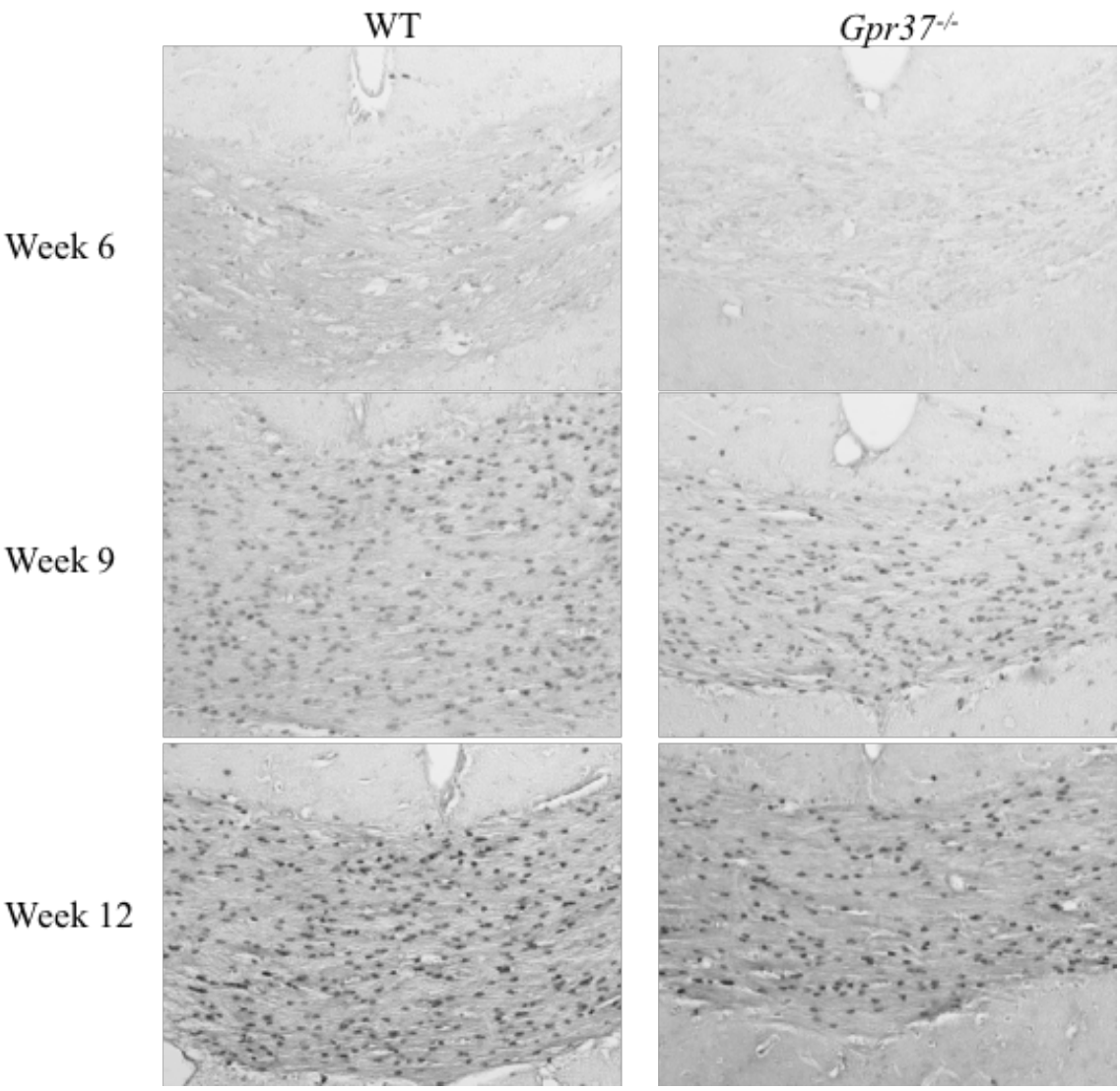
WT
Gpr37-/-
Week 6
Week 9
Week 12

B

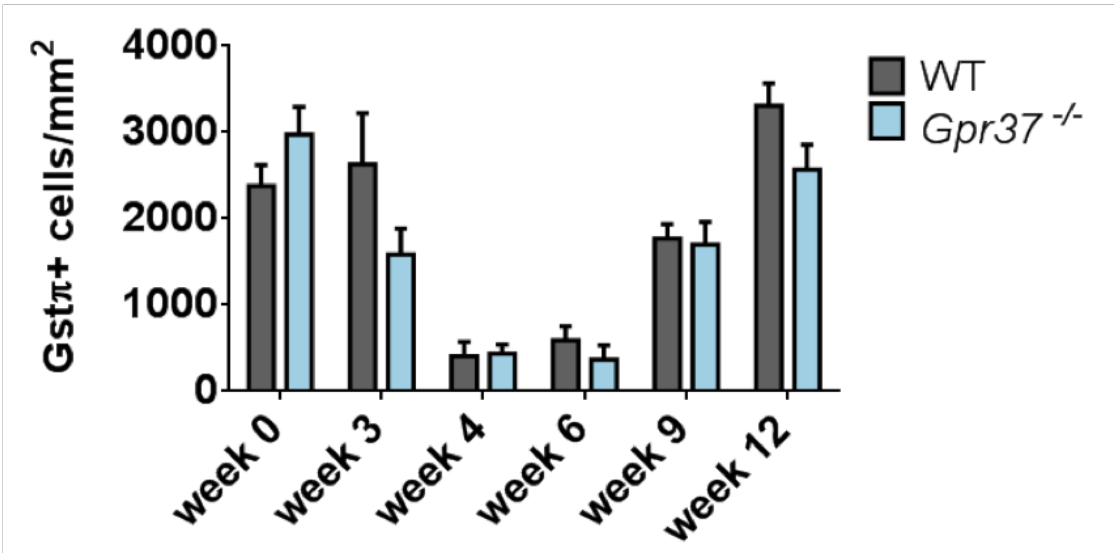
Gstπ+ cells/mm2
4000
3000
2000
1000
0
week 0
week 3
week 4
week 6
week 9
week 12
WT
Gpr37 -/-

3.5 Discussion

GPR37 is an orphan GPCR that has not previously been associated with demyelinating disorders. This receptor, which is also known as the "parkin-associated endothelin receptor-like receptor" (Pael-R), is expressed predominantly in the brain (Donohue et al., 1998; Leng et al., 1999; Marazziti et al., 1998; Valdenaire et al., 1998; Zeng et al., 1997). Several peptides have been reported to bind to GPR37, including head activator peptide (Gandia et al., 2013; Rezgaoui et al., 2006) and prosaptide (Lundius et al., 2014; Meyer et al., 2013), but activation of GPR37 signaling by these peptides is modest at best and not observed at significant levels in all studies (Coleman et al., 2016; Dunham et al., 2009) and thus GPR37 is still considered an orphan receptor. Most of the focus of GPR37 research over the past twenty years has been on the potential role of GPR37 in Parkinson's disease (Imai et al., 2002; Imai et al., 2001; Kubota et al., 2006; Lundius et al., 2013; Murakami et al., 2004; Yang et al., 2003) and regulation of the dopamine system (Imai et al., 2007; Marazziti et al., 2011; Marazziti et al., 2004; Marazziti et al., 2007). In the absence of parkin, GPR37 is prone to aggregation and misfolding, resulting in cytotoxicity to dopaminergic neurons (Imai et al., 2002; Imai et al., 2001).

Although most work to date on GPR37 has focused on the receptor's role in certain neuronal populations, such as dopaminergic neurons, the highest expression levels of GPR37 are observed in mature oligodendrocytes (Cahoy et al., 2008; Imai et al., 2001; Yang et al., 2016). Indeed, a recent report presented evidence that GPR37 is a negative regulator of myelination during development (Yang et al., 2016), but this report did not

assess the effect of GPR37 on responses to demyelinating insults. In the studies described in this chapter, we observed that loss of GPR37 results in a striking increase in the extent of demyelination following cuprizone treatment. Additionally, we observed that overall numbers of OPCs and mature oligodendrocytes were unaffected by loss of Gpr37 at all stages of cuprizone-induced demyelination. These findings suggest that Gpr37 regulates the stability of myelin or resistance of myelin itself to demyelination, rather than regulating OPC recruitment or behaving in a cytoprotective fashion in mature oligodendrocytes. This apparent decrease in myelin stability is consistent with the idea presented in chapter two that *Gpr37*$^{-/-}$ mice might have a demyelination phenotype that is related to decreased Mag protein expression.

Mag$^{-/-}$ mice display sufficient expression of myelin proteins during development, and no gross myelination phenotype is observed at baseline in adult Mag-deficient mice (Li et al., 1994; Montag et al., 1994). However, when Mag$^{-/-}$ mice are exposed to insults such as injury, age, or demyelinating agents, they are more susceptible to demyelination and degeneration of myelinated axons than wild type mice (Jones et al., 2013; Lopez et al., 2011; Weiss et al., 2000). Mag is expressed at the periaxonal membrane (Sternberger et al., 1979) and thought to regulate spacing between axons and myelin and attachment of myelin to axons via interaction with axonal receptors (Pronker et al., 2016; Quarles, 2009). Mag expression is restricted to myelinating oligodendrocytes in the CNS and Schwann cells in the PNS, and so it makes sense that phenotypes observed in Mag$^{-/-}$ mice specifically affect mature myelinating cells. Furthermore, demyelination observed in Mag-deficient mice begins with a characteristic dying-back oligodendrogliopathy

(Lassmann et al., 1997), with periaxonal myelin breakdown occurring before oligodendrocyte apoptosis or axonal degeneration. If deficient Mag expression in *Gpr37*$^{-/-}$ mice contributes to their demyelination phenotype, we would expect to first see loss of myelin without effects on density of mature oligodendrocytes or OPCs. Further work will be needed to conclusively show that decreased Mag expression in *Gpr37*$^{-/-}$ mice contributes causally to the observed decrease in myelin stability, but the data presented in this chapter are consistent with the possibility of destabilized myelin secondary to insufficient Mag expression.

In the studies described in this chapter, we found that *Gpr37*$^{-/-}$ mice display lower average g ratio at week four, but a higher average g ratio at week six and week nine of the cuprizone paradigm, with no significant differences between WT and *Gpr37*$^{-/-}$ mice observed at any other time point. The g ratio, or ratio of inner axon diameter to the total outer diameter of the myelinated axon, is generally considered a reliable method for measuring myelination. A higher g ratio indicates a thinner myelin sheath if axon caliber is constant. For large-caliber axons, g ratio is also a useful tool for determining if a population of axons has been remyelinated, since remyelinated axons have thinner myelin sheaths, and thus higher than average g ratios (Blakemore, 1974; Franklin and Ffrench-Constant, 2008). However, for the smaller axons of the corpus callosum, remyelinated axons are frequently indistinguishable from baseline g ratio (Stidworthy et al., 2003).

A recently published report focusing on the role of GPR37 in myelin development found that *Gpr37*$^{-/-}$ mice display a small but significant decrease in g ratio at baseline,

indicating thicker myelin sheaths in *Gpr37*$^{-/-}$ mice (Yang et al., 2016). This difference in g ratio was first observed at postnatal data (P)14 and sustained throughout adulthood. In the studies presented here, we also observed a trend toward reduced g ratios in the *Gpr37*$^{-/-}$ mice. At baseline, the difference from WT was not statistically significant, but at an early stage (week four) of cuprizone administration, the reduced g ratios of the *Gpr37*$^{-/-}$ mice were significantly different from WT mice. Conversely, at weeks six and nine, this observation was reversed, with WT mice exhibiting significantly lower g ratios, indicating that their myelin sheaths were thicker on average. This finding is consistent with our parallel observation that *Gpr37*$^{-/-}$ mice displayed far more extensive demyelination than WT mice: the higher g ratios observed in *Gpr37*$^{-/-}$ mice during the remyelination phase may plausibly reflect a higher percentage of axons observed being remyelinated. This would make sense, given that *Gpr37*$^{-/-}$ mice would have more demyelinated axons in need of remyelination following cuprizone withdrawal.

Interpretation of the capacity for remyelination in *Gpr37*$^{-/-}$ mice is complicated by the fact that WT mice did not reach complete demyelination during cuprizone administration. Typically, remyelination following cuprizone administration follows a pattern of over-remyelination, with increased density of myelinated axons early in remyelination eventually tapering off to baseline levels (Franklin and Ffrench-Constant, 2008). We observed this pattern in WT mice, with a peak density of myelinated axons occurring at week nine. Conversely, *Gpr37*$^{-/-}$ mice displayed significantly fewer myelinated axons per area observed at week nine. However, both the density of myelinated axons and the average g ratios of *Gpr37*$^{-/-}$ mice had evened out to that of WT

mice by week twelve at the end of the remyelination phase of the cuprizone paradigm, suggesting that *Gpr37*$^{-/-}$ mice have the capacity to eventually reach complete remyelination in this context.

The data presented in this chapter indicate that loss of Gpr37 increases susceptibility to demyelination. These results suggest that GPR37 may be an attractive drug target in the treatment of demyelinating diseases. Elucidation of the mechanisms through which GPR37 regulates susceptibility to demyelination will require the ability to activity and inhibit receptor signaling. The identification of pharmacological tools for studying GPR37 signaling was the focus of the studies described in the next chapter.

Chapter IV: Identification of Modulators of GPR37 Signaling

4.1 Abstract

Work in the preceding chapters identified GPR37 as a regulator of MAG protein expression and a factor contributing to protection against demyelination. Furthermore, previous work from our lab and others have shown that GPR37 is cytoprotective in several different contexts. Previously identified putative ligands are only able to elicit modest signaling effects from GPR37, and thus GPR37 maintains its classification as an orphan receptor. This presents a major challenge to studying the mechanism through which GPR37 mediates its myriad protective effects. In this chapter, we sought to identify synthetic surrogate ligands of GPR37. The pathway-independent biophysical dynamic mass redistribution assay (DMR) was used to complete a high throughput screen of 16,640 small molecule compounds for activity at GPR37. Subsequent confirmatory and counter screens resulted in the identification of two compounds with activity against GPR37. One compound, termed C18 for its location on the screening plate, potentiated constitutive GPR37-mediated activity to both NFAT and SRE in luciferase-based reporter gene assays. However, C18 also appeared to show activity at BAI1, an unrelated GPCR, indicating that it may increase NFAT signaling in a mechanism independent of GPR37 signaling. The second compound, octoclothepin maleate, inhibited constitutive GPR37 signaling to NFAT with an estimated K_i of 65 μM. Octoclothepin is a small synthetic compound that is known to be an antagonist of several other GPCRs. Thus, octoclothepin is not a selective antagonist of GPR37. However, it is the first identified antagonist of GPR37 signaling, and it may prove useful in the future as a scaffold for the synthesis for more selective inhibitors of GPR37. Ongoing small molecule screens aim to identify agonists and other modulators of GPR37 signaling.

4.2 Introduction

The studies described in the preceding chapter revealed that loss of GPR37 results in greatly exacerbated damage in a model of demyelination. These findings suggest that agonism of GPR37 might be protective against demyelination. At present, no synthetic agonist for GPR37 are known, and little is known in general about the regulation of GPR37 signaling. Thus, we sought to identify synthetic ligands and/or interacting partners that could modulate GPR37 signaling. The identification of small molecule activators of GPR37 is of interest both in terms of developing tools to better understand the physiological importance of GPR37 in native tissues and also in terms of the potential therapeutic targeting of GPR37 in the treatment of neurological diseases. Furthermore, the characterization of GPR37-interacting partners could shed light on how GPR37 activity is regulated in native cell types, which is important for designing and interpreting studies on receptor signaling.

It has previously been reported that GPR37 couples predominantly to $G\alpha_i$ (Meyer et al., 2013). High-throughput screening efforts involving $G\alpha_i$-coupled receptors are challenging, mainly because the most widely-utilized readout of $G\alpha_i$ activation is the inhibition of stimulated cAMP production. Thus, the dynamic range of these assays is limited, given that these assays traditionally involve a measurement of inhibition of forskolin-induced cAMP accumulation (Gilissen et al., 2015). Thus, we chose a pathway-independent screening method to avoid these challenges related to screening $G\alpha_i$-coupled receptors.

Dyanmic mass redistribution (DMR) has previously been used to successfully identify specific ligands for the $G\alpha_i$-coupled orphan GPCR GPR17, a receptor involved in oligodendrocyte differentiation and myelination (Hennen et al., 2013; Simon et al., 2016). DMR is a biophysical assay that measures movement of cells, or mass redistribution, on a biosensor plate upon ligand stimulation. The mass redistribution is measured by shining broadband light through the biosensor plate before and after ligand stimulation; changes in the incident wavelength of light indicate movement. In this chapter, we describe the results of screening 16,640 compounds in the DMR high throughput screening assay.

In addition to screening for small molecule ligands capable of activating GPR37, we also explored the effect of several GPR37-interacting partners on receptor signaling. In the studies shown in Chapter 2, MAG was identified as an interacting partner of GPR37. Because of the high expression of GPR37 in oligodendrocytes, it is possible that MAG and GPR37 could interact in vivo to modulate GPR37 signaling activity. Thus, we assessed the effect of MAG co-expression on GPR37 signaling in HEK-293T cells. Additionally, the regenerating islet-derived family member 4 (REG4) was identified as a potential agonist or modulator of GPR37 (Wang et al., 2016). REG proteins are secreted factors known for their pro-regenerative effects after injury. REG4 expression is highly restricted to the gastrointestinal tract, but other REG family members are ectopically expressed, especially in the context of tissue injury (Hartupee et al., 2001; Parikh et al., 2012; Violette et al., 2003). REG2, also called Reg3β in mice or pancreatitis-associated

protein (PAP1) in humans, is expressed in the central and peripheral nervous systems (Bartoli et al., 1998). REG2 is released after sensory or motor neuron injury (Averill et al., 2002; Livesey et al., 1997), and it promotes regeneration in a mouse model of diabetic peripheral neuropathy (Tam et al., 2004). Deletion of REG2 also disrupts CNTF signaling and delays myelination (Tebar et al., 2008). Given the potential role for REG2 in myelination, its close relationship to REG4, and the evidence that REG4 might activate GPR37, we explored the potential of both REG2 and REG4 to modulate GPR37 signaling *in vitro*.

4.3 Experimental Procedures

Cell Culture: HEK-293T/17 cells were acquired from ATCC (Manassas, VA) and maintained in DMEM (Life Technologies) supplemented with 10% fetal bovine serum and 1% penicillin/streptomycin in a humid, 5% CO_2, 37°C incubator.CHO-K1 cells were acquired from ATCC and maintained in F12-K medium (ATCC) supplemented with 10% fetal bovine serum. Cells were transfected using Mirus (Madison, WI) TransIT-LT1 according to the manufacturer's protocol.

Compounds*:* Octoclothepin maleate, amantadine hydrochloride, and α-methyl-L-tyrosine were purchased from Sigma-Aldrich (St Louis, MO). All other compounds were acquired from Chemical Diversity (San Diego, CA).

Dynamic Mass Redistribution: CHO-K1 cells were seeded in 384-well Epic assay microplates from Corning (Corning, NY) 24 hours prior to transfection. Each well was transfected with 15ng GFP-tagged GPR37 or mock DNA when cells reached 50% confluency. Complete cell media was exchanged for serum-free assay buffer (1% DMSO in HBSS) 46 hours after transfection. Following a two-hour serum starve, a baseline read of mass distribution was determined for each plate using an Epic microplate reader (Corning). Cells were then treated with compounds at 50uM in 1% DMSO. Plates were immediately returned to the Epic plate reader to assess dynamic mass redistribution. A total of 16,640 compounds were screened from the Sigma-Aldrich library of

pharmacologically active compounds (LOPAC) and Sigma-Aldrich and Asinex (Winston-Salem, NC) compound diversity libraries.

Luciferase Reporter Assays: HEK-293T/17 cells were seeded in 96-well plates 20-24 hours prior to transfection. When cells reached 50% confluency, each well was transfected with 50ng of firefly reporter, 1ng of *Renilla* luciferase, and 10ng of receptor or mock DNA. Reporter constructs (NFAT: pGL4.30, SRE: pGL4.33, *Renilla* pRLSV40) were acquired from Promega (Madison, WI). Cells were treated with drug or vehicle 24-42hrs after transfection. 48 hours after transfection, Dual-Glo luciferase assays (Promega) were performed according to the manufacturer's protocol and plates were read on a BMG Omega plate reader. Results were calculated for each assay by determining the luminescence ratio of firefly:*Renilla* luciferase counts, normalized to empty vector (EV) transfected, vehicle-treated wells.

Western Blotting: Protein samples were reduced and denatured in Laemmli buffer, loaded into 4-20% Tris-Glycine gels (Bio-Rad) for SDS-PAGE, and then were run at 120V for 20 minutes followed by 180V for 40 minutes. Proteins were transferred to nitrocellulose membranes for 10 minutes using the Trans-Blot Turbo transfer system (Bio-Rad). Blots were blocked for 30 minutes at room temperature with 2% milk (in 50mM NaCl, 10mM HEPES, pH 7.3 with 0.1% Tween-20 (Sigma)) and then incubated in milk with primary antibodies overnight at 4°C. The following day, blots were washed with milk three times for five minutes. Blots were then incubated in milk with secondary antibody at a 1:20,000 dilution for 30 minutes at room temperature. Secondary antibody

incubation was followed by three seven-minute washes. Blots were developed using SuperSignal West Pico, West Dura, or West Femto chemiluminescent substrate (Thermo) and visualized using a LiCor imaging platform. Proteins were quantified using densitometry, performed with Image Studio Lite software.

Coimmunoprecipitation: HEK-293T/17 cells were transfected in 10 cm dishes with 2µg of either empty vector plasmid, GFP-tagged GPR37, FLAG-tagged REG4, His-tagged prosaposin, or a combination of the three constructs at 50% confluency. After a 48-hour incubation, cells were harvested in 500 µl of lysis buffer (1% Triton X-100, 25 mM HEPES, 150 mM NaCl, 10 mM $MgCl_2$, 1 mM EDTA, HALT protease inhibitor mix, and 2% glycerol) and lysed by slowly rotating for 60 min at 4 °C. Cells were subjected to centrifugation to clear cellular debris, and soluble cell lysates were incubated with 60µl of anti-FLAG antibody-conjugated protein A/G beads for 1 h at 4 °C. Following five washes with lysis buffer, beads were resuspended in 60 µl of 2X Laemmli buffer.

AP-TGFα Shedding Assay: HEK-293T/17 cells were transfected in 10 cm dishes with 3 µg AP-TGFα, either 2 µg GFP-tagged GPR37 or EV, and 2 µg of REG2, REG4, or EV plasmid DNA 48 hours prior to the assay. Transfected cells were detached by treatment with 0.05% trypsin EDTA and pelleted by centrifugation at 1,200 rotations per minute for five minutes. Cells from each plate were resuspended in 10 mL Hank's balanced salt solution (HBSS) with 5 mM HEPES and reseeded at 90 µl per well in a 96-well plate. The cells were then returned to the incubator for 30 minutes, after which 80 µl of conditioned medium were transferred to new wells. A baseline absorbance read at 405

nm was read on a BMG Omega plate reader, and then a p-NPP solution (10 mM *p*-NPP, 40 mM Tris-HCl (pH 9.5), 40 mM NaCl, 10 mM $MgCl_2$) was added at 80 µl per well to wells containing both adherent cells and conditioned medium. Cells were incubated for one hour, and then absorbance was read again at 405 nm. Relative percentage of alkaline phosphatase in each well was calculated as follows:

$$\boldsymbol{Relative\ AP\ activity} = \frac{\mathbf{\Delta OD\ 405CM}}{\mathbf{\Delta OD\ 405CM} + \mathbf{\Delta OD\ 405Cells}}$$

where ΔOD 405CM refers to the change in absorbance from baseline in the conditioned medium wells and ΔOD 405Cells refers to the change in absorbance from baseline in the wells containing adherent cells.

4.4 Results

4.4.1 High-throughput screening for small molecule modulators of GPR37 signaling

Primary screening of compounds was completed in CHO-K1 cells transiently transfected with GFP-tagged GPR37 (Figure IV-1). Initial hits from the DMR screen were selected based on their ability to induce changes in DMR compared to cells transfected with empty vector (EV). For secondary assays, the ability of identified compounds to enhance constitutive GPR37-mediated signaling to NFAT luciferase in a reporter gene assay was utilized (Figure IV-2A). This signaling was found to be inhibited by the Gβγ inhibitor gallein (Figure IV-2A), revealing that this signaling represents G protein-mediated signaling downstream of GPR37.

Three compounds were selected from the LOPAC library for secondary screening: amantadine, α-methyl-L-tyrosine (AMPT), and octoclothepin maleate (octoclothepin) (Figure IV-3A). These compounds were assessed for the ability to enhance GPR37-mediated signaling to NFAT-luciferase. Surprisingly, octoclothepin appeared to attenuate GPR37-mediated signaling at high doses. In contrast, AMPT and amantadine exhibited no effect on GPR37-mediated signaling to NFAT luciferase (data not shown), so no further studies were pursued with these compounds.

Dose-response experiments were then carried out to characterize the activity of octoclothepin on GPR37 signaling. A dose-response curve ranging in concentration from 10 nM to 100 μM octoclothepin revealed a dramatic and dose-dependent inhibition of

signaling between 10 μM and 100 μM (Figure IV-3B). Thus, we utilized a narrower range of doses from 10 μM to 100 μM and calculated an IC_{50} of 65 μM for octoclothepin inhibition of GPR37-mediated signaling in this assay (Figure IV-3C).

Following the LOPAC library, we screened compounds from the Sigma-Aldrich and Asinex compound diversity libraries. A total of 12 hits were detected in the primary screen and assessed in the NFAT luciferase secondary assay, but most of the compounds exhibited no ability to modulate NFAT luciferase activation by GPR37 (data not shown). However, one compound (5HD[1,2,4]triazino[5,6Db]indolD3Dylthio)acetamide; (termed "C18" for its plate position) did yield substantial increases in GPR37-mediated signaling in the NFAT-luciferase assay (figure IV-3A). A full list of all compounds screened and their identities is presented in table IV-1.

We confirmed that C18 significantly potentiates GPR37-mediated signaling to NFAT (Figure IV-3B). Subsequent dose-response studies revealed an EC_{50} of 1.2 μM (Figure IV-3C). To further confirm that C18 activates GPR37, we tested the ability of C18 to induce signaling to the serum response element (SRE) reporter. SRE is activated downstream of the MAPK/ERK signaling pathway, and we have previously reported that activation of GPR37 results in ERK phosphorylation (Meyer et al., 2013). Unlike the NFAT assay, GPR37 does not exhibit constitutive activity in the SRE-luciferase assay (Figure IV-3D). However, treatment of cells with C18 resulted in significant activation of SRE in the presence of GPR37 but not EV DNA.

We next sought to determine if the activation of signaling by C18 was specific for GPR37. To this end, we treated a stalkless truncated version of the adhesion G protein-coupled receptor BAI1/ADGRB1 (BAI1-SL) with C18. Like GPR37, BAI1-SL exhibits substantial constitutive activity in the NFAT-luciferase assay (Kishore et al., 2016) but is only distantly related to GPR37. We observed both NFAT activation (figure IV-4A) and SRE activation (figure IV-4B) upon treatment of BAI-SL-transfected cells with C18. Based on these results, we concluded that C18 is not a specific activator of GPR37 but rather a non-selective activator of GPCR-mediated signaling.

Figure IV-1. Transiently transfected CHOK-1 cells express GFP-tagged GPR37 48 hours after transfection. Transfections were confirmed via visualization of GFP before each screening session.

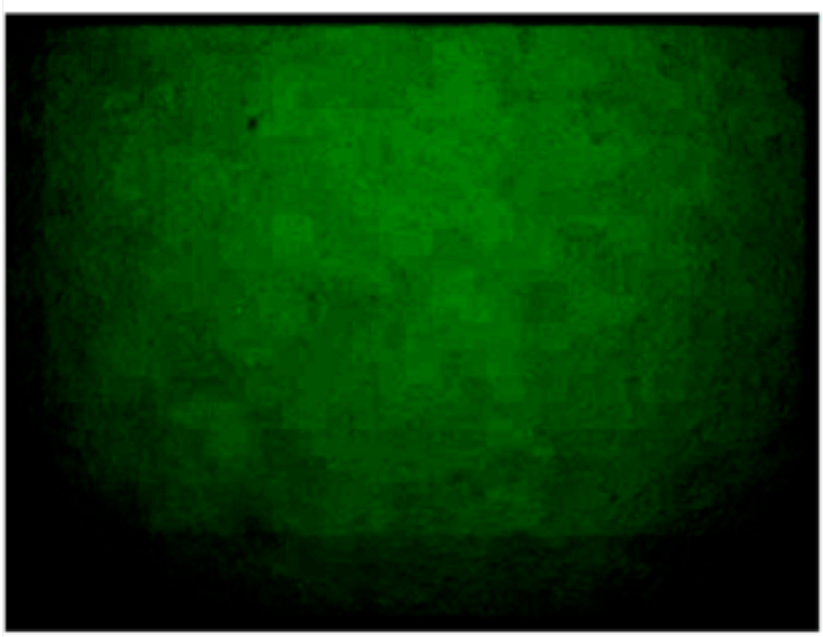

Empty Vector

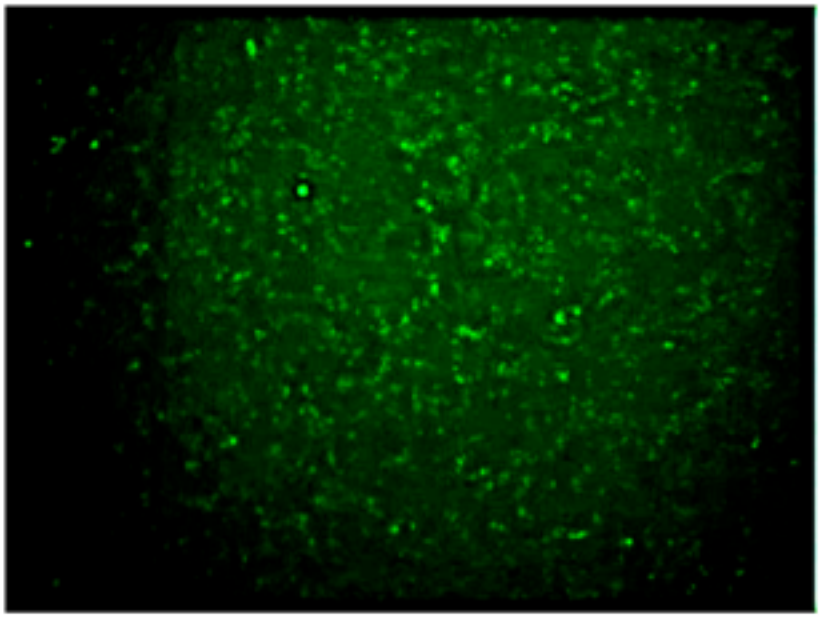

GFP37

Figure IV-2. GPR37 signals to NFAT via Gβγ. A) GFP-tagged and Flag-tagged GPR37 constructs, but not an untagged GPR37 construct, signal constitutively to NFAT in a luciferase reporter assay. B) Constitutive GFP37 signaling is reduced by the Gβγ inhibitor gallein (n = 5).

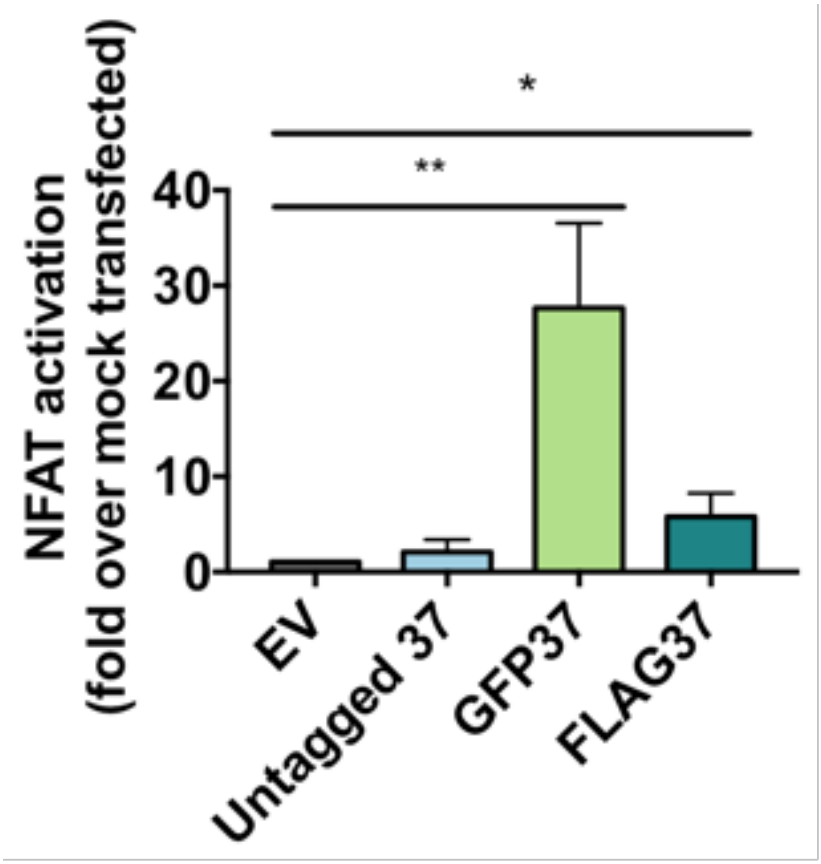
NFAT activation
(fold over mock transfected)
*
**
40
30
20
10
0
EV
Untagged 37
GFP37
FLAG37

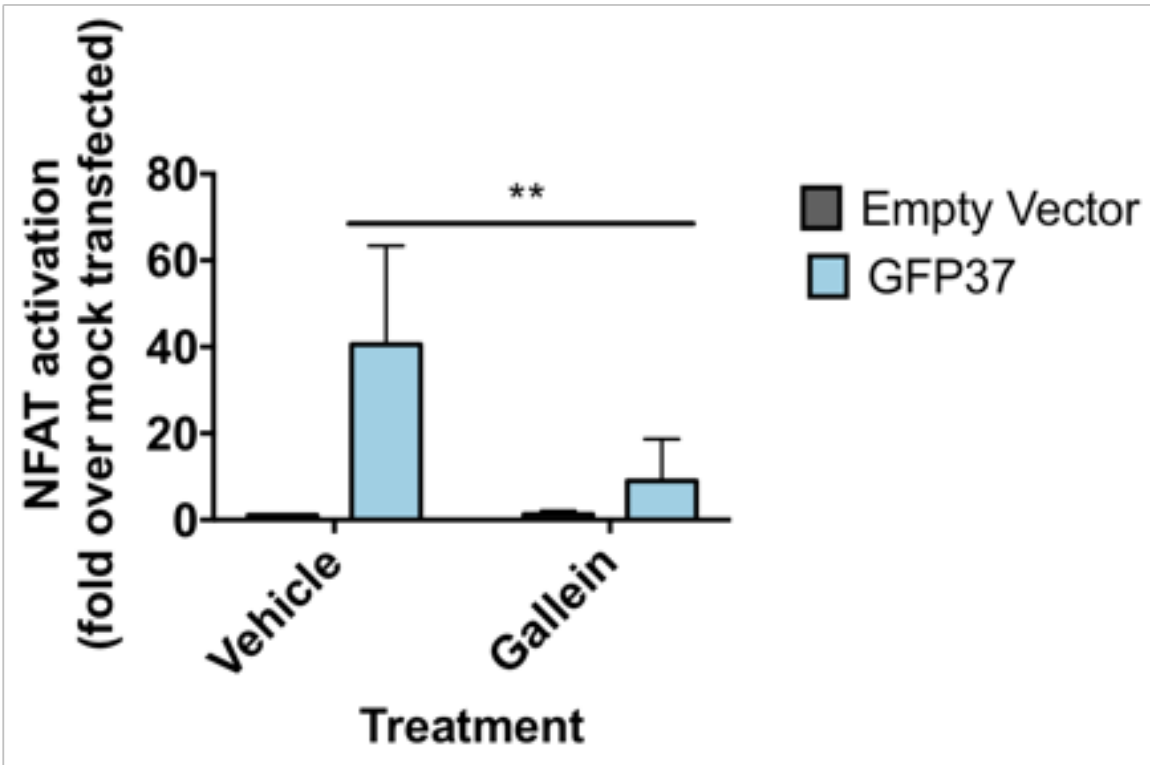
NFAT activation
(fold over mock transfected)
**
80
60
40
20
0
Vehicle
Gallein
Treatment
Empty Vector
GFP37

Figure IV-3. Octoclothepin is a low-affinity inverse agonist of GPR37. A) Secondary screening of hits from the LOPAC library revealed that octoclothepin attenuates constitutive GPR37-mediated NFAT signaling (n=5). B) Octoclothepin inhibits GPR37-mediated signaling most effectively at doses higher than 10 uM (n=2). C) An inhibition curve revealed an IC_{50} of 65 μM (n=4).

A

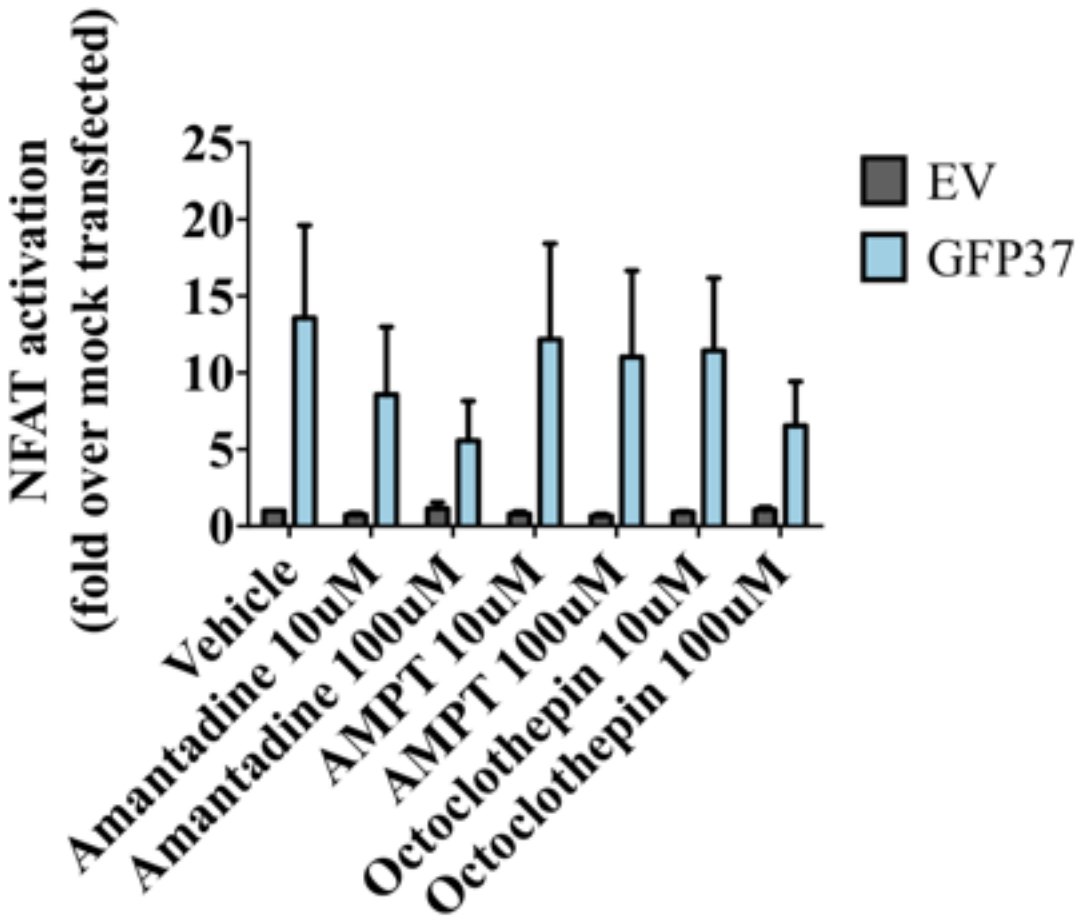
NFAT activation
(fold over mock transfected)
25
20
15
10
5
0
EV
GFP37
Vehicle
Amantadine 10uM
Amantadine 100uM
AMPT 10uM
AMPT 100uM
Octoclothepin 10uM
Octoclothepin 100uM

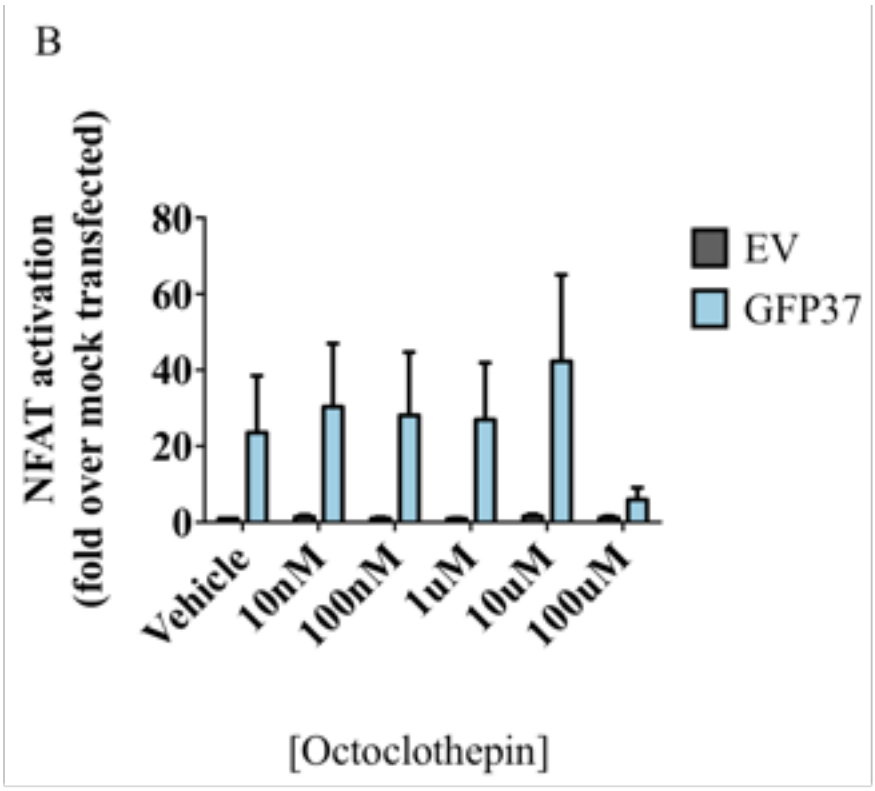
B
NFAT activation
(fold over mock transfected)
80
60
40
20
0
EV
GFP37
Vehicle
10nM
100nM
1uM
10uM
100uM
[Octoclothepin]

C

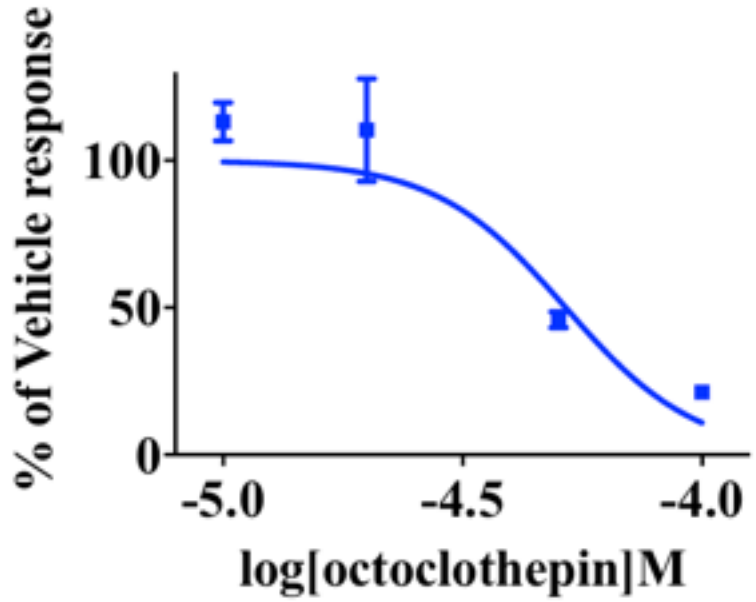
% of Vehicle response
100
50
0
-5.0
-4.5
-4.0
log[octoclothepin]M

Figure IV-4. C18 promotes GPR37 signaling to NFAT and SRE. Treatment of cells with both 10 μM and 100 μM C18 (n=3) resulted in significantly increased GPR37-mediated signaling to NFAT [$F(2,4)=7.642$, $p=0.0430$] (A) with an EC_{50} of 1.2 μM (B). C) Two-way ANOVA indicated that C18 treatment also resulted in GPR37-mediated activation of SRE [$F(1,1)=348.8$, $p=0.0341$] (n=2). *$p<0.05$ via Sidak's post-hoc analysis

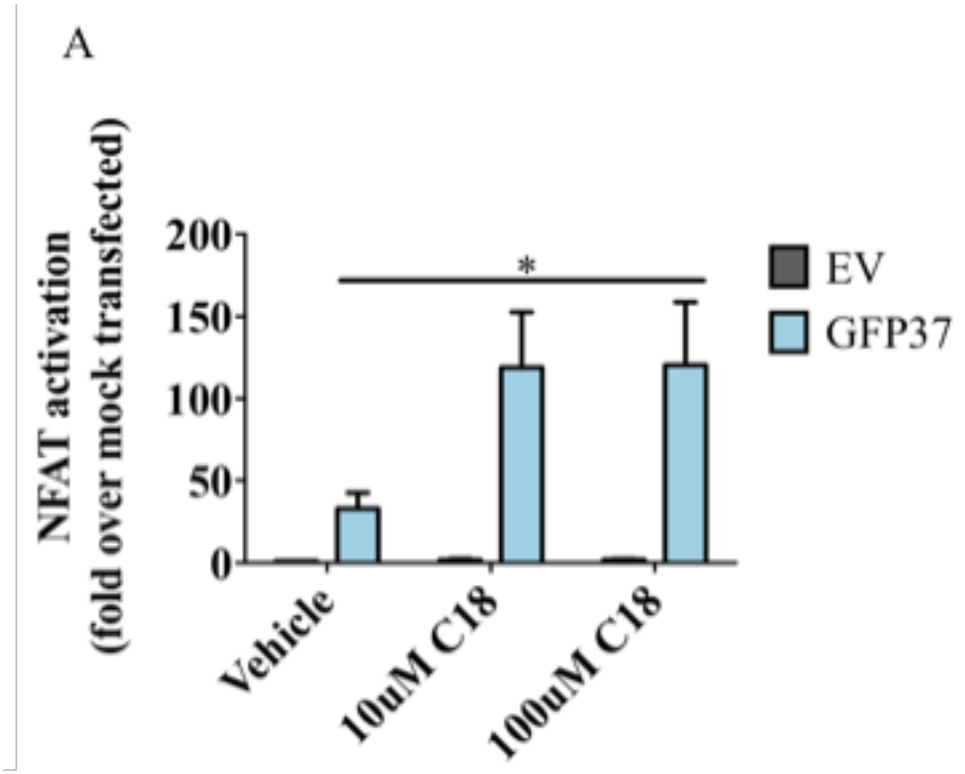
A
NFAT activation
(fold over mock transfected)
200
150
100
50
0
*
EV
GFP37
Vehicle
10uM C18
100uM C18

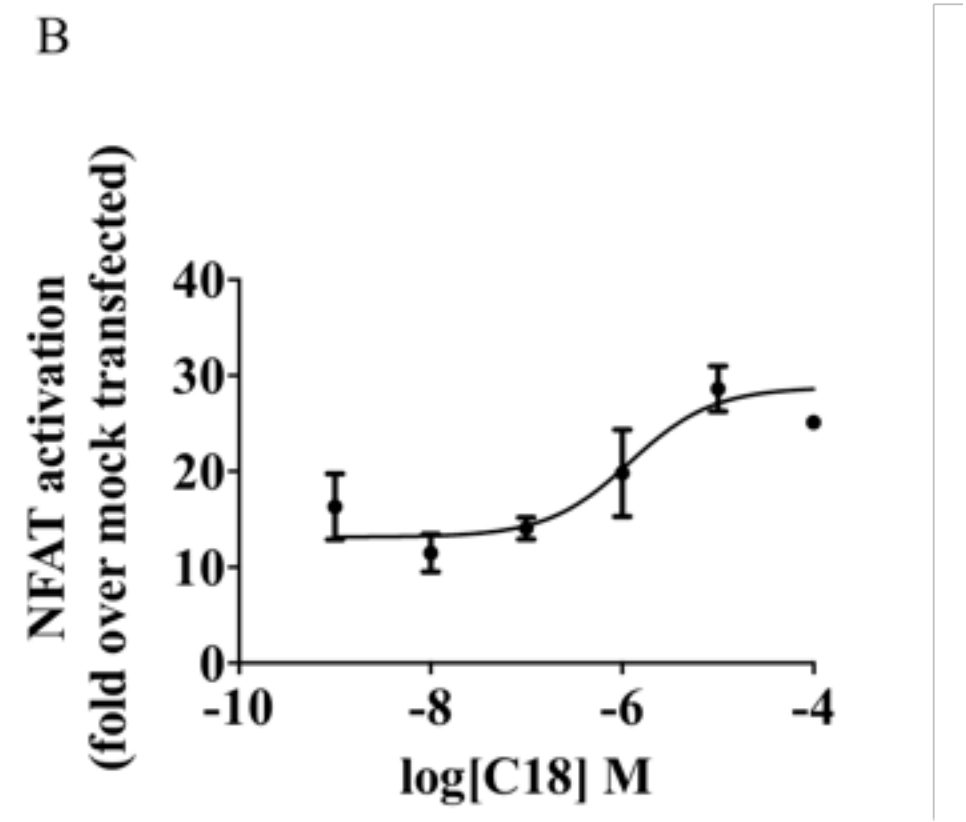
B
NFAT activation
(fold over mock transfected)
40
30
20
10
0
-10
-8
-6
-4
log[C18] M

C

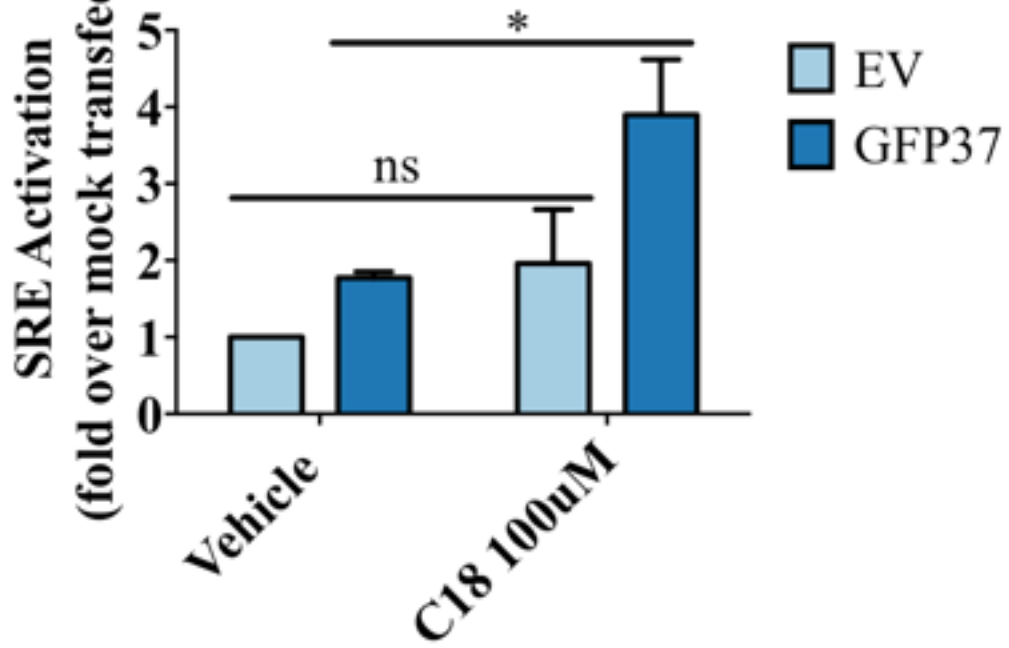
SRE Activation
(fold over mock transfected)
5
4
3
2
1
0
*
ns
EV
GFP37
Vehicle
C18 100uM

Figure IV-5. C18 potentiates BAI1 signaling to NFAT and SRE. Treatment with C18 increases BAI-SL-mediated signaling to NFAT (A) and SRE (B) (n=2).

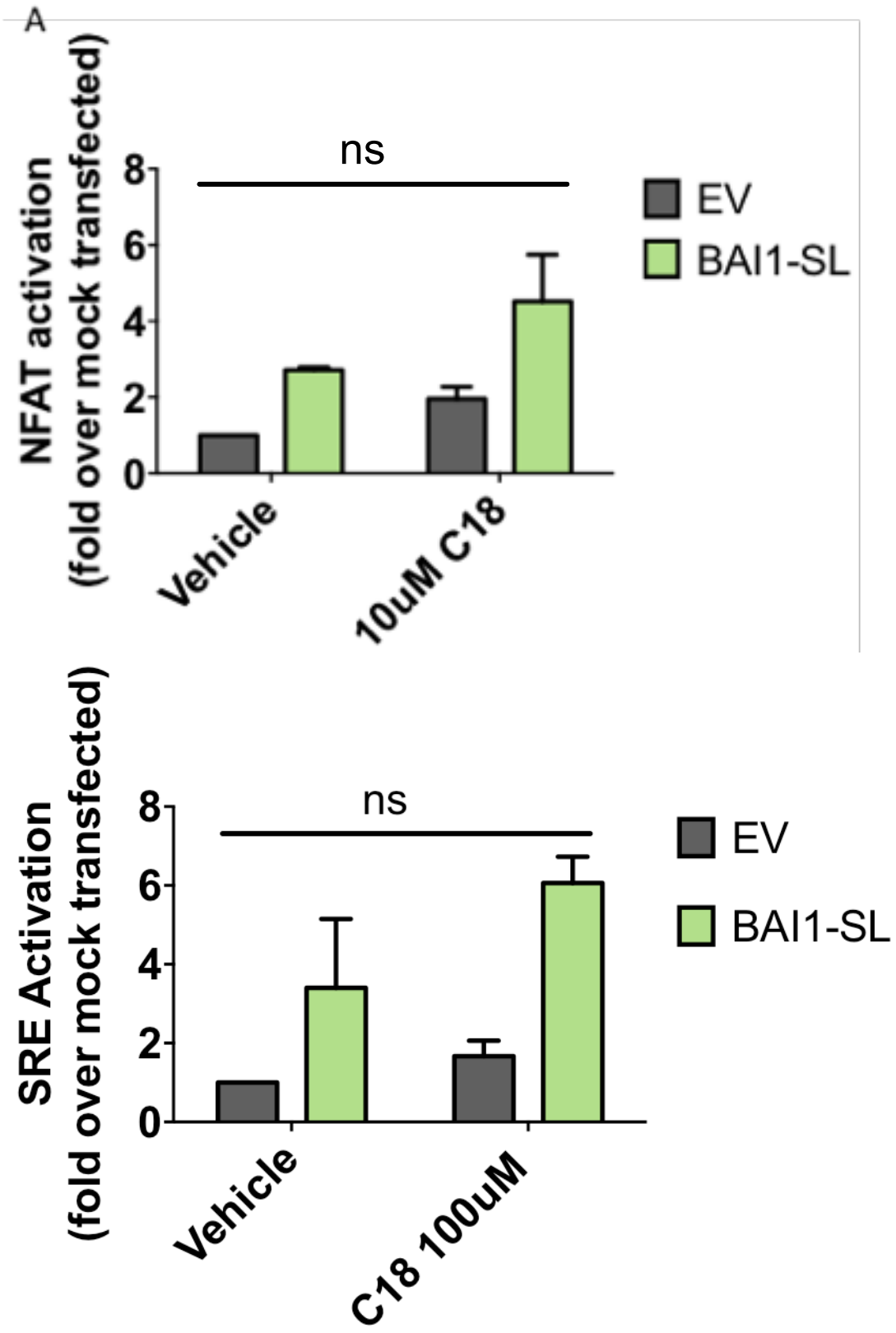
A
NFAT activation
(fold over mock transfected)
ns
EV
BAI1-SL
0
2
4
6
8
Vehicle
10uM C18
SRE Activation
(fold over mock transfected)
ns
EV
BAI1-SL
0
2
4
6
8
Vehicle
C18 100uM

Table IV-1. List of compounds used in secondary assays. All compounds except for amantadine hydrochloride, octoclothepin maleate, and α-methyl-L-tyrosine are identified by their IUPAC names. LOPAC=Library of Pharmacologically Active Compounds, CDL=Chemical Diversity Library, ANXLG=Asinex Library, SID=Pubchem Substance Accession Identifier.

Library	Screened	Secondary	SID	Identity
LOPAC	1280	3	17404569	amantadine hydrochloride
			17405444	octoclothepin maleate
			117393519	α-methyl-L-tyrosine
CDL	12480	6	24341625	2-chloro-N-(3-nitrophenyl)-5-sulfamoylbenzamide
			24347677	4-nitro-N,N-bis(prop-2-ynyl)aniline
			24338919	1-(2,6-dimethoxyphenoxy)-3-[4-(2-fluorophenyl)piperazin-1-yl]propan-2-ol
			24335619	4-(2-chlorophenyl)-N-(2,3-dimethylphenyl)-6-methyl-2-oxo-1,2,3,4-tetrahydropyrimidine-5-carboxamide
			24335703	1-(2-pyrrolidin-1-ylethyl)chromeno[3,4-d]imidazol-4-one
			24285191	N-(2-fluorophenyl)-2-(5H-[1,2,4]triazino[5,6-b]indol-3-ylsulfanyl)acetamide
ANXLG	2880	3	24285191	8-chloro-9-nitro-4-(4-nitrophenyl)-3a,4,5,9b-tetrahydro-3H-cyclopenta[c]quinolin-6-ol
			26614794	1-(1-ethylbenzimidazol-2-yl)-N-(5-propan-2-yl-1,3,4-thiadiazol-2-yl)piperidine-4-carboxamide
			26613709	9-cyclohexyl-2-(2-fluorophenyl)-8-oxo-7H-purine-6-carboxamide
TOTAL	16640	12		

4.4.2 Effect of interacting partners on GPR37 signaling

In addition to the high-throughput screening efforts to find activators or modulators of GPR37 signaling activity, we explored the possibility that certain GPR37-interacting partners might modulate receptor signaling. Given the data shown in Chapter 2 that MAG can interact with GPR37, we sought to determine if co-transfection of MAG with GPR37 might alter constitutive GPR37-mediated signaling to NFAT. In the course of these studies, three different GPR37 constructs were identified as having different levels of constitutive activity in the NFAT-luciferase signaling assay. GFP-tagged GPR37 (GFP37) exhibits robust constitutive signaling to NFAT (figure IV-5A), perhaps because of its extremely high level of expression, while Flag-tagged GPR37 (figure IV-5B) and untagged GPR37 (figure IV-5C) do not display any significant constitutive activity in the NFAT-luciferase assay. However, co-transfection of MAG with each of the three GPR37 constructs resulted in no significant differences in signaling to NFAT luciferase.

In a recent publication, GPR37 was reported to be found in a complex with prosaposin and REG4 (Wang et al., 2016). We confirmed this interaction via co-immunoprecipitation, and further found that GPR37 can interact with REG4 in both the absence and presence of prosaposin (figure IV-6). Wang et al. (2016) also reported that siRNA knockdown of GPR37 resulted in decreased REG4-evoked TGFα release in a gastric cancer cell line, concluding that REG4 might be a ligand for GPR37.

We tested the ability of REG2 and REG4 to activate GPR37 in the NFAT-luciferase reporter gene assay. Unexpectedly, both REG2 and REG4 attenuated GPR37-mediated signaling to NFAT (Figure IV-8A). Because REG proteins are secreted factors, we next sought to determine if REG inhibition of GPR37 signaling was the result of released REG2 or REG4 acting extracellularly on GPR37. To test this, cells transfected with GPR37 were co-cultured with cells that were transfected with either REG2 or REG4. In the co-culture context, neither REG2 or REG4 inhibited GPR37 signaling to NFAT (Figure IV-8B). From these data, we concluded that the REG-mediated inhibition of GPR37 signaling that we observed was the result of REG2 or REG4 interacting with GPR37 within the same cell.

Finally, we explored the ability of REG2 and REG4 to activate GPR37 in an AP-TGFα activity assay. REG4-evoked TGFα release was reported to be dramatically decreased when GPR37 was knocked down in gastric cancer cells (Wang et al., 2016). Thus, we sought to confirm this finding in HEK293 cells by co-transfecting GPR37 with REG4 and investigate whether REG2 might also activate GPR37 *in vitro*. However, no significant differences in relative secreted alkaline phosphatase activity was observed between cells transfected with only GPR37 compared to cells transfected with GPR37 and REG2 or REG4 (figure IV-8C). Thus, we concluded that co-transfection of REG2 or REG4 did not stimulate TGFα release via GPR37 in this cellular context. However, a significant decrease in alkaline phosphatase activity was observed in cells transfected with GPR37 compared to EV, regardless of presence or absence of REG proteins.

Figure IV-6. Co-expression of MAG does not alter GPR37-mediated signaling to NFAT Co-transfection of 5ng/well or 10ng/well MAG with GFP-tagged GPR37 (GFP37) (A), Flag-tagged GPR37 (FLAG37) (B), or untagged GPR37 (UT37) (C) did not result in altered GPR37 signaling to NFAT luciferase (n=3).

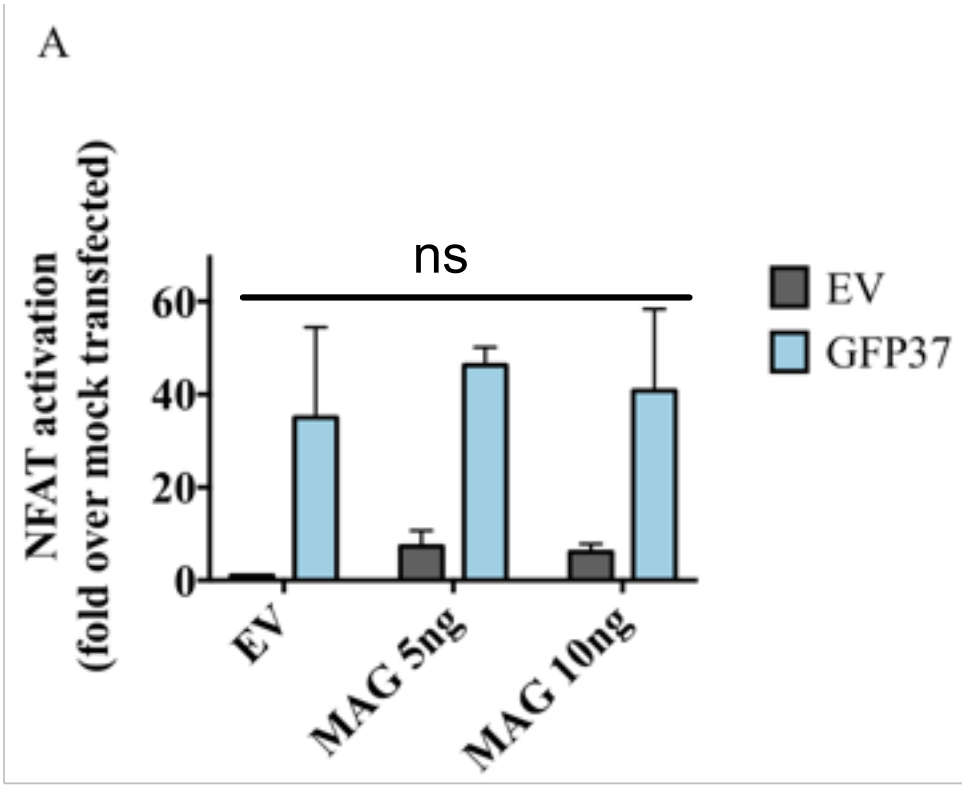
A
NFAT activation
(fold over mock transfected)
60
40
20
0
ns
EV
GFP37
EV
MAG 5ng
MAG 10ng

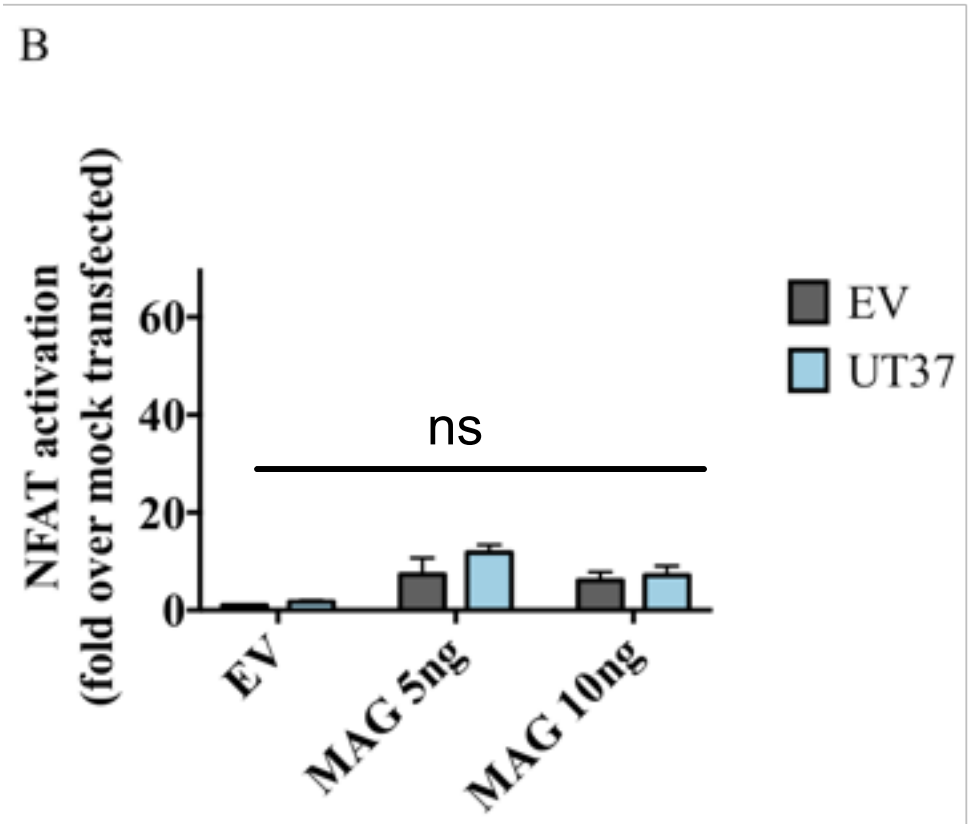
B
NFAT activation
(fold over mock transfected)
60
40
20
0
ns
EV
UT37
EV
MAG 5ng
MAG 10ng

C

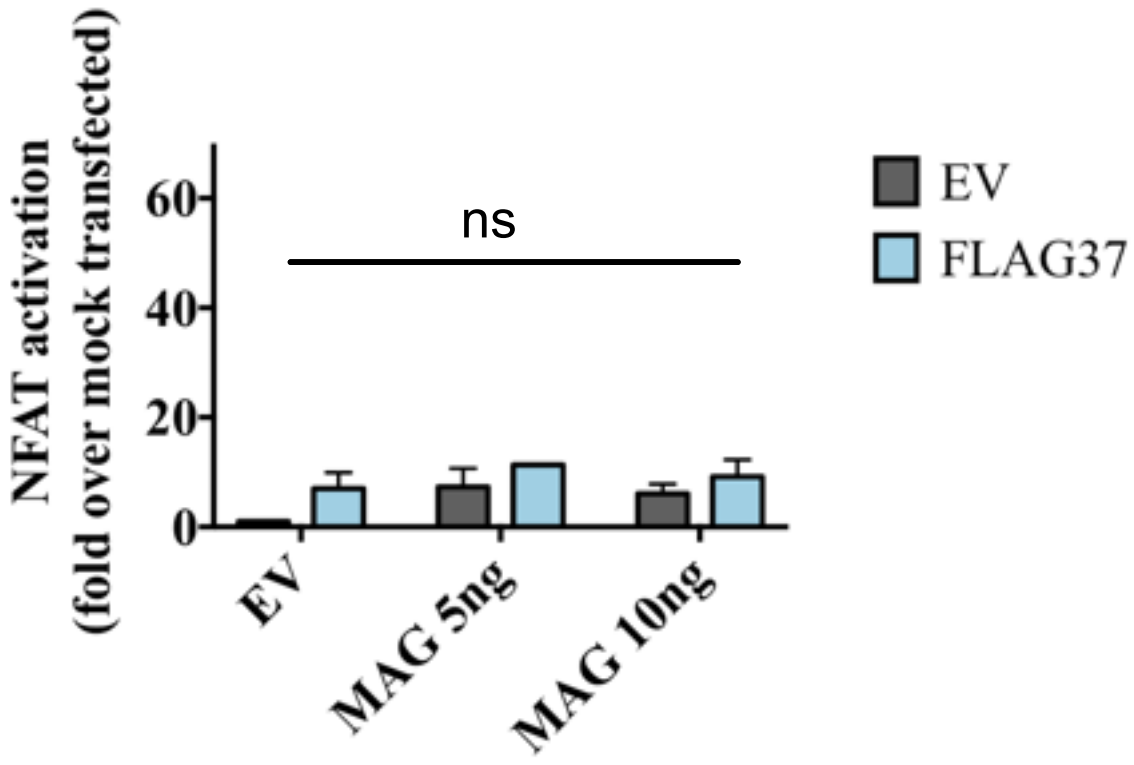
NFAT activation
(fold over mock transfected)
60
40
20
0
ns
EV
FLAG37
EV
MAG 5ng
MAG 10ng

Figure IV-7. GPR37 Co-immunoprecipitates with REG4. GPR37 co-immunoprecipitates with Flag-tagged REG4 in the presence or absence of prosaposin (n=3). Molecular weight markers are shown in kDa to the left of each immunoblot. IP=immunoprecipitation.

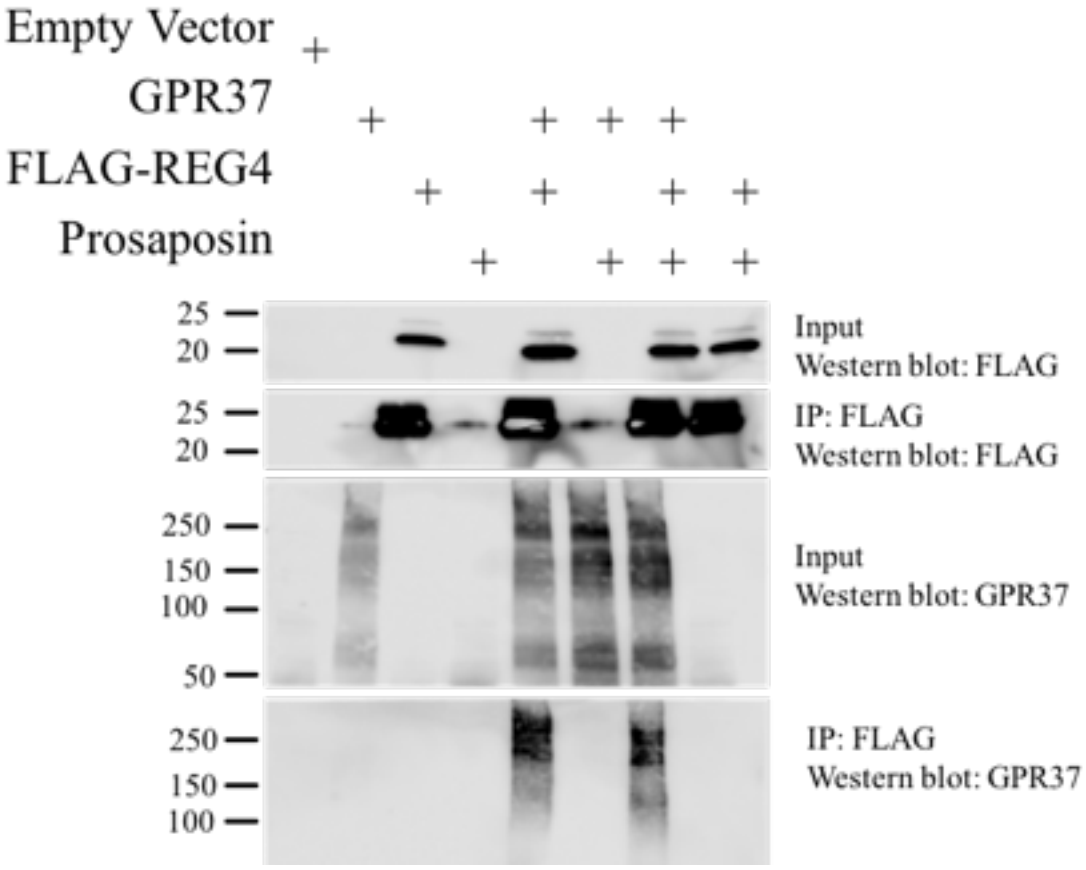
Empty Vector
GPR37
FLAG-REG4
Prosaposin
+
+ + + +
+ + + +
+ + + +
25
20
Input
Western blot: FLAG
25
20
IP: FLAG
Western blot: FLAG
250
150
100
50
Input
Western blot: GPR37
250
150
100
IP: FLAG
Western blot: GPR37

Figure IV-8. REG2 and REG4 inhibit constitutive NFAT signaling but not constitutive TGFα shedding mediated by GPR37. A) GPR37-mediated signaling to NFAT was significantly reduced by co-transfection of either REG2 or REG4 [$F(1,6)=9.926$, $p=0.0198$]. B) Co-culture of cells transfected with GPR37 and either REG2 or REG4 did not result in altered GPR37-mediated signaling to NFAT. C) Relative AP-TGFα activity present in media of cells transfected with GPR37 was significantly decreased compared to empty vector (EV) transfection, but co-transfection of REG2 or REG4 did not significantly affect GPR37-mediated AP-TGFα release , n=3, *$p<0.05$ by two-way ANOVA.

A

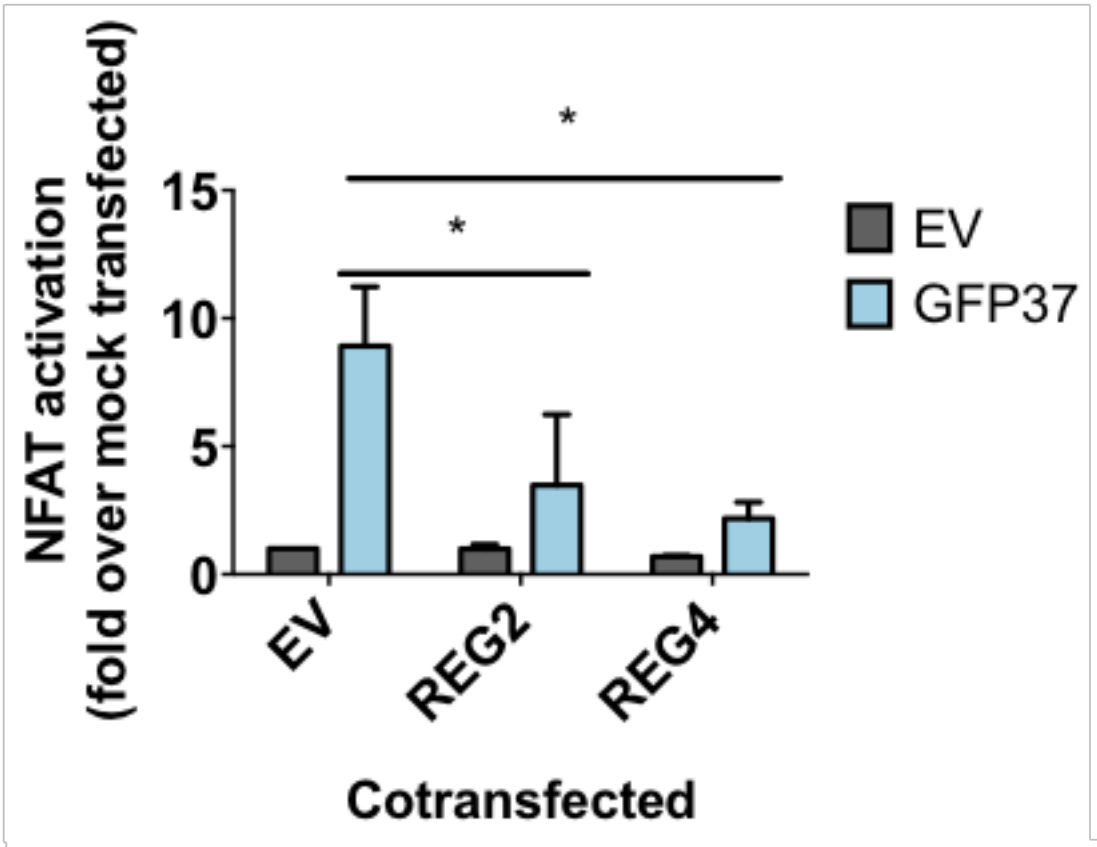
NFAT activation
(fold over mock transfected)
15
10
5
0
*
*
EV
GFP37
EV
REG2
REG4
Cotransfected

B

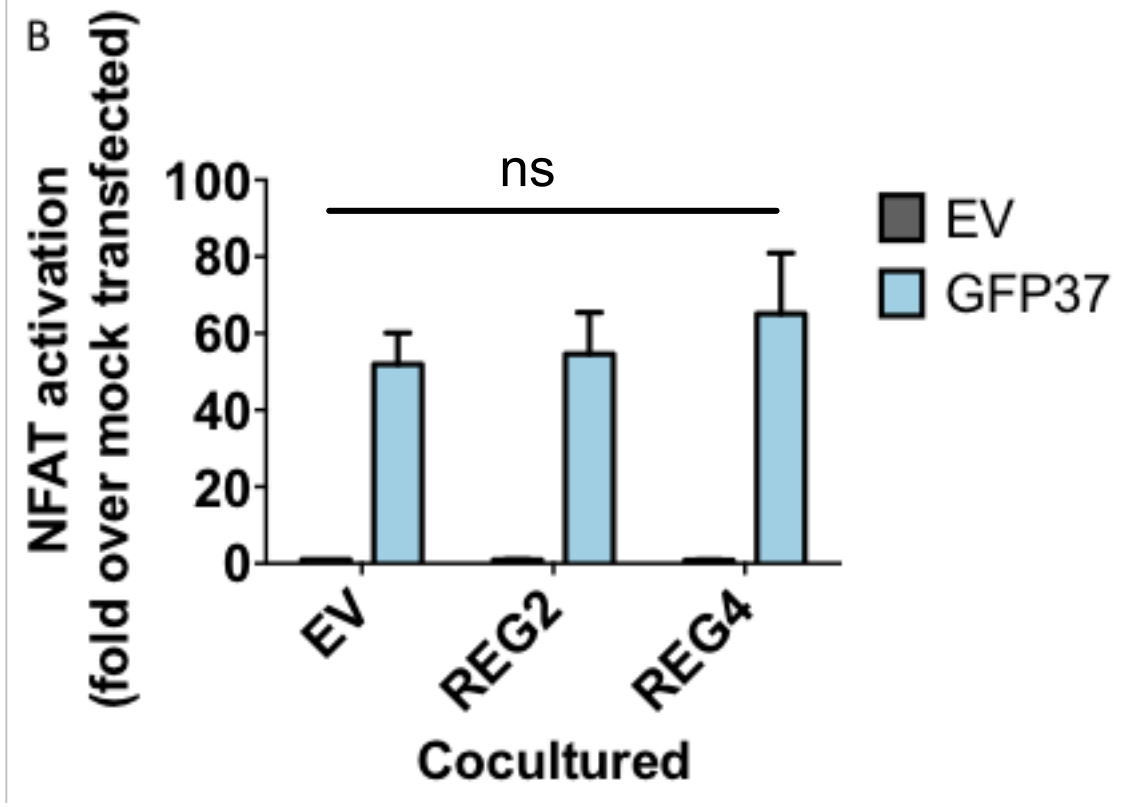
NFAT activation
(fold over mock transfected)
100
80
60
40
20
0
ns
EV
GFP37
EV
REG2
REG4
Cocultured

C

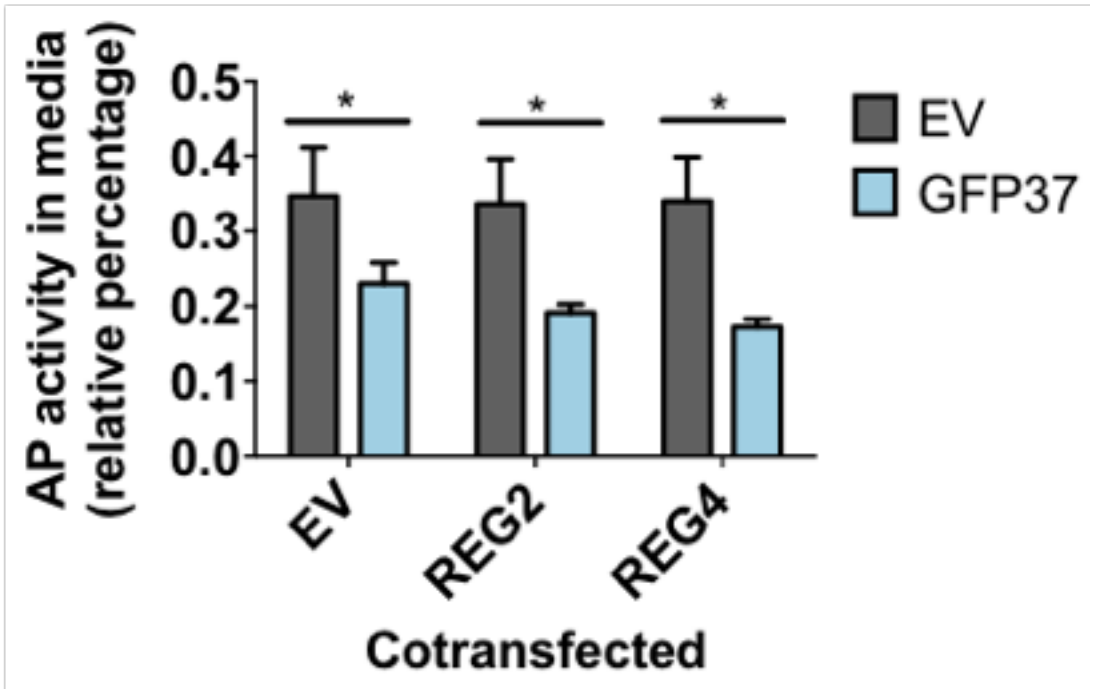
AP activity in media
(relative percentage)
0.5
0.4
0.3
0.2
0.1
0.0
*
*
*
EV
GFP37
EV
REG2
REG4
Cotransfected

4.5 Discussion

In studies described in this chapter, octoclothepin was identified as a low-affinity inverse agonist of GPR37-mediated signaling. The high IC_{50} of 65 μM suggests that octoclothepin itself will not be a particularly useful tool in studying the signaling of GPR37. The potential utility of octoclothepin as a pharmacological modulator of GPR37 is further reduced by the fact that this compound is known to act as an antagonist and/or inverse agonist at a number of dopamine (Burstein et al., 2005; Campiani et al., 2002), serotonin (Bogeso et al., 1991; Campiani et al., 2002; Roth et al., 1994), histamine (Lim et al., 2005), and α-adrenergic receptor subtypes (Kristensen et al., 2010). Octoclothepin is also a norepinephrine reuptake inhibitor (Liljefors and Bogeso, 1988). However, even though octoclothepin is a non-selective antagonist for many GPCRs, this compound nonetheless represents the first antagonist discovered for GPR37 and may prove useful as a lead compound that could be modified to increase specificity for GPR37 in future work.

We also observed that C18 potentiates GPR37-mediated signaling to NFAT. However, the activity of C18 was not specific for GPR37, as it also potentiated BAI1-mediated signaling to NFAT. Baseline increases in NFAT signaling were not observed when EV-transfected cells are treated with C18, indicating that C18 may act to nonspecifically potentiate GPCR signaling in the NFAT luciferase assay. As discussed in Chapter 1, GPCR-mediated signaling in regulated through several distinct pathways. C18 could act as an inhibitor of GRKs or β-arrestins, thereby decreasing the downregulation of chronically activated GPCRs. Additionally, C18 could exert effects on regulation of G

protein-mediated signaling by guanine nucleotide exchange factors (GEFs). GEFs facilitate the exchange of GDP for GTP during G protein activation, and they can increase the rate of activation by several orders of magnitude (Bos et al., 2007; Murga et al., 1999; Vetter and Wittinghofer, 2001). C18 could potentiate G protein-mediated signaling to NFAT by activating GEFs and accelerating guanine nucleotide exchange during GPCR activation. Finally, G proteins have intrinsic GTPase activity, through which G protein-mediated signaling is terminated. C18 could possibly inhibit GTPase-activating proteins (GAPs) to slow the termination of G protein-mediated signaling. GEFs and GAPs are pharmaceutical targets, particularly in the treatment of cancer (Stephen et al., 2014; Vigil et al., 2010), and so C18 signaling may be of interest in future work in that field. However, based on the data presented in this chapter, our conclusion is that C18 will not be a useful tool for specifically studying GPR37-mediated signaling because of the non-specificity of C18 action.

No effect of MAG co-expression on constitutive GPR37 signaling to NFAT was observed in the experiments shown in this chapter. Thus, the functional significance of the interaction between GPR37 and MAG remains uncertain. The studies shown in Chapter 2 reveal that GPR37 regulates MAG expression, but it is unclear if this regulation is dependent in any way on the interaction of the two proteins. Similarly, it is uncertain if MAG has any effect on GPR37 signaling. Further work in this area could explore potential effects on MAG on GPR37 localization as well as exploring effects of MAG on GPR37 signaling activity in different signaling assays and in different cellular contexts.

In the studies described in this chapter, we found that co-expression of REG4 with GPR37 did not activate GPR37 in either the NFAT luciferase or TGFα shedding assays. Indeed, in the NFAT-luciferase assay, co-transfection of REG2 or REG4 with GPR37 resulted in decreased constitutive signaling of GPR37, but this effect was not seen upon co-culture of cells transfected with GPR37 and either REG2 or REG4 separately. These results suggest that REG2- and REG4-mediated modulation of GPR37 signaling is cell-intrinsic. Further work will be needed to determine whether REG proteins inhibit GPR37 signaling per se or instead impair GPR37 trafficking to the plasma membrane. Also, it will be interesting to elucidate the structural determinants of the GPR37/REG association and perform further studies to shed light on the functional significance of this interaction.

Chapter V: Further Discussion and Future Directions

5.1 GPR37 as a regulator of the myelin-associated glycoprotein MAG

5.1.1 Further discussion: GPR37 regulation of MAG expression

The work presented in this dissertation identifies Mag as a significantly downregulated protein in *Gpr37*$^{-/-}$ mice, indicating that GPR37 regulates MAG expression. Furthermore, we show that there is not a significant difference in *Mag* mRNA expression between WT and *Gpr37*$^{-/-}$ mice, which suggests that this regulation happens at the protein level. One other report of a GPCR, VLGR1, regulating MAG expression *in vivo* was able to recapitulate MAG regulation *in vitro* in transfected cells, which allowed exploration of the mechanism through which MAG is regulated (Shin et al., 2013). However, GPR37-mediated MAG regulation was not recapitulated upon transfection of GPR37 and MAG into HEK-293T cells. It is possible that the regulation of MAG expression by GPR37 is cell-context dependent, and the model system utilized may lack a critical component of the signaling machinery that allows GPR37 to promote MAG protein expression. How this regulation occurs will be the focus of future studies. MAG is known to be regulated in a variety of ways, and GPR37 could potentially impinge on one or several of these known pathways by which MAG is regulated.

One intensively-studied mechanism by which MAG is regulated is via cleavage by matrix metalloproteinases (MMPs) MMP-2, MMP-7, and MMP-9 (Milward et al., 2008). Cleavage at L509 occurs near the transmembrane domain and results in the release of an N-terminal fragment that matches the previously-identified derivative of MAG (dMAG) in size (Tang et al., 2001; Yanagisawa et al., 1985). Both release of dMAG and

increased MMP activity in the CNS are associated with neurological disorders, including MS. The remaining C-terminal fragment of MAG left after MMP cleavage is subsequently internalized and broken down. The activity of MMPs is reduced by tissue inhibitors of metalloproteinases (TIMPs) (Murphy, 2011). GPCRs are known to be capable of regulating both MMPs (Hsieh, 2014; Thornton et al., 2016; Vacas et al., 2016) and TIMPS (Hsiao et al., 2014; Khokha et al., 2013). It is possible that GPR37 promotes MAG stability by positively regulating TIMPS or negatively regulating MMPs, thus preventing MAG cleavage by MMPS (Figure V-1A).

Data presented in this dissertation show that GPR37 coimmunoprecipitates with MAG. The functional significance of this interaction is yet to be determined, but previously identified interacting partners of MAG suggest that GPR37 could be a critical regulator of myelination and myelin stability in its capacity as a MAG-interacting protein. For example, the non-receptor tyrosine kinase Fyn is one of the major identified interacting partners of MAG in oligodendrocytes (Umemori et al., 1994). After MAG antibody crosslinking, specific Fyn activity is increased, suggesting that Fyn acts downstream of MAG activation. Fyn is also known to be critical in the initiation of myelination. However, knockout mice lacking both *Fyn* and *Mag* have a more severe myelination phenotype than either $Mag^{-/-}$ or $Fyn^{-/-}$ mice individually (Biffiger et al., 2000). These results suggest that, although Fyn and MAG can interact in oligodendrocytes, at least some of Fyn's activity occurs independently of MAG; if the two proteins were restricted to the same signaling axis, $Mag^{-/-}$ and $Fyn^{-/-}$ mice should have similar a similar phenotype to the *Mag*/*Fyn* double knockout. Given the possibility for

GPR37 to act as a novel regulator of myelination, the *in vivo* relevance of the GPR37/MAG interaction is likely to be of interest in future exploration of GPR37's potential as a drug target for the treatment of demyelinating diseases.

GPR37 could act as a cis-interacting partner of MAG in oligodendrocytes. MAG typically does not reside in lipid raft fractions of the cell membrane (Taylor et al., 2002; Vinson et al., 2003). However, it is translocated to lipid rafts following antibody crosslinking (Marta et al., 2004). GPR37 is localized to lipid rafts (Lundius et al., 2014), and it is possible that the receptor facilitates MAG translocation to lipid rafts (figure V-1C). This could occur either through GPR37 downstream signaling or physical interaction with MAG. For example, GPCR activation results in activation of various downstream pathways that frequently lead to phosphorylation of proteins. The cytoplasmic tail of L-MAG is phosphorylated *in vitro* and *in vivo* (Bambrick and Braun, 1991; Edwards et al., 1989; Kirchhoff et al., 1993; Yim et al., 1995). This phosphorylation appears to be mediated by PKC and other calcium-dependent kinases. The signaling pathways activated by GPR37 in oligodendrocytes are incompletely characterized, but it is possible that GPR37 activation ultimately leads to phosphorylation of MAG (Figure V-1B).

Whether or not signaling pathways downstream of GPR37 lead to changes in MAG phosphorylation, the physical interaction between GPR37 and MAG could facilitate GPR37-mediated translocation of MAG into lipid rafts (Figure V-1C). Raft-raft interactions between axons and periaxonal membranes of myelinating oligodendrocytes

are known to stabilize axoglial structure and regulate spacing between axons and myelin membranes (Vinson et al., 2003). In particular, lipid raft localization seems to be important for MAG binding to axonal MAG receptors. In addition to facilitating interaction of ligands and receptors on opposing cell membranes, lipid rafts create microenvironments where intracellular signal transduction molecules are closely associated with MAG; this signaling of MAG back into myelinating oligodendrocytes is known to promote oligodendrocyte health and myelin stability. Thus, if GPR37 helps MAG segregate into lipid rafts in the cell membrane, then the interaction of MAG with GPR37 could possibly serve to enhance stability of myelin.

In trans, MAG activates axonal receptors to signal to Rho (Yamashita et al., 2002), facilitate neurofilament phosphorylation (Yin et al., 1998), and regulate the actin cytoskeleton (Filbin, 2006; Quarles, 2007). Given the expression of GPR37 in certain neuronal populations, the receptor could act as a trans-interacting partner of MAG (Figure V-1D). MAG is known to exert sialic acid-dependent (DeBellard et al., 1996; Tang et al., 1997) and sialic acid-independent (Domeniconi et al., 2002; Liu et al., 2002) effects on axons. Given that MAG is likely to have a wide variety of axonal binding partners and GPR37 is localized to lipid rafts, it is possible that MAG interaction with GPR37 could bring it into close contact with signaling molecules necessary for mediating certain effects on axons. This would allow MAG to have selective activity in certain neuronal populations, depending on the presence or absence of GPR37.

Figure V-1. Potential pathways through which GPR37 might regulate MAG expression. A) GPR37 could promote TIMP activity or inhibit MMP activity to reduce MAG cleavage, thereby stabilizing MAG expression levels. B) Signaling downstream of GPR37 could result in MAG phosphorylation. C) Physical association of GPR37 and MAG could result in MAG translocation to lipid rafts. D) GPR37 and MAG could interact in trans across the periaxonal space.

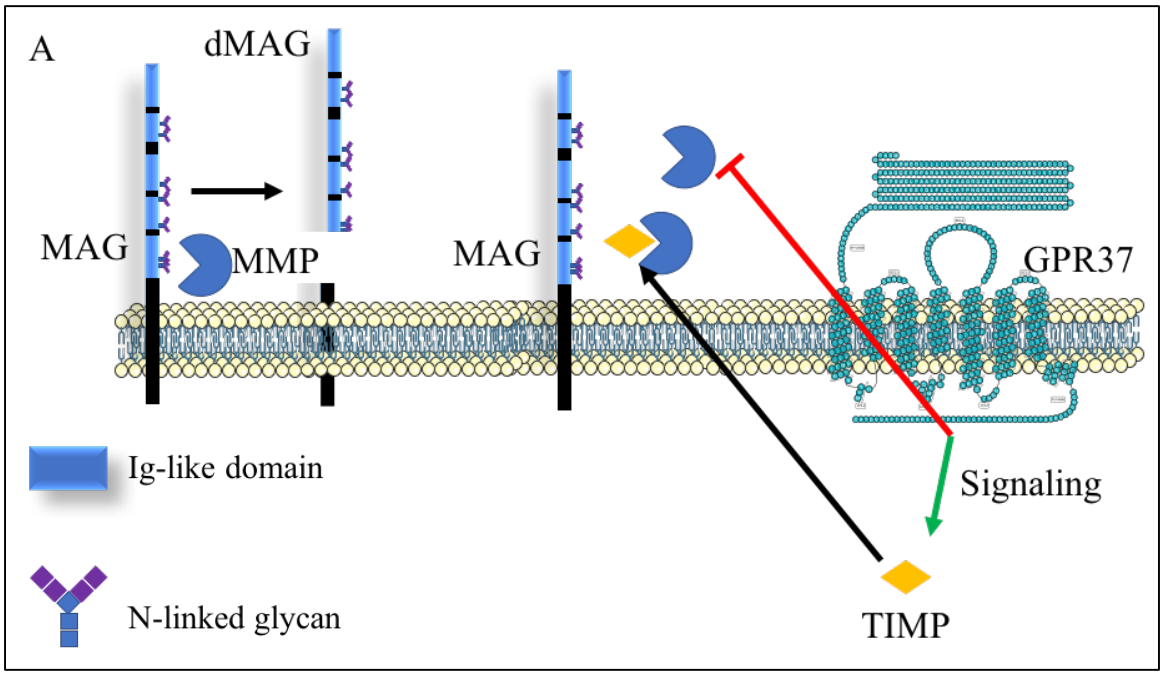
A
dMAG
MAG
MMP
MAG
GPR37
Ig-like domain
Signaling
N-linked glycan
TIMP

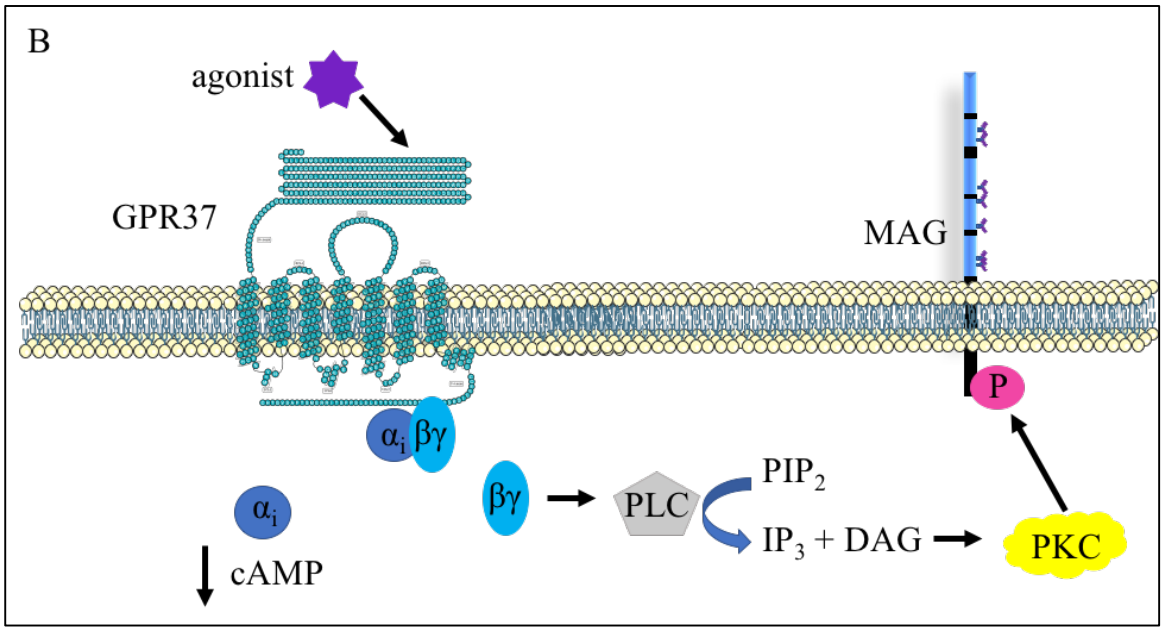
B
agonist
GPR37
MAG
P
αi βγ
βγ
PLC
PIP2
IP3 + DAG
PKC
αi
cAMP

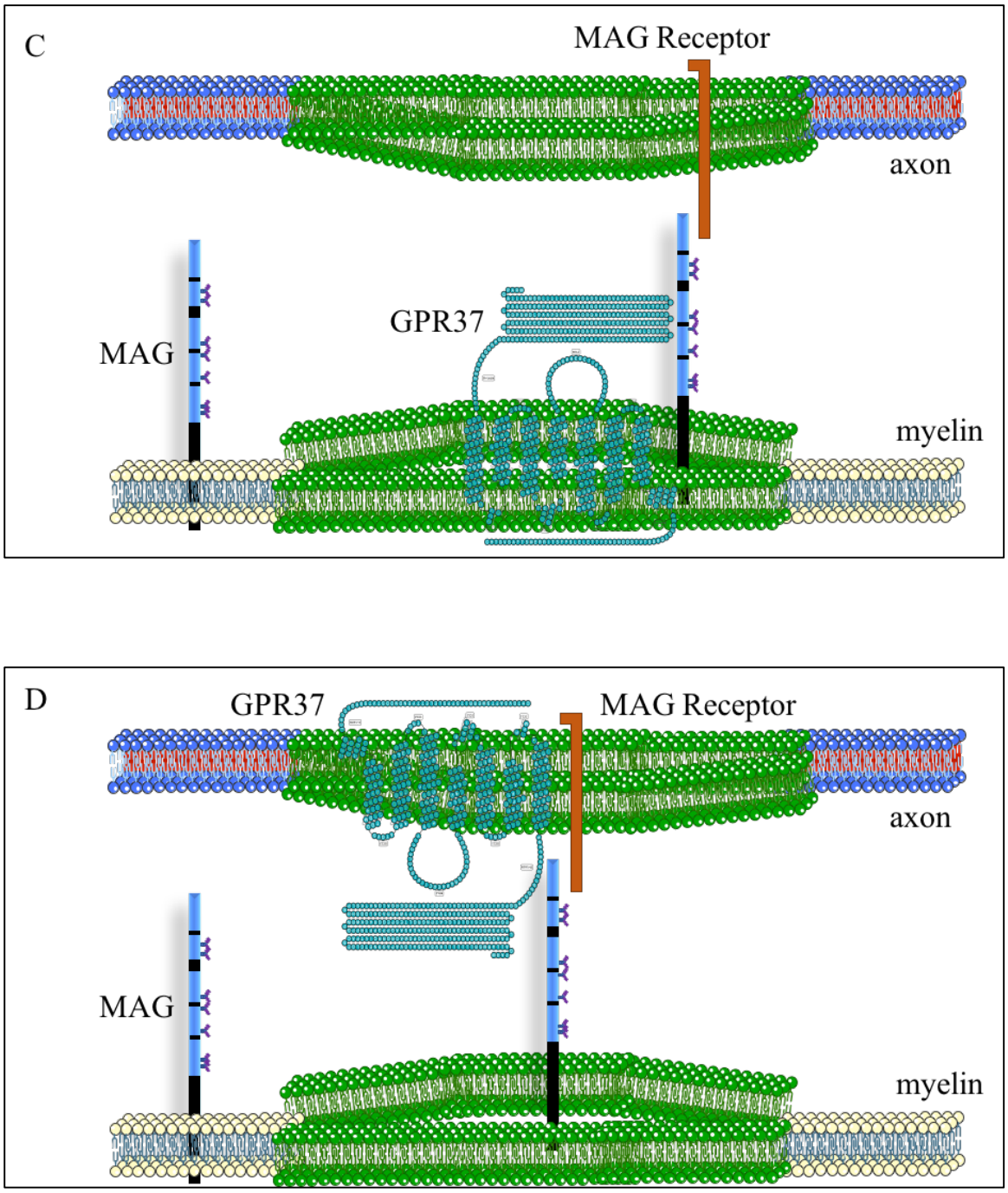
C
MAG Receptor
axon
GPR37
MAG
myelin
D
GPR37
MAG Receptor
axon
MAG
myelin
Ig-like domain
Lipid raft
N-linked glycan

5.1.2 Future directions: GPR37 regulation of MAG expression

This dissertation lays the groundwork for future studies on the mechanism(s) behind and functional significance of GPR37-mediated regulation of MAG expression. The developmental profile of Mag expression in *Gpr37*$^{-/-}$ mice could reveal if timing of Mag expression is disrupted in the *Gpr37*$^{-/-}$ animal model. Results from such studies could provide insight into why GPR37 seems to act as a negative regulator of myelination during development (Yang et al., 2016) but yet data presented in this dissertation suggest that GPR37 stabilizes myelin in the adult brain. Furthermore, viral reintroduction of Mag in *Gpr37*$^{-/-}$ mice in models of disease could confirm if there is a causal link between decreased Mag expression and the phenotype observed in *Gpr37*$^{-/-}$ mice. In addition to the increased susceptibility to demyelination presented in this dissertation, *Gpr37*$^{-/-}$ mice also have increased susceptibility to seizure models (Giddens, 2017) (*in submission*). Loss of MAG is also associated with increased susceptibility to brain insults beyond demyelination, for example excitotoxicity (Lopez et al., 2011; Mehta et al., 2010; Schnaar and Lopez, 2009).

Because of the potential relevance to the etiology of multiple neurological disorders, understanding the mechanism(s) by which GPR37 regulates MAG expression is an important future direction. Addressing this question will likely require studies on primary cultures and/or *in vivo* experiments, as it seems that HEK cells lack some fundamental part of the cellular machinery required for Gpr37 to regulate Mag. Oli-neu cells (Jung et al., 1995) and CG4 (Louis et al., 1992) cells are also possible cell lines for exploring this question. Myelin mutant animals resulting from dysregulated Mag exhibit

issues such as irregular glycosylation (Bartoszewicz et al., 1995), increased endocytosis and decreased production of Mag (Bo et al., 1995), increased proteasomal degradation of Mag (Shin et al., 2013), and mislocalization of OPCs during development (Myers et al., 2016). Identification of the mechanisms underlying GPR37 regulation of MAG expression will illuminate a previously undefined aspect of GPR37 signaling and provide direction for future efforts aimed at pharmacologically targeting GPR37 in the treatment of human disease.

5.2 GPR37-mediated protection against demyelination

5.2.1 Further discussion: Gpr37$^{-/-}$ mice are more susceptible to cuprizone-induced demyelination

GPR37 is highly expressed in oligodendrocytes (Cahoy et al., 2008; Imai et al., 2001; Yang et al., 2016), and data presented in this dissertation show that expression of Mag is significantly decreased in *Gpr37*$^{-/-}$ mice. Furthermore, mice deficient in Mag show mild perturbations in myelination (Li et al., 1994; Montag et al., 1994) that are enhanced upon exposure to injury and demyelinating toxins (Jones et al., 2013; Lassmann et al., 1997; Lopez et al., 2011). Mag expression is selectively lost in early lesions in human demyelinating disease (Rodriguez and Scheithauer, 1994), and many cases of demyelination in humans begin with dying-back oligodendrogliopathy (Lucchinetti et al., 2000), which is a common myelination feature in Mag-deficient mice. *Gpr37*$^{-/-}$ mice have been previously reported to display precocious myelination during development and slightly thicker myelin sheaths compared to WT mice (Yang et al., 2016), leading to the

conclusion that GPR37 is a negative regulator of myelination. However, no previously published work has explored the phenotype of *Gpr37*$^{-/-}$ mice under demyelinating conditions. Given the evidence that GPR37 negatively regulates the myelin-stabilizing MAG, we tested the hypothesis that *Gpr37*$^{-/-}$ mice would be more susceptible to cuprizone-induced demyelination than WT mice.

Cuprizone is a copper chelator that selectively induces apoptosis in oligodendrocytes and results in reliable demyelination in the corpus callosum (Kipp et al., 2016; Skripuletz et al., 2011), with few peripheral side effects at demyelinating doses. Furthermore, cuprizone toxicity is a non-T cell-mediated model of demyelination, which would allow us to focus on the role of GPR37 in demyelination without having to consider contributions or variability arising from immune system involvement. Mice of the C57/Bl6 background, on which the *Gpr37*$^{-/-}$ mice were bred, are particularly susceptible to cuprizone-induced demyelination (Skripuletz et al., 2008). Finally, withdrawal of cuprizone treatment following demyelination results in consistent remyelination.

Here, we report that *Gpr37*$^{-/-}$ mice displayed more extensive demyelination than WT mice in the cuprizone model of demyelination. Although significant differences in extent of myelination were observed between *Gpr37*$^{-/-}$ mice and WT mice at the beginning of the remyelination phase, the interpretation of data from this phase is complicated by the fact that WT mice did not reach complete demyelination during the study. Furthermore, the cuprizone paradigm is theoretically divided into discrete

demyelination and remyelination phases. However spontaneous remyelination also occurs during the first phase, while cuprizone is still being administered. Therefore, we were unable to determine conclusively if loss of Gpr37 resulted in changes in remyelination capacity.

Additionally, we found that *Gpr37*$^{-/-}$ mice did not exhibit differences in density of OPCs or mature oligodendrocytes at any time point during cuprizone-induced demyelination and subsequent remyelination. Taken together, these data suggest that GPR37 contributes to myelin stability per se, rather than exerting cytoprotective effects on oligodendrocytes or OPCs that result in stabilized myelin, expanding our understanding of the role of GPR37 in oligodendroglial biology. Further experiments will be needed to further explore the mechanism through which GPR37 stabilizes myelin and to establish what role, if any, GPR37 plays in remyelination.

Figure V-2. Potential model of GPR37 contribution to myelin stability. A) GPR37 regulates MAG expression (Chapter 2) and can increase ERK phosphorylation *(Meyer et al., 2013)*. It is possible that these and/or other yet to be identified downstream signaling pathways contribute to the maintenance of myelin sheaths under demyelinating conditions. B) The data presented in this dissertation suggest that loss of GPR37 increases susceptibility of axons to demyelinating attack. The mechanism through which this occurs will be the focus of future work.

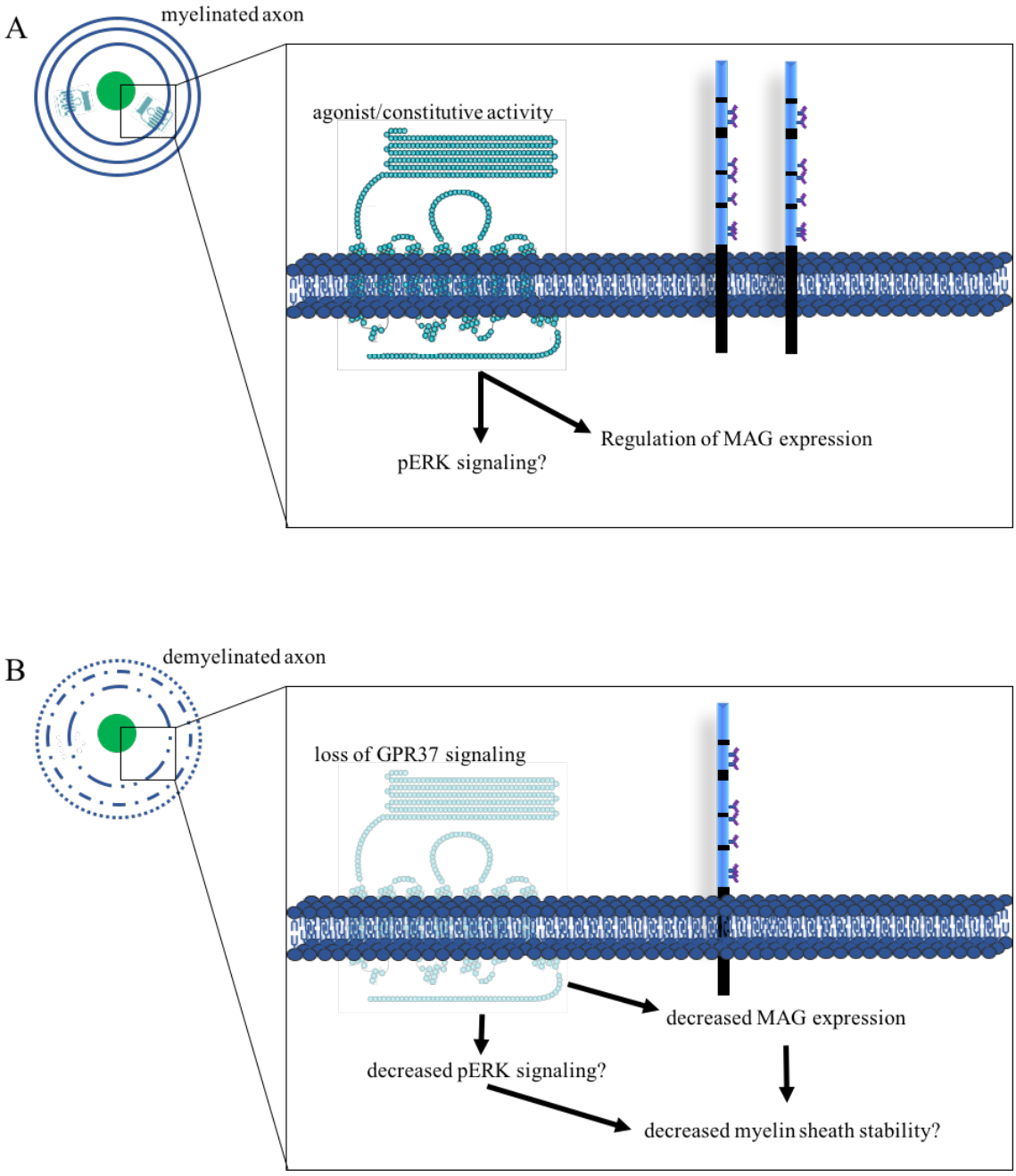
A
myelinated axon
agonist/constitutive activity
pERK signaling?
Regulation of MAG expression
B
demyelinated axon
loss of GPR37 signaling
decreased MAG expression
decreased pERK signaling?
decreased myelin sheath stability?

5.2.2 Future directions: GPR37-mediated protection against demyelination

The potential role of GPR37 in the process of remyelination is of interest to study further for two main reasons: (1) such studies would shed light on the role of GPR37 in oligodendroglial biology, given the apparent conflict between GPR37 activity as a negative regulator of differentiation and a stabilizer of myelin and (2) drug targets that are involved in remyelination are highly attractive for the treatment of demyelinating diseases like MS. To assess differences in remyelination capacity between WT and *Gpr37*$^{-/-}$ mice, complete demyelination would need to be achieved for both genotypes. More complete demyelination can be achieved by extending the timeline of cuprizone treatment (Skripuletz et al., 2008). However, extended treatment with cuprizone can result in axonal degeneration, which would add another complication in interpreting the remyelination data. The mammalian target of rapamycin (mTOR) signaling pathway has been implicated in stabilizing myelin and promoting remyelination (Sachs et al., 2014). Furthermore, treatment with rapamycin augments cuprizone toxicity to achieve more complete demyelination in shorter amounts of time. Rapamycin treatment could be added to future cuprizone studies involving *Gpr37*$^{-/-}$ mice to more definitively establish the effect of knocking out Gpr37 on remyelination.

Despite the advantages of the cuprizone model in studying demyelination and remyelination, it fails to fully recapitulate the features physiological demyelination observed in MS. Thus, future studies could complement the cuprizone data by using an inflammatory model of demyelination, such as experimental autoimmune encephalomyelitis (EAE). In EAE, mice develop clinical features of demyelination, such

as hind limb paralysis, that are not seen in cuprizone-induced demyelination (Denic et al., 2011). Demyelination is also observed in disparate brain regions and the spinal cord in EAE, a feature present in MS.

In addition to using complementary models of demyelination to confirm the conclusion that GPR37 protects against demyelination, another important unanswered question is whether the loss of GPR37 in oligodendrocytes specifically increases myelin stability. GPR37 is known to be expressed in other glia and certain neuronal populations. While evidence for a protective role of GPR37 is dependent on cell context, it is known that GPR37 is protective in other cell types (Lundius et al., 2013; Lundius et al., 2014; Meyer et al., 2013). Furthermore, other cells in the brain affect cuprizone-induced toxicity. Astrocytes and microglia are activated during cuprizone administration (Groebe et al., 2009; Skripuletz et al., 2013). Additionally, demyelination can occur secondary to axonal degeneration. Conditional knockout mice that lack Gpr37 in different cell types in the brain can be used in the future to identify which cell type is relevant in Gpr37-mediated protection against cuprizone-induced demyelination. For example, since GPR37 is known to be expressed in certain neuronal populations, it will be important to determine whether expression of GPR37 in axons contributes to the stability of the myelin sheath. Finally, the future identification of small molecule GPR37 agonists would allow for validation of GPR37 as a drug target in the treatment of MS.

5.3 Signaling modulators of GPR37

5.3.1 Further discussion: signaling modulators of GPR37

A challenge in fully understanding the mechanism(s) through which GPR37 mediates its myelin-stabilizing effects is the lack of a widely-accepted endogenous agonist. Activation by the putative ligands HA (Gandia et al., 2013; Rezgaoui et al., 2006) and prosaptide (Lundius et al., 2014; Meyer et al., 2013) is modest and inconsistent across cell types. In fact, neither putative ligand could be confirmed in oligodendrocytes (Yang et al., 2016). We sought to work around the lack of a definitive endogenous ligand by identifying small molecules and interacting partners that modulate GPR37 signaling. To that end, we completed a high throughput drug screen and tested several recently identified GPR37 interacting partners in signaling assays. We chose dynamic mass redistribution (DMR), a pathway-independent method, for the high throughput screen, because the signaling pathways activated downstream of GPR37 are not completely characterized.

We identified octoclothepin maleate as a low-affinity inverse agonist of constitutive GPR37 signaling to NFAT. While octoclothepin reliably attenuated GPR37 signaling to NFAT, an IC_{50} of 65 μM was observed. This affinity constant is much higher than the IC_{50} of octoclothepin for any of its other many targets (Bogeso et al., 1991; Burstein et al., 2005; Campiani et al., 2002; Kristensen et al., 2010; Liljefors and Bogeso, 1988; Lim et al., 2005; Roth et al., 1994). From this, we conclude that octoclothepin is unlikely to be useful as a tool to selectively study GPR37 signaling *in vitro* or for manipulation of GPR37 signaling *in vivo,* although the possibility exists that

octoclothepin could serve as a lead compound to develop more selective and higher-affinity GPR37 antagonists.

Another compound, (5HD[1,2,4]triazino[5,6Db]indolD3Dylthio)acetamide (C18), was identified in the screen as an activator of GPR37. However, C18 also potentiated signaling of BAI1, a distantly-related GPCR, in secondary assays. From this, we concluded that C18 is a general potentiator of GPCR-mediated signaling. The multistep process of GPCR signal initiation and termination presents several mechanisms through which C18 could potentiate signaling. For example, C18 could inhibit GTPase activating proteins (GAPs) to prolong GPCR signaling. This possibility could be assessed using fluorescence-based GTPase activity assays (Willard et al., 2005). Another potential target of C18 is β-arrestin-mediated receptor internalization. Fluorescence-based β-arrestin mobilization assays could be used to determine if C18 inhibits β-arrestin recruitment to GPCRs, resulting in inhibited termination of GPCR-mediated signaling. Further characterization of the mechanism of action of C18 may reveal a more specific utility for the compound as a pharmacological tool than was determined by these studies.

Earlier in this chapter, the interaction of MAG with GPR37 was discussed in terms of the potential impact of this association on MAG function. Given that MAG is known to be part of a bidirectional signaling complex, we also tested the possibility that MAG co-expression might modulate GPR37 signaling. However, we found that MAG did not alter constitutive GPR37 signaling to NFAT. It is possible that MAG regulates GPR37-mediated signaling to other pathways, such as pERK, and it is also possible that

MAG association with GPR37 has no effect on the receptor's signaling. Further studies will be needed to conclusively determine whether MAG modulates GPR37 signaling activity.

We also tested whether regenerating islet-derived family members 2 (REG2) and 4 (REG4) could activate GPR37. REG2 is expressed in the brain, is secreted after injury (Averill et al., 2002; Livesey et al., 1997), and is closely related to REG4, which was recently suggested to be capable of activating GPR37 (Wang et al., 2016). Furthermore, mice lacking Reg2 exhibit myelination deficits (Tebar et al., 2008). If indeed REG2 could activate GPR37 signaling, the known involvement of this protein in myelination would be tantalizing. However, we found that both REG2 and REG4 co-expression attenuated constitutive GPR37 signaling. Further work will be needed to ascertain whether this regulation reflects an effect on receptor trafficking or signaling, or conversely reflects an effect on signaling pathways downstream of GPR37.

In sum, our efforts to identify either small molecules or endogenous interacting partners that could activate GPR37 resulted in the identification of three inhibitors of constitutive GPR37 signaling. Efforts to identify small molecule agonists of GPR37 and refine some of the inhibitors identified here are ongoing.

5.3.2 Future directions: Small molecule ligands for GPR37

While high throughput screening is a common and often successful method for identifying agonists of GPCRs, novel strategies are emerging for virtually screening

receptors (Kumari et al., 2015). These methods depend on knowledge of three-dimensional structures or receptor-ligand pairs. At present, no crystal structures are available for GPR37. However, efforts have been made based on primary sequence to predict ligands that might bind to the closely-related receptor GPR37L1 (Ngo et al., 2017). Several small molecule ligands were identified via this approach, but these ligands were all found to be antagonists (Ngo et al., 2017).

The study of heteromeric receptor complexes has expanded drug targets in GPCR signaling systems (Fuxe et al., 2014; George et al., 2002). Many GPCRs are believed to exist in a monomer-dimer equilibrium (Gurevich and Gurevich, 2008b; Lambert, 2010), except for class C receptors, which are believed to exist as more stable dimers (Gurevich and Gurevich, 2008a). It is becoming increasingly apparent that most signaling molecules exist as members of larger complexes or signaling structures, highlighting the importance of taking a signaling system-wide approach in developing pharmaceuticals targeted at GPCRs. For example, multivalent agonists of receptors have shown increased affinity for the desired receptors compared to monovalent agonists (Halazy et al., 1996; Perez et al., 1998). Furthermore, agonists targeting certain opioid dimers over others have been shown to increase opiate analgesia without increasing tolerance (Daniels et al., 2005; George et al., 2000; Gomes et al., 2004). This evidence suggests that understanding all members of the signaling complex and developing agonists selectively targeted at all members of that complex can significantly improve clinical outcomes.

Because GPR37 signaling has been implicated in several different disease states, it may be beneficial to focus future efforts in small molecule agonist development at creating multivalent ligands that might target GPR37 in complex with a disease-specific interacting partner, like MAG. This approach could be particularly important for targets like GPR37. While we show here that GPR37 protects against demyelination, other reports indicate that GPR37 over-expression is deleterious and can cause cytotoxicity due to protein misfolding and endoplasmic reticulum stress (Imai et al., 2002; Imai et al., 2001; Marazziti et al., 2009; Omura et al., 2006; Yang et al., 2003; Zeng et al., 1997). The development of agonists that target the GPR37/MAG signaling complex could possibly promote myelin-protective GPR37 signaling while avoiding GPR37 signaling in dopaminergic neurons or other cell populations where the activity of the receptor might be less desirable.

Another method for achieving specific modulation of signaling is through the development of biased agonists. Such agonists allow for the selective activation of one signaling pathway downstream of a receptor over other pathways (Fisher et al., 1993; Gurwitz et al., 1994; Reiter et al., 2017). GPR37 has been shown to couple to $G\alpha_i$, resulting in inhibition of cAMP formation (Meyer et al., 2013). Increased pERK signaling has also been identified downstream of GPR37, which could be the result of β-arrestin mediated signaling, rather than G protein-mediated signaling. Activation of the MEK/ERK signaling pathway has been implicated in oligodendrocyte process extension and myelination (Gaesser and Fyffe-Maricich, 2016). However, further work will be

required to determine the downstream signaling pathway relevant to GPR37-mediated protection against demyelination.

5.4 Concluding remarks

The work described in this dissertation provides new knowledge concerning GPR37 regulation of myelin proteins and demyelination. We also describe GPR37-mediated activation of a previously unreported downstream signaling pathway and identify novel inhibitors of GPR37 signaling. Prior to this work, little was known about the role of GPR37 in oligodendroglial biology, as most previous reports focused on GPR37-mediated effects on dopaminergic signaling and parkinsonism. During the course of the studies presented here, a paper was published demonstrating a role for GPR37 as a negative regulator of oligodendrocyte differentiation during development (Yang et al., 2016). This study represents a useful complement to the studies described in this dissertation, as the work presented here focused on the role of GPR37 in adult mice, rather than development, and also focused on the role of GPR37 in response to a demyelinating insult, rather than under normal conditions.

In conclusion, the work presented here identifies GPR37 as a novel regulator of MAG expression and an interacting partner of MAG. Furthermore, this work has advanced the understanding of the role played by GPR37 in myelin maintenance by demonstrating that loss of GPR37 increases susceptibility to demyelination. Thus, the results described in this dissertation provide new insights into the fundamental biology of

GPR37. These findings may prove useful in the future therapeutic targeting of GPR37 for the treatment of neurological disorders, especially myelination disorders such as multiple sclerosis.

References

Adler, E., Hoon, M. A., Mueller, K. L., Chandrashekar, J., Ryba, N. J., Zuker, C. S., 2000. A novel family of mammalian taste receptors. Cell. 100**,** 693-702.

Ahmad, R., Wojciech, S., Jockers, R., 2015. Hunting for the function of orphan GPCRs - beyond the search for the endogenous ligand. Br J Pharmacol. 172**,** 3212-28.

Alexander, S. P., Davenport, A. P., Kelly, E., Marrion, N., Peters, J. A., Benson, H. E., Faccenda, E., Pawson, A. J., Sharman, J. L., Southan, C., Davies, J. A., Collaborators, C., 2015. The Concise Guide to PHARMACOLOGY 2015/16: G protein-coupled receptors. Br J Pharmacol. 172**,** 5744-869.

Arac, D., Boucard, A. A., Bolliger, M. F., Nguyen, J., Soltis, S. M., Sudhof, T. C., Brunger, A. T., 2012. A novel evolutionarily conserved domain of cell-adhesion GPCRs mediates autoproteolysis. EMBO J. 31**,** 1364-78.

Arroyo, E. J., Scherer, S. S., 2000. On the molecular architecture of myelinated fibers. Histochem Cell Biol. 113**,** 1-18.

Attramadal, H., Arriza, J. L., Aoki, C., Dawson, T. M., Codina, J., Kwatra, M. M., Snyder, S. H., Caron, M. G., Lefkowitz, R. J., 1992. Beta-arrestin2, a novel member of the arrestin/beta-arrestin gene family. J Biol Chem. 267**,** 17882-90.

Attwood, T. K., Findlay, J. B., 1994. Fingerprinting G-protein-coupled receptors. Protein Eng. 7**,** 195-203.

Aube, B., Levesque, S. A., Pare, A., Chamma, E., Kebir, H., Gorina, R., Lecuyer, M. A., Alvarez, J. I., De Koninck, Y., Engelhardt, B., Prat, A., Cote, D., Lacroix, S., 2014. Neutrophils mediate blood-spinal cord barrier disruption in demyelinating neuroinflammatory diseases. J Immunol. 193**,** 2438-54.

Averill, S., Davis, D. R., Shortland, P. J., Priestley, J. V., Hunt, S. P., 2002. Dynamic pattern of reg-2 expression in rat sensory neurons after peripheral nerve injury. J Neurosci. 22**,** 7493-501.

Baldwin, J. M., 1994. Structure and function of receptors coupled to G proteins. Curr Opin Cell Biol. 6**,** 180-90.

Bambrick, L. L., Braun, P. E., 1991. Phosphorylation of myelin-associated glycoprotein in cultured oligodendrocytes. Dev Neurosci. 13**,** 412-6.

Barnabe-Heider, F., Goritz, C., Sabelstrom, H., Takebayashi, H., Pfrieger, F. W., Meletis, K., Frisen, J., 2010. Origin of new glial cells in intact and injured adult spinal cord. Cell Stem Cell. 7**,** 470-82.

Bartoli, C., Baeza, N., Figarella, C., Pellegrini, I., Figarella-Branger, D., 1998. Expression of peptide-23/pancreatitis-associated protein and Reg genes in human pituitary and adenomas: comparison with other fetal and adult human tissues. J Clin Endocrinol Metab. 83**,** 4041-6.

Bartoszewicz, Z. P., Noronha, A. B., Fujita, N., Sato, S., Bo, L., Trapp, B. D., Quarles, R. H., 1995. Abnormal expression and glycosylation of the large and small isoforms of myelin-associated glycoprotein in dysmyelinating quaking mutants. J Neurosci Res. 41**,** 27-38.

Batoulis, H., Recks, M. S., Addicks, K., Kuerten, S., 2011. Experimental autoimmune encephalomyelitis--achievements and prospective advances. APMIS. 119**,** 819-30.

Baumann, N., Pham-Dinh, D., 2001. Biology of oligodendrocyte and myelin in the mammalian central nervous system. Physiol Rev. 81**,** 871-927.

Bean, B. P., 2007. The action potential in mammalian central neurons. Nat Rev Neurosci. 8**,** 451-65.

Benovic, J. L., Pike, L. J., Cerione, R. A., Staniszewski, C., Yoshimasa, T., Codina, J., Caron, M. G., Lefkowitz, R. J., 1985. Phosphorylation of the mammalian beta-adrenergic receptor by cyclic AMP-dependent protein kinase. Regulation of the rate of receptor phosphorylation and dephosphorylation by agonist occupancy and effects on coupling of the receptor to the stimulatory guanine nucleotide regulatory protein. J Biol Chem. 260**,** 7094-101.

Bercury, K. K., Macklin, W. B., 2015. Dynamics and mechanisms of CNS myelination. Dev Cell. 32**,** 447-58.

Biffiger, K., Bartsch, S., Montag, D., Aguzzi, A., Schachner, M., Bartsch, U., 2000. Severe hypomyelination of the murine CNS in the absence of myelin-associated glycoprotein and fyn tyrosine kinase. J Neurosci. 20**,** 7430-7.

Bjarnadottir, T. K., Fredriksson, R., Schioth, H. B., 2005. The gene repertoire and the common evolutionary history of glutamate, pheromone (V2R), taste(1) and other related G protein-coupled receptors. Gene. 362**,** 70-84.

Bjarnadottir, T. K., Gloriam, D. E., Hellstrand, S. H., Kristiansson, H., Fredriksson, R., Schioth, H. B., 2006. Comprehensive repertoire and phylogenetic analysis of the G protein-coupled receptors in human and mouse. Genomics. 88**,** 263-73.

Blakemore, W. F., 1974. Pattern of remyelination in the CNS. Nature. 249**,** 577-8.

Bo, L., Quarles, R. H., Fujita, N., Bartoszewicz, Z., Sato, S., Trapp, B. D., 1995. Endocytic depletion of L-MAG from CNS myelin in quaking mice. J Cell Biol. 131**,** 1811-20.

Bockaert, J., Pin, J. P., 1999. Molecular tinkering of G protein-coupled receptors: an evolutionary success. EMBO J. 18**,** 1723-9.

Bodenmuller, H., Schaller, H. C., 1981. Conserved amino acid sequence of a neuropeptide, the head activator, from coelenterates to humans. Nature. 293**,** 579-80.

Bogeso, K. P., Liljefors, T., Arnt, J., Hyttel, J., Pedersen, H., 1991. Octoclothepin enantiomers. A reinvestigation of their biochemical and pharmacological activity in relation to a new receptor-interaction model for dopamine D-2 receptor antagonists. J Med Chem. 34**,** 2023-30.

Bos, J. L., Rehmann, H., Wittinghofer, A., 2007. GEFs and GAPs: critical elements in the control of small G proteins. Cell. 129**,** 865-77.

Boulanger, J. J., Messier, C., 2014. From precursors to myelinating oligodendrocytes: contribution of intrinsic and extrinsic factors to white matter plasticity in the adult brain. Neuroscience. 269**,** 343-66.

Bourne, H. R., Sanders, D. A., McCormick, F., 1990. The GTPase superfamily: a conserved switch for diverse cell functions. Nature. 348**,** 125-32.

Breer, H., Boekhoff, I., Tareilus, E., 1990. Rapid kinetics of second messenger formation in olfactory transduction. Nature. 345**,** 65-8.

Bronnum-Hansen, H., Koch-Henriksen, N., Stenager, E., 2004. Trends in survival and cause of death in Danish patients with multiple sclerosis. Brain. 127**,** 844-50.

Bunge, R. P., 1968. Glial cells and the central myelin sheath. Physiol Rev. 48**,** 197-251.

Burstein, E. S., Ma, J., Wong, S., Gao, Y., Pham, E., Knapp, A. E., Nash, N. R., Olsson, R., Davis, R. E., Hacksell, U., Weiner, D. M., Brann, M. R., 2005. Intrinsic

efficacy of antipsychotics at human D2, D3, and D4 dopamine receptors: identification of the clozapine metabolite N-desmethylclozapine as a D2/D3 partial agonist. J Pharmacol Exp Ther. 315**,** 1278-87.

Cahoy, J. D., Emery, B., Kaushal, A., Foo, L. C., Zamanian, J. L., Christopherson, K. S., Xing, Y., Lubischer, J. L., Krieg, P. A., Krupenko, S. A., Thompson, W. J., Barres, B. A., 2008. A transcriptome database for astrocytes, neurons, and oligodendrocytes: a new resource for understanding brain development and function. The Journal of neuroscience : the official journal of the Society for Neuroscience. 28**,** 264-78.

Campiani, G., Butini, S., Gemma, S., Nacci, V., Fattorusso, C., Catalanotti, B., Giorgi, G., Cagnotto, A., Goegan, M., Mennini, T., Minetti, P., Di Cesare, M. A., Mastroianni, D., Scafetta, N., Galletti, B., Stasi, M. A., Castorina, M., Pacifici, L., Ghirardi, O., Tinti, O., Carminati, P., 2002. Pyrrolo[1,3]benzothiazepine-based atypical antipsychotic agents. Synthesis, structure-activity relationship, molecular modeling, and biological studies. J Med Chem. 45**,** 344-59.

Cerione, R. A., Sibley, D. R., Codina, J., Benovic, J. L., Winslow, J., Neer, E. J., Birnbaumer, L., Caron, M. G., Lefkowitz, R. J., 1984. Reconstitution of a hormone-sensitive adenylate cyclase system. The pure beta-adrenergic receptor and guanine nucleotide regulatory protein confer hormone responsiveness on the resolved catalytic unit. J Biol Chem. 259**,** 9979-82.

Cerione, R. A., Strulovici, B., Benovic, J. L., Lefkowitz, R. J., Caron, M. G., 1983. Pure beta-adrenergic receptor: the single polypeptide confers catecholamine responsiveness to adenylate cyclase. Nature. 306**,** 562-6.

Chen, Y., Wu, H., Wang, S., Koito, H., Li, J., Ye, F., Hoang, J., Escobar, S. S., Gow, A., Arnett, H. A., Trapp, B. D., Karandikar, N. J., Hsieh, J., Lu, Q. R., 2009. The oligodendrocyte-specific G protein-coupled receptor GPR17 is a cell-intrinsic timer of myelination. Nat Neurosci. 12**,** 1398-406.

Chong, S. Y., Rosenberg, S. S., Fancy, S. P., Zhao, C., Shen, Y. A., Hahn, A. T., McGee, A. W., Xu, X., Zheng, B., Zhang, L. I., Rowitch, D. H., Franklin, R. J., Lu, Q. R., Chan, J. R., 2012. Neurite outgrowth inhibitor Nogo-A establishes spatial segregation and extent of oligodendrocyte myelination. Proc Natl Acad Sci U S A. 109**,** 1299-304.

Clark, A. J., 1933. The mode of action of drugs on cells. Edward Arnold, London.

Coleman, J. L., Ngo, T., Schmidt, J., Mrad, N., Liew, C. K., Jones, N. M., Graham, R. M., Smith, N. J., 2016. Metalloprotease cleavage of the N terminus of the orphan G protein-coupled receptor GPR37L1 reduces its constitutive activity. Sci Signal. 9**,** ra36.

Compston, A., Coles, A., 2008. Multiple sclerosis. Lancet. 372**,** 1502-17.

Congreve, M., Langmead, C. J., Mason, J. S., Marshall, F. H., 2011. Progress in structure based drug design for G protein-coupled receptors. J Med Chem. 54**,** 4283-311.

Costa, T., Herz, A., 1989. Antagonists with negative intrinsic activity at delta opioid receptors coupled to GTP-binding proteins. Proc Natl Acad Sci U S A. 86**,** 7321-5.

Daniels, D. J., Kulkarni, A., Xie, Z., Bhushan, R. G., Portoghese, P. S., 2005. A bivalent ligand (KDAN-18) containing delta-antagonist and kappa-agonist

pharmacophores bridges delta2 and kappa1 opioid receptor phenotypes. J Med Chem. 48**,** 1713-6.

De Lean, A., Stadel, J. M., Lefkowitz, R. J., 1980. A ternary complex model explains the agonist-specific binding properties of the adenylate cyclase-coupled beta-adrenergic receptor. J Biol Chem. 255**,** 7108-17.

DeBellard, M. E., Tang, S., Mukhopadhyay, G., Shen, Y. J., Filbin, M. T., 1996. Myelin-associated glycoprotein inhibits axonal regeneration from a variety of neurons via interaction with a sialoglycoprotein. Mol Cell Neurosci. 7**,** 89-101.

Denic, A., Johnson, A. J., Bieber, A. J., Warrington, A. E., Rodriguez, M., Pirko, I., 2011. The relevance of animal models in multiple sclerosis research. Pathophysiology. 18**,** 21-9.

Deshmukh, V. A., Tardif, V., Lyssiotis, C. A., Green, C. C., Kerman, B., Kim, H. J., Padmanabhan, K., Swoboda, J. G., Ahmad, I., Kondo, T., Gage, F. H., Theofilopoulos, A. N., Lawson, B. R., Schultz, P. G., Lairson, L. L., 2013. A regenerative approach to the treatment of multiple sclerosis. Nature. 502**,** 327-32.

Dixon, R. A., Kobilka, B. K., Strader, D. J., Benovic, J. L., Dohlman, H. G., Frielle, T., Bolanowski, M. A., Bennett, C. D., Rands, E., Diehl, R. E., Mumford, R. A., Slater, E. E., Sigal, I. S., Caron, M. G., Lefkowitz, R. J., Strader, C. D., 1986. Cloning of the gene and cDNA for mammalian beta-adrenergic receptor and homology with rhodopsin. Nature. 321**,** 75-9.

Dohlman, H. G., Thorner, J., Caron, M. G., Lefkowitz, R. J., 1991. Model systems for the study of seven-transmembrane-segment receptors. Annu Rev Biochem. 60**,** 653-88.

Domeniconi, M., Cao, Z., Spencer, T., Sivasankaran, R., Wang, K., Nikulina, E., Kimura, N., Cai, H., Deng, K., Gao, Y., He, Z., Filbin, M., 2002. Myelin-associated glycoprotein interacts with the Nogo66 receptor to inhibit neurite outgrowth. Neuron. 35**,** 283-90.

Dong, M., Pinon, D. I., Cox, R. F., Miller, L. J., 2004. Importance of the amino terminus in secretin family G protein-coupled receptors. Intrinsic photoaffinity labeling establishes initial docking constraints for the calcitonin receptor. J Biol Chem. 279**,** 1167-75.

Donohue, P. J., Shapira, H., Mantey, S. A., Hampton, L. L., Jensen, R. T., Battey, J. F., 1998. A human gene encodes a putative G protein-coupled receptor highly expressed in the central nervous system. Brain Res Mol Brain Res. 54**,** 152-60.

Du, C., Duan, Y., Wei, W., Cai, Y., Chai, H., Lv, J., Du, X., Zhu, J., Xie, X., 2016. Kappa opioid receptor activation alleviates experimental autoimmune encephalomyelitis and promotes oligodendrocyte-mediated remyelination. Nat Commun. 7**,** 11120.

Dunham, J. H., Meyer, R. C., Garcia, E. L., Hall, R. A., 2009. GPR37 surface expression enhancement via N-terminal truncation or protein-protein interactions. Biochemistry. 48**,** 10286-97.

Ebers, G., 2013. Interactions of environment and genes in multiple sclerosis. J Neurol Sci. 334**,** 161-3.

Edwards, A. M., Braun, P. E., Bell, J. C., 1989. Phosphorylation of myelin-associated glycoprotein in vivo and in vitro occurs only in the cytoplasmic domain of the large isoform. J Neurochem. 52**,** 317-20.

Fancy, S. P., Baranzini, S. E., Zhao, C., Yuk, D. I., Irvine, K. A., Kaing, S., Sanai, N., Franklin, R. J., Rowitch, D. H., 2009. Dysregulation of the Wnt pathway inhibits timely myelination and remyelination in the mammalian CNS. Genes Dev. 23**,** 1571-85.

Fancy, S. P., Harrington, E. P., Baranzini, S. E., Silbereis, J. C., Shiow, L. R., Yuen, T. J., Huang, E. J., Lomvardas, S., Rowitch, D. H., 2014. Parallel states of pathological Wnt signaling in neonatal brain injury and colon cancer. Nat Neurosci. 17**,** 506-12.

Fanning, A. S., Anderson, J. M., 1999. PDZ domains: fundamental building blocks in the organization of protein complexes at the plasma membrane. J Clin Invest. 103**,** 767-72.

Felts, P. A., Woolston, A. M., Fernando, H. B., Asquith, S., Gregson, N. A., Mizzi, O. J., Smith, K. J., 2005. Inflammation and primary demyelination induced by the intraspinal injection of lipopolysaccharide. Brain. 128**,** 1649-66.

Ferguson, S. S., Downey, W. E., 3rd, Colapietro, A. M., Barak, L. S., Menard, L., Caron, M. G., 1996. Role of beta-arrestin in mediating agonist-promoted G protein-coupled receptor internalization. Science. 271**,** 363-6.

Fields, R. D., 2015. A new mechanism of nervous system plasticity: activity-dependent myelination. Nat Rev Neurosci. 16**,** 756-67.

Filbin, M. T., 2006. Recapitulate development to promote axonal regeneration: good or bad approach? Philos Trans R Soc Lond B Biol Sci. 361**,** 1565-74.

Fisher, A., Heldman, E., Gurwitz, D., Haring, R., Barak, D., Meshulam, H., Marciano, D., Brandeis, R., Pittel, Z., Segal, M., et al., 1993. Selective signaling via unique M1 muscarinic agonists. Ann N Y Acad Sci. 695**,** 300-3.

Franklin, R. J., Ffrench-Constant, C., 2008. Remyelination in the CNS: from biology to therapy. Nat Rev Neurosci. 9**,** 839-55.

Fredriksson, R., Lagerstrom, M. C., Lundin, L. G., Schioth, H. B., 2003. The G-protein-coupled receptors in the human genome form five main families. Phylogenetic analysis, paralogon groups, and fingerprints. Mol Pharmacol. 63**,** 1256-72.

Fredriksson, R., Schioth, H. B., 2005. The repertoire of G-protein-coupled receptors in fully sequenced genomes. Mol Pharmacol. 67**,** 1414-25.

Fruttiger, M., Montag, D., Schachner, M., Martini, R., 1995. Crucial role for the myelin-associated glycoprotein in the maintenance of axon-myelin integrity. Eur J Neurosci. 7**,** 511-5.

Fujita, N., Kemper, A., Dupree, J., Nakayasu, H., Bartsch, U., Schachner, M., Maeda, N., Suzuki, K., Popko, B., 1998. The cytoplasmic domain of the large myelin-associated glycoprotein isoform is needed for proper CNS but not peripheral nervous system myelination. J Neurosci. 18**,** 1970-8.

Fumagalli, M., Daniele, S., Lecca, D., Lee, P. R., Parravicini, C., Fields, R. D., Rosa, P., Antonucci, F., Verderio, C., Trincavelli, M. L., Bramanti, P., Martini, C., Abbracchio, M. P., 2011. Phenotypic changes, signaling pathway, and functional correlates of GPR17-expressing neural precursor cells during oligodendrocyte differentiation. J Biol Chem. 286**,** 10593-604.

Fuxe, K., Borroto-Escuela, D. O., Romero-Fernandez, W., Palkovits, M., Tarakanov, A. O., Ciruela, F., Agnati, L. F., 2014. Moonlighting proteins and protein-protein

interactions as neurotherapeutic targets in the G protein-coupled receptor field. Neuropsychopharmacology. 39**,** 131-55.

Gaesser, J. M., Fyffe-Maricich, S. L., 2016. Intracellular signaling pathway regulation of myelination and remyelination in the CNS. Exp Neurol. 283**,** 501-11.

Gandia, J., Fernandez-Duenas, V., Morato, X., Caltabiano, G., Gonzalez-Muniz, R., Pardo, L., Stagljar, I., Ciruela, F., 2013. The Parkinson's disease-associated GPR37 receptor-mediated cytotoxicity is controlled by its intracellular cysteine-rich domain. J Neurochem. 125**,** 362-72.

Gandia, J., Morato, X., Stagljar, I., Fernandez-Duenas, V., Ciruela, F., 2015. Adenosine A2A receptor-mediated control of pilocarpine-induced tremulous jaw movements is Parkinson's disease-associated GPR37 receptor-dependent. Behav Brain Res. 288**,** 103-6.

Gard, A. L., Maughon, R. H., Schachner, M., 1996. In vitro oligodendrogliotrophic properties of cell adhesion molecules in the immunoglobulin superfamily: myelin-associated glycoprotein and N-CAM. J Neurosci Res. 46**,** 415-26.

George, S. R., Fan, T., Xie, Z., Tse, R., Tam, V., Varghese, G., O'Dowd, B. F., 2000. Oligomerization of mu- and delta-opioid receptors. Generation of novel functional properties. J Biol Chem. 275**,** 26128-35.

George, S. R., O'Dowd, B. F., Lee, S. P., 2002. G-protein-coupled receptor oligomerization and its potential for drug discovery. Nat Rev Drug Discov. 1**,** 808-20.

Giddens, M. M. W., J.C.; Schroeder, J.P.; Farrow, E.G.; Smith, B.M.; Owino, S.; Soden, S.E.; Meyer, R.C.; Saunders, C.; LePichon, J.B.; Weinshenker, D.; Escayg, A.; Hall, R.A., 2017. A mutation in the brain-expressed receptor GPR37L1 is associated with a novel progressive myoclonus epilepsy. In submission.

Gilissen, J., Geubelle, P., Dupuis, N., Laschet, C., Pirotte, B., Hanson, J., 2015. Forskolin-free cAMP assay for Gi-coupled receptors. Biochem Pharmacol. 98**,** 381-91.

Gilman, A. G., 1987. G proteins: transducers of receptor-generated signals. Annu Rev Biochem. 56**,** 615-49.

Gomes, I., Gupta, A., Filipovska, J., Szeto, H. H., Pintar, J. E., Devi, L. A., 2004. A role for heterodimerization of mu and delta opiate receptors in enhancing morphine analgesia. Proc Natl Acad Sci U S A. 101**,** 5135-9.

Groebe, A., Clarner, T., Baumgartner, W., Dang, J., Beyer, C., Kipp, M., 2009. Cuprizone treatment induces distinct demyelination, astrocytosis, and microglia cell invasion or proliferation in the mouse cerebellum. Cerebellum. 8**,** 163-74.

Gurevich, V. V., Gurevich, E. V., 2008a. GPCR monomers and oligomers: it takes all kinds. Trends Neurosci. 31**,** 74-81.

Gurevich, V. V., Gurevich, E. V., 2008b. How and why do GPCRs dimerize? Trends Pharmacol Sci. 29**,** 234-40.

Gurwitz, D., Haring, R., Heldman, E., Fraser, C. M., Manor, D., Fisher, A., 1994. Discrete activation of transduction pathways associated with acetylcholine m1 receptor by several muscarinic ligands. Eur J Pharmacol. 267**,** 21-31.

Halazy, S., Perez, M., Fourrier, C., Pallard, I., Pauwels, P. J., Palmier, C., John, G. W., Valentin, J. P., Bonnafous, R., Martinez, J., 1996. Serotonin dimers: application

of the bivalent ligand approach to the design of new potent and selective 5-HT(1B/1D) agonists. J Med Chem. 39**,** 4920-7.

Han, H., Myllykoski, M., Ruskamo, S., Wang, C., Kursula, P., 2013. Myelin-specific proteins: a structurally diverse group of membrane-interacting molecules. Biofactors. 39**,** 233-41.

Hartline, D. K., Colman, D. R., 2007. Rapid conduction and the evolution of giant axons and myelinated fibers. Curr Biol. 17**,** R29-35.

Hartupee, J. C., Zhang, H., Bonaldo, M. F., Soares, M. B., Dieckgraefe, B. K., 2001. Isolation and characterization of a cDNA encoding a novel member of the human regenerating protein family: Reg IV. Biochim Biophys Acta. 1518**,** 287-93.

Hennen, S., Wang, H., Peters, L., Merten, N., Simon, K., Spinrath, A., Blattermann, S., Akkari, R., Schrage, R., Schroder, R., Schulz, D., Vermeiren, C., Zimmermann, K., Kehraus, S., Drewke, C., Pfeifer, A., Konig, G. M., Mohr, K., Gillard, M., Muller, C. E., Lu, Q. R., Gomeza, J., Kostenis, E., 2013. Decoding signaling and function of the orphan G protein-coupled receptor GPR17 with a small-molecule agonist. Sci Signal. 6**,** ra93.

Hildebrand, C., Remahl, S., Persson, H., Bjartmar, C., 1993. Myelinated nerve fibres in the CNS. Prog Neurobiol. 40**,** 319-84.

Ho, M. K., Wong, Y. H., 2001. G(z) signaling: emerging divergence from G(i) signaling. Oncogene. 20**,** 1615-25.

Hoon, M. A., Adler, E., Lindemeier, J., Battey, J. F., Ryba, N. J., Zuker, C. S., 1999. Putative mammalian taste receptors: a class of taste-specific GPCRs with distinct topographic selectivity. Cell. 96**,** 541-51.

Hopkins, A. L., Groom, C. R., 2002. The druggable genome. Nat Rev Drug Discov. 1**,** 727-30.

Hsiao, C. C., Wang, W. C., Kuo, W. L., Chen, H. Y., Chen, T. C., Hamann, J., Lin, H. H., 2014. CD97 inhibits cell migration in human fibrosarcoma cells by modulating TIMP-2/MT1- MMP/MMP-2 activity--role of GPS autoproteolysis and functional cooperation between the N- and C-terminal fragments. FEBS J. 281**,** 4878-91.

Hsieh, H.-L. Y., Chuen-Mao, 2014. The role of matrix metalloproteinase-9 in pro-inflammatory
factors-induced brain inflammation and neurodegenerative
diseases. Inflammation and Cell Signaling. 1.

Hughes, E. G., Kang, S. H., Fukaya, M., Bergles, D. E., 2013. Oligodendrocyte progenitors balance growth with self-repulsion to achieve homeostasis in the adult brain. Nat Neurosci. 16**,** 668-76.

Huxley, A. F., Stampfli, R., 1949. Evidence for saltatory conduction in peripheral myelinated nerve fibres. J Physiol. 108**,** 315-39.

Imai, Y., Inoue, H., Kataoka, A., Hua-Qin, W., Masuda, M., Ikeda, T., Tsukita, K., Soda, M., Kodama, T., Fuwa, T., Honda, Y., Kaneko, S., Matsumoto, S., Wakamatsu, K., Ito, S., Miura, M., Aosaki, T., Itohara, S., Takahashi, R., 2007. Pael receptor is involved in dopamine metabolism in the nigrostriatal system. Neurosci Res. 59**,** 413-25.

Imai, Y., Soda, M., Hatakeyama, S., Akagi, T., Hashikawa, T., Nakayama, K. I., Takahashi, R., 2002. CHIP is associated with Parkin, a gene responsible for

familial Parkinson's disease, and enhances its ubiquitin ligase activity. Mol Cell. 10**,** 55-67.

Imai, Y., Soda, M., Inoue, H., Hattori, N., Mizuno, Y., Takahashi, R., 2001. An unfolded putative transmembrane polypeptide, which can lead to endoplasmic reticulum stress, is a substrate of Parkin. Cell. 105**,** 891-902.

Ito, J., Ito, M., Nambu, H., Fujikawa, T., Tanaka, K., Iwaasa, H., Tokita, S., 2009. Anatomical and histological profiling of orphan G-protein-coupled receptor expression in gastrointestinal tract of C57BL/6J mice. Cell Tissue Res. 338**,** 257-69.

Itoyama, Y., Sternberger, N. H., Webster, H. D., Quarles, R. H., Cohen, S. R., Richardson, E. P., Jr., 1980. Immunocytochemical observations on the distribution of myelin-associated glycoprotein and myelin basic protein in multiple sclerosis lesions. Ann Neurol. 7**,** 167-77.

Jaramillo, M. L., Afar, D. E., Almazan, G., Bell, J. C., 1994. Identification of tyrosine 620 as the major phosphorylation site of myelin-associated glycoprotein and its implication in interacting with signaling molecules. J Biol Chem. 269**,** 27240-5.

Johnson, D., Sato, S., Quarles, R. H., Inuzuka, T., Brady, R. O., Tourtellotte, W. W., 1986. Quantitation of the myelin-associated glycoprotein in human nervous tissue from controls and multiple sclerosis patients. J Neurochem. 46**,** 1086-93.

Jones, M. V., Nguyen, T. T., Ewaleifoh, O., Lebson, L., Whartenby, K. A., Griffin, J. W., Calabresi, P. A., 2013. Accelerated axon loss in MOG35-55 experimental autoimmune encephalomyelitis (EAE) in myelin-associated glycoprotein-deficient (MAGKO) mice. J Neuroimmunol. 262**,** 53-61.

Joost, P., Methner, A., 2002. Phylogenetic analysis of 277 human G-protein-coupled receptors as a tool for the prediction of orphan receptor ligands. Genome Biol. 3**,** RESEARCH0063.

Jordan, B. A., Devi, L. A., 1999. G-protein-coupled receptor heterodimerization modulates receptor function. Nature. 399**,** 697-700.

Jung, M., Kramer, E., Grzenkowski, M., Tang, K., Blakemore, W., Aguzzi, A., Khazaie, K., Chlichlia, K., von Blankenfeld, G., Kettenmann, H., et al., 1995. Lines of murine oligodendroglial precursor cells immortalized by an activated neu tyrosine kinase show distinct degrees of interaction with axons in vitro and in vivo. Eur J Neurosci. 7**,** 1245-65.

Kang, J., Shi, Y., Xiang, B., Qu, B., Su, W., Zhu, M., Zhang, M., Bao, G., Wang, F., Zhang, X., Yang, R., Fan, F., Chen, X., Pei, G., Ma, L., 2005. A nuclear function of beta-arrestin1 in GPCR signaling: regulation of histone acetylation and gene transcription. Cell. 123**,** 833-47.

Kelm, S., Pelz, A., Schauer, R., Filbin, M. T., Tang, S., de Bellard, M. E., Schnaar, R. L., Mahoney, J. A., Hartnell, A., Bradfield, P., et al., 1994. Sialoadhesin, myelin-associated glycoprotein and CD22 define a new family of sialic acid-dependent adhesion molecules of the immunoglobulin superfamily. Curr Biol. 4**,** 965-72.

Khokha, R., Murthy, A., Weiss, A., 2013. Metalloproteinases and their natural inhibitors in inflammation and immunity. Nat Rev Immunol. 13**,** 649-65.

Kipp, M., Nyamoya, S., Hochstrasser, T., Amor, S., 2016. Multiple sclerosis animal models: a clinical and histopathological perspective. Brain Pathol.

Kirby, B. B., Takada, N., Latimer, A. J., Shin, J., Carney, T. J., Kelsh, R. N., Appel, B., 2006. In vivo time-lapse imaging shows dynamic oligodendrocyte progenitor behavior during zebrafish development. Nat Neurosci. 9**,** 1506-11.

Kirchhoff, F., Hofer, H. W., Schachner, M., 1993. Myelin-associated glycoprotein is phosphorylated by protein kinase C. J Neurosci Res. 36**,** 368-81.

Kishore, A., Purcell, R. H., Nassiri-Toosi, Z., Hall, R. A., 2016. Stalk-dependent and Stalk-independent Signaling by the Adhesion G Protein-coupled Receptors GPR56 (ADGRG1) and BAI1 (ADGRB1). J Biol Chem. 291**,** 3385-94.

Kobilka, B. K., Matsui, H., Kobilka, T. S., Yang-Feng, T. L., Francke, U., Caron, M. G., Lefkowitz, R. J., Regan, J. W., 1987. Cloning, sequencing, and expression of the gene coding for the human platelet alpha 2-adrenergic receptor. Science. 238**,** 650-6.

Kohout, T. A., Nicholas, S. L., Perry, S. J., Reinhart, G., Junger, S., Struthers, R. S., 2004. Differential desensitization, receptor phosphorylation, beta-arrestin recruitment, and ERK1/2 activation by the two endogenous ligands for the CC chemokine receptor 7. J Biol Chem. 279**,** 23214-22.

Kolakowski, L. F., Jr., 1994. GCRDb: a G-protein-coupled receptor database. Receptors Channels. 2**,** 1-7.

Kristensen, J. L., Puschl, A., Jensen, M., Risgaard, R., Christoffersen, C. T., Bang-Andersen, B., Balle, T., 2010. Exploring the neuroleptic substituent in octoclothepin: potential ligands for positron emission tomography with subnanomolar affinity for alpha(1)-adrenoceptors. J Med Chem. 53**,** 7021-34.

Kristiansen, K., 2004. Molecular mechanisms of ligand binding, signaling, and regulation within the superfamily of G-protein-coupled receptors: molecular modeling and mutagenesis approaches to receptor structure and function. Pharmacol Ther. 103**,** 21-80.

Kubo, T., Fukuda, K., Mikami, A., Maeda, A., Takahashi, H., Mishina, M., Haga, T., Haga, K., Ichiyama, A., Kangawa, K., et al., 1986. Cloning, sequencing and expression of complementary DNA encoding the muscarinic acetylcholine receptor. Nature. 323**,** 411-6.

Kubota, K., Niinuma, Y., Kaneko, M., Okuma, Y., Sugai, M., Omura, T., Uesugi, M., Uehara, T., Hosoi, T., Nomura, Y., 2006. Suppressive effects of 4-phenylbutyrate on the aggregation of Pael receptors and endoplasmic reticulum stress. J Neurochem. 97**,** 1259-68.

Kuhn, H., Wilden, U., 1987. Deactivation of photoactivated rhodopsin by rhodopsin-kinase and arrestin. J Recept Res. 7**,** 283-98.

Kumari, P., Ghosh, E., Shukla, A. K., 2015. Emerging Approaches to GPCR Ligand Screening for Drug Discovery. Trends Mol Med. 21**,** 687-701.

La Sala, G., Marazziti, D., Di Pietro, C., Golini, E., Matteoni, R., Tocchini-Valentini, G. P., 2015. Modulation of Dhh signaling and altered Sertoli cell function in mice lacking the GPR37-prosaposin receptor. FASEB J. 29**,** 2059-69.

Lagerstrom, M. C., Schioth, H. B., 2008. Structural diversity of G protein-coupled receptors and significance for drug discovery. Nat Rev Drug Discov. 7**,** 339-57.

Lambert, N. A., 2010. GPCR dimers fall apart. Sci Signal. 3**,** pe12.

Langenhan, T., Aust, G., Hamann, J., 2013. Sticky signaling--adhesion class G protein-coupled receptors take the stage. Sci Signal. 6**,** re3.

Langenhan, T., Piao, X., Monk, K. R., 2016. Adhesion G protein-coupled receptors in nervous system development and disease. Nat Rev Neurosci. 17**,** 550-61.

Lassmann, H., Bartsch, U., Montag, D., Schachner, M., 1997. Dying-back oligodendrogliopathy: a late sequel of myelin-associated glycoprotein deficiency. Glia. 19**,** 104-10.

Lefkowitz, R. J., Shenoy, S. K., 2005. Transduction of receptor signals by beta-arrestins. Science. 308**,** 512-7.

Lehmann, F., Gathje, H., Kelm, S., Dietz, F., 2004. Evolution of sialic acid-binding proteins: molecular cloning and expression of fish siglec-4. Glycobiology. 14**,** 959-68.

Leng, N., Gu, G., Simerly, R. B., Spindel, E. R., 1999. Molecular cloning and characterization of two putative G protein-coupled receptors which are highly expressed in the central nervous system. Brain Res Mol Brain Res. 69**,** 73-83.

Lewis, M. M., Watts, V. J., Lawler, C. P., Nichols, D. E., Mailman, R. B., 1998. Homologous desensitization of the D1A dopamine receptor: efficacy in causing desensitization dissociates from both receptor occupancy and functional potency. J Pharmacol Exp Ther. 286**,** 345-53.

Li, C., Tropak, M. B., Gerlai, R., Clapoff, S., Abramow-Newerly, W., Trapp, B., Peterson, A., Roder, J., 1994. Myelination in the absence of myelin-associated glycoprotein. Nature. 369**,** 747-50.

Liebscher, I., Schon, J., Petersen, S. C., Fischer, L., Auerbach, N., Demberg, L. M., Mogha, A., Coster, M., Simon, K. U., Rothemund, S., Monk, K. R., Schoneberg, T., 2014. A tethered agonist within the ectodomain activates the adhesion G protein-coupled receptors GPR126 and GPR133. Cell Rep. 9**,** 2018-26.

Liljefors, T., Bogeso, K. P., 1988. Conformational analysis and structural comparisons of (1R,3S)-(+)- and (1S,3R)-(-)-tefludazine, (S)-(+)- and (R)-(-)-octoclothepin, and (+)-dexclamol in relation to dopamine receptor antagonism and amine-uptake inhibition. J Med Chem. 31**,** 306-12.

Lim, H. D., van Rijn, R. M., Ling, P., Bakker, R. A., Thurmond, R. L., Leurs, R., 2005. Evaluation of histamine H1-, H2-, and H3-receptor ligands at the human histamine H4 receptor: identification of 4-methylhistamine as the first potent and selective H4 receptor agonist. J Pharmacol Exp Ther. 314**,** 1310-21.

Liu, B. P., Fournier, A., GrandPre, T., Strittmatter, S. M., 2002. Myelin-associated glycoprotein as a functional ligand for the Nogo-66 receptor. Science. 297**,** 1190-3.

Liu, L., Belkadi, A., Darnall, L., Hu, T., Drescher, C., Cotleur, A. C., Padovani-Claudio, D., He, T., Choi, K., Lane, T. E., Miller, R. H., Ransohoff, R. M., 2010. CXCR2-positive neutrophils are essential for cuprizone-induced demyelination: relevance to multiple sclerosis. Nat Neurosci. 13**,** 319-26.

Livesey, F. J., O'Brien, J. A., Li, M., Smith, A. G., Murphy, L. J., Hunt, S. P., 1997. A Schwann cell mitogen accompanying regeneration of motor neurons. Nature. 390**,** 614-8.

Logan, C. Y., Nusse, R., 2004. The Wnt signaling pathway in development and disease. Annu Rev Cell Dev Biol. 20**,** 781-810.

Lohse, M. J., Andexinger, S., Pitcher, J., Trukawinski, S., Codina, J., Faure, J. P., Caron, M. G., Lefkowitz, R. J., 1992. Receptor-specific desensitization with purified

proteins. Kinase dependence and receptor specificity of beta-arrestin and arrestin in the beta 2-adrenergic receptor and rhodopsin systems. J Biol Chem. 267**,** 8558-64.

Lopez, P. H., 2014. Role of myelin-associated glycoprotein (siglec-4a) in the nervous system. Adv Neurobiol. 9**,** 245-62.

Lopez, P. H., Ahmad, A. S., Mehta, N. R., Toner, M., Rowland, E. A., Zhang, J., Dore, S., Schnaar, R. L., 2011. Myelin-associated glycoprotein protects neurons from excitotoxicity. J Neurochem. 116**,** 900-8.

Louis, J. C., Magal, E., Muir, D., Manthorpe, M., Varon, S., 1992. CG-4, a new bipotential glial cell line from rat brain, is capable of differentiating in vitro into either mature oligodendrocytes or type-2 astrocytes. J Neurosci Res. 31**,** 193-204.

Lucchinetti, C., Bruck, W., Parisi, J., Scheithauer, B., Rodriguez, M., Lassmann, H., 2000. Heterogeneity of multiple sclerosis lesions: implications for the pathogenesis of demyelination. Ann Neurol. 47**,** 707-17.

Ludwin, S. K., Johnson, E. S., 1981. Evidence for a "dying-back" gliopathy in demyelinating disease. Ann Neurol. 9**,** 301-5.

Lundius, E. G., Stroth, N., Vukojevic, V., Terenius, L., Svenningsson, P., 2013. Functional GPR37 trafficking protects against toxicity induced by 6-OHDA, MPP+ or rotenone in a catecholaminergic cell line. J Neurochem. 124**,** 410-7.

Lundius, E. G., Vukojevic, V., Hertz, E., Stroth, N., Cederlund, A., Hiraiwa, M., Terenius, L., Svenningsson, P., 2014. GPR37 protein trafficking to the plasma membrane regulated by prosaposin and GM1 gangliosides promotes cell viability. J Biol Chem. 289**,** 4660-73.

Mandillo, S., Golini, E., Marazziti, D., Di Pietro, C., Matteoni, R., Tocchini-Valentini, G. P., 2013. Mice lacking the Parkinson's related GPR37/PAEL receptor show non-motor behavioral phenotypes: age and gender effect. Genes Brain Behav. 12**,** 465-77.

Marazziti, D., Di Pietro, C., Golini, E., Mandillo, S., La Sala, G., Matteoni, R., Tocchini-Valentini, G. P., 2013. Precocious cerebellum development and improved motor functions in mice lacking the astrocyte cilium-, patched 1-associated Gpr37l1 receptor. Proceedings of the National Academy of Sciences of the United States of America. 110**,** 16486-91.

Marazziti, D., Di Pietro, C., Golini, E., Mandillo, S., Matteoni, R., Tocchini-Valentini, G. P., 2009. Induction of macroautophagy by overexpression of the Parkinson's disease-associated GPR37 receptor. FASEB J. 23**,** 1978-87.

Marazziti, D., Di Pietro, C., Mandillo, S., Golini, E., Matteoni, R., Tocchini-Valentini, G. P., 2011. Absence of the GPR37/PAEL receptor impairs striatal Akt and ERK2 phosphorylation, DeltaFosB expression, and conditioned place preference to amphetamine and cocaine. FASEB J. 25**,** 2071-81.

Marazziti, D., Gallo, A., Golini, E., Matteoni, R., Tocchini-Valentini, G. P., 1998. Molecular cloning and chromosomal localization of the mouse Gpr37 gene encoding an orphan G-protein-coupled peptide receptor expressed in brain and testis. Genomics. 53**,** 315-24.

Marazziti, D., Golini, E., Gallo, A., Lombardi, M. S., Matteoni, R., Tocchini-Valentini, G. P., 1997. Cloning of GPR37, a gene located on chromosome 7 encoding a

putative G-protein-coupled peptide receptor, from a human frontal brain EST library. Genomics. 45**,** 68-77.

Marazziti, D., Golini, E., Mandillo, S., Magrelli, A., Witke, W., Matteoni, R., Tocchini-Valentini, G. P., 2004. Altered dopamine signaling and MPTP resistance in mice lacking the Parkinson's disease-associated GPR37/parkin-associated endothelin-like receptor. Proceedings of the National Academy of Sciences of the United States of America. 101**,** 10189-94.

Marazziti, D., Mandillo, S., Di Pietro, C., Golini, E., Matteoni, R., Tocchini-Valentini, G. P., 2007. GPR37 associates with the dopamine transporter to modulate dopamine uptake and behavioral responses to dopaminergic drugs. Proc Natl Acad Sci U S A. 104**,** 9846-51.

Marcus, J., Dupree, J. L., Popko, B., 2002. Myelin-associated glycoprotein and myelin galactolipids stabilize developing axo-glial interactions. J Cell Biol. 156**,** 567-77.

Margolskee, R. F., 2002. Molecular mechanisms of bitter and sweet taste transduction. J Biol Chem. 277**,** 1-4.

Marta, C. B., Taylor, C. M., Cheng, S., Quarles, R. H., Bansal, R., Pfeiffer, S. E., 2004. Myelin associated glycoprotein cross-linking triggers its partitioning into lipid rafts, specific signaling events and cytoskeletal rearrangements in oligodendrocytes. Neuron Glia Biol. 1**,** 35-46.

Masu, Y., Nakayama, K., Tamaki, H., Harada, Y., Kuno, M., Nakanishi, S., 1987. cDNA cloning of bovine substance-K receptor through oocyte expression system. Nature. 329**,** 836-8.

Matsunami, H., Montmayeur, J. P., Buck, L. B., 2000. A family of candidate taste receptors in human and mouse. Nature. 404**,** 601-4.

Matsushima, G. K., Morell, P., 2001. The neurotoxicant, cuprizone, as a model to study demyelination and remyelination in the central nervous system. Brain pathology. 11**,** 107-16.

Matthews, M. A., Duncan, D., 1971. A quantitative study of morphological changes accompanying the initiation and progress of myelin production in the dorsal funiculus of the rat spinal cord. J Comp Neurol. 142**,** 1-22.

Mattila, S. O., Tuusa, J. T., Petaja-Repo, U. E., 2016. The Parkinson's-disease-associated receptor GPR37 undergoes metalloproteinase-mediated N-terminal cleavage and ectodomain shedding. J Cell Sci. 129**,** 1366-77.

McKerracher, L., Winton, M. J., 2002. Nogo on the go. Neuron. 36**,** 345-8.

Mehta, N. R., Nguyen, T., Bullen, J. W., Jr., Griffin, J. W., Schnaar, R. L., 2010. Myelin-associated glycoprotein (MAG) protects neurons from acute toxicity using a ganglioside-dependent mechanism. ACS Chem Neurosci. 1**,** 215-222.

Mei, F., Mayoral, S. R., Nobuta, H., Wang, F., Desponts, C., Lorrain, D. S., Xiao, L., Green, A. J., Rowitch, D., Whistler, J., Chan, J. R., 2016. Identification of the Kappa-Opioid Receptor as a Therapeutic Target for Oligodendrocyte Remyelination. J Neurosci. 36**,** 7925-35.

Meyer, R. C., Giddens, M. M., Schaefer, S. A., Hall, R. A., 2013. GPR37 and GPR37L1 are receptors for the neuroprotective and glioprotective factors prosaptide and prosaposin. Proceedings of the National Academy of Sciences of the United States of America. 110**,** 9529-34.

Milward, E., Kim, K. J., Szklarczyk, A., Nguyen, T., Melli, G., Nayak, M., Deshpande, D., Fitzsimmons, C., Hoke, A., Kerr, D., Griffin, J. W., Calabresi, P. A., Conant, K., 2008. Cleavage of myelin associated glycoprotein by matrix metalloproteinases. J Neuroimmunol. 193**,** 140-8.

Min, K. D., Asakura, M., Liao, Y., Nakamaru, K., Okazaki, H., Takahashi, T., Fujimoto, K., Ito, S., Takahashi, A., Asanuma, H., Yamazaki, S., Minamino, T., Sanada, S., Seguchi, O., Nakano, A., Ando, Y., Otsuka, T., Furukawa, H., Isomura, T., Takashima, S., Mochizuki, N., Kitakaze, M., 2010. Identification of genes related to heart failure using global gene expression profiling of human failing myocardium. Biochem Biophys Res Commun. 393**,** 55-60.

Minden, S. L., Schiffer, R. B., 1990. Affective disorders in multiple sclerosis. Review and recommendations for clinical research. Arch Neurol. 47**,** 98-104.

Montag, D., Giese, K. P., Bartsch, U., Martini, R., Lang, Y., Bluthmann, H., Karthigasan, J., Kirschner, D. A., Wintergerst, E. S., Nave, K. A., et al., 1994. Mice deficient for the myelin-associated glycoprotein show subtle abnormalities in myelin. Neuron. 13**,** 229-46.

Mukherjee, C., Caron, M. G., Coverstone, M., Lefkowitz, R. J., 1975. Identification of adenylate cyclase-coupled beta-adrenergic receptors in frog erythrocytes with (minus)-[3-H] alprenolol. J Biol Chem. 250**,** 4869-76.

Murakami, T., Shoji, M., Imai, Y., Inoue, H., Kawarabayashi, T., Matsubara, E., Harigaya, Y., Sasaki, A., Takahashi, R., Abe, K., 2004. Pael-R is accumulated in Lewy bodies of Parkinson's disease. Ann Neurol. 55**,** 439-42.

Murga, C., Fukuhara, S., Gutkind, J. S., 1999. Novel Molecular Mediators in the Pathway Connecting G-protein-coupled Receptors to MAP Kinase Cascades. Trends Endocrinol Metab. 10**,** 122-127.

Murphy, G., 2011. Tissue inhibitors of metalloproteinases. Genome Biol. 12**,** 233.

Myers, K. R., Liu, G., Feng, Y., Zheng, J. Q., 2016. Oligodendroglial defects during quakingviable cerebellar development. Dev Neurobiol. 76**,** 972-82.

Nathans, J., Hogness, D. S., 1983. Isolation, sequence analysis, and intron-exon arrangement of the gene encoding bovine rhodopsin. Cell. 34**,** 807-14.

Nave, K. A., 2010. Myelination and the trophic support of long axons. Nat Rev Neurosci. 11**,** 275-83.

Nelson, G., Chandrashekar, J., Hoon, M. A., Feng, L., Zhao, G., Ryba, N. J., Zuker, C. S., 2002. An amino-acid taste receptor. Nature. 416**,** 199-202.

Nelson, G., Hoon, M. A., Chandrashekar, J., Zhang, Y., Ryba, N. J., Zuker, C. S., 2001. Mammalian sweet taste receptors. Cell. 106**,** 381-90.

Neves, S. R., Ram, P. T., Iyengar, R., 2002. G protein pathways. Science. 296**,** 1636-9.

Ngo, T., Ilatovskiy, A. V., Stewart, A. G., Coleman, J. L., McRobb, F. M., Riek, R. P., Graham, R. M., Abagyan, R., Kufareva, I., Smith, N. J., 2017. Orphan receptor ligand discovery by pickpocketing pharmacological neighbors. Nat Chem Biol. 13**,** 235-242.

Oldham, W. M., Hamm, H. E., 2008. Heterotrimeric G protein activation by G-protein-coupled receptors. Nat Rev Mol Cell Biol. 9**,** 60-71.

Omura, T., Kaneko, M., Okuma, Y., Orba, Y., Nagashima, K., Takahashi, R., Fujitani, N., Matsumura, S., Hata, A., Kubota, K., Murahashi, K., Uehara, T., Nomura, Y.,

2006. A ubiquitin ligase HRD1 promotes the degradation of Pael receptor, a substrate of Parkin. J Neurochem. 99**,** 1456-69.

Orton, S. M., Herrera, B. M., Yee, I. M., Valdar, W., Ramagopalan, S. V., Sadovnick, A. D., Ebers, G. C., Canadian Collaborative Study, G., 2006. Sex ratio of multiple sclerosis in Canada: a longitudinal study. Lancet Neurol. 5**,** 932-6.

Overington, J. P., Al-Lazikani, B., Hopkins, A. L., 2006. How many drug targets are there? Nat Rev Drug Discov. 5**,** 993-6.

Paavola, K. J., Stephenson, J. R., Ritter, S. L., Alter, S. P., Hall, R. A., 2011. The N terminus of the adhesion G protein-coupled receptor GPR56 controls receptor signaling activity. J Biol Chem. 286**,** 28914-21.

Pan, B., Fromholt, S. E., Hess, E. J., Crawford, T. O., Griffin, J. W., Sheikh, K. A., Schnaar, R. L., 2005. Myelin-associated glycoprotein and complementary axonal ligands, gangliosides, mediate axon stability in the CNS and PNS: neuropathology and behavioral deficits in single- and double-null mice. Exp Neurol. 195**,** 208-17.

Parikh, A., Stephan, A. F., Tzanakakis, E. S., 2012. Regenerating proteins and their expression, regulation and signaling. Biomol Concepts. 3**,** 57-70.

Perez, M., Jorand-Lebrun, C., Pauwels, P. J., Pallard, I., Halazy, S., 1998. Dimers of 5HT1 ligands preferentially bind to 5HT1B/1D receptor subtypes. Bioorg Med Chem Lett. 8**,** 1407-12.

Pert, C. B., Snyder, S. H., 1973. Opiate receptor: demonstration in nervous tissue. Science. 179**,** 1011-4.

Petersen, S. C., Luo, R., Liebscher, I., Giera, S., Jeong, S. J., Mogha, A., Ghidinelli, M., Feltri, M. L., Schoneberg, T., Piao, X., Monk, K. R., 2015. The adhesion GPCR GPR126 has distinct, domain-dependent functions in Schwann cell development mediated by interaction with laminin-211. Neuron. 85**,** 755-69.

Pitcher, J., Lohse, M. J., Codina, J., Caron, M. G., Lefkowitz, R. J., 1992. Desensitization of the isolated beta 2-adrenergic receptor by beta-adrenergic receptor kinase, cAMP-dependent protein kinase, and protein kinase C occurs via distinct molecular mechanisms. Biochemistry. 31**,** 3193-7.

Probst, W. C., Snyder, L. A., Schuster, D. I., Brosius, J., Sealfon, S. C., 1992. Sequence alignment of the G-protein coupled receptor superfamily. DNA Cell Biol. 11**,** 1-20.

Procaccini, C., De Rosa, V., Pucino, V., Formisano, L., Matarese, G., 2015. Animal models of Multiple Sclerosis. Eur J Pharmacol. 759**,** 182-91.

Pronker, M. F., Lemstra, S., Snijder, J., Heck, A. J., Thies-Weesie, D. M., Pasterkamp, R. J., Janssen, B. J., 2016. Structural basis of myelin-associated glycoprotein adhesion and signalling. Nat Commun. 7**,** 13584.

Quarles, R. H., 2007. Myelin-associated glycoprotein (MAG): past, present and beyond. J Neurochem. 100**,** 1431-48.

Quarles, R. H., 2009. A hypothesis about the relationship of myelin-associated glycoprotein's function in myelinated axons to its capacity to inhibit neurite outgrowth. Neurochem Res. 34**,** 79-86.

Rasband, M. N., Peles, E., 2015. The Nodes of Ranvier: Molecular Assembly and Maintenance. Cold Spring Harb Perspect Biol. 8**,** a020495.

Regard, J. B., Sato, I. T., Coughlin, S. R., 2008. Anatomical profiling of G protein-coupled receptor expression. Cell. 135**,** 561-71.

Reiter, E., Ayoub, M. A., Pellissier, L. P., Landomiel, F., Musnier, A., Trefier, A., Gandia, J., De Pascali, F., Tahir, S., Yvinec, R., Bruneau, G., Poupon, A., Crepieux, P., 2017. beta-arrestin signalling and bias in hormone-responsive GPCRs. Mol Cell Endocrinol.

Rezgaoui, M., Susens, U., Ignatov, A., Gelderblom, M., Glassmeier, G., Franke, I., Urny, J., Imai, Y., Takahashi, R., Schaller, H. C., 2006. The neuropeptide head activator is a high-affinity ligand for the orphan G-protein-coupled receptor GPR37. J Cell Sci. 119**,** 542-9.

Ritter, S. L., Hall, R. A., 2011. Detection and characterization of receptor interactions with PDZ domains. Methods Mol Biol. 756**,** 345-56.

Robak, L. A., Venkatesh, K., Lee, H., Raiker, S. J., Duan, Y., Lee-Osbourne, J., Hofer, T., Mage, R. G., Rader, C., Giger, R. J., 2009. Molecular basis of the interactions of the Nogo-66 receptor and its homolog NgR2 with myelin-associated glycoprotein: development of NgROMNI-Fc, a novel antagonist of CNS myelin inhibition. J Neurosci. 29**,** 5768-83.

Robison, G. A., Butcher, R. W., Sutherland, E. W., 1967. Adenyl cyclase as an adrenergic receptor. Ann N Y Acad Sci. 139**,** 703-23.

Rodbell, M., Krans, H. M., Pohl, S. L., Birnbaumer, L., 1971. The glucagon-sensitive adenyl cyclase system in plasma membranes of rat liver. IV. Effects of guanylnucleotides on binding of 125I-glucagon. J Biol Chem. 246**,** 1872-6.

Rodriguez, M., Scheithauer, B., 1994. Ultrastructure of multiple sclerosis. Ultrastruct Pathol. 18**,** 3-13.

Rosenbluth, J., 1980. Central myelin in the mouse mutant shiverer. J Comp Neurol. 194**,** 639-48.

Roth, B. L., Craigo, S. C., Choudhary, M. S., Uluer, A., Monsma, F. J., Jr., Shen, Y., Meltzer, H. Y., Sibley, D. R., 1994. Binding of typical and atypical antipsychotic agents to 5-hydroxytryptamine-6 and 5-hydroxytryptamine-7 receptors. J Pharmacol Exp Ther. 268**,** 1403-10.

Sachs, H. H., Bercury, K. K., Popescu, D. C., Narayanan, S. P., Macklin, W. B., 2014. A new model of cuprizone-mediated demyelination/remyelination. ASN Neuro. 6.

Samama, P., Cotecchia, S., Costa, T., Lefkowitz, R. J., 1993. A mutation-induced activated state of the beta 2-adrenergic receptor. Extending the ternary complex model. J Biol Chem. 268**,** 4625-36.

Santos, R., Ursu, O., Gaulton, A., Bento, A. P., Donadi, R. S., Bologa, C. G., Karlsson, A., Al-Lazikani, B., Hersey, A., Oprea, T. I., Overington, J. P., 2017. A comprehensive map of molecular drug targets. Nat Rev Drug Discov. 16**,** 19-34.

Schleicher, S., Boekhoff, I., Arriza, J., Lefkowitz, R. J., Breer, H., 1993. A beta-adrenergic receptor kinase-like enzyme is involved in olfactory signal termination. Proc Natl Acad Sci U S A. 90**,** 1420-4.

Schnaar, R. L., Lopez, P. H., 2009. Myelin-associated glycoprotein and its axonal receptors. J Neurosci Res. 87**,** 3267-76.

Shenoy, S. K., McDonald, P. H., Kohout, T. A., Lefkowitz, R. J., 2001. Regulation of receptor fate by ubiquitination of activated beta 2-adrenergic receptor and beta-arrestin. Science. 294**,** 1307-13.

Shimazaki, T., 2016. Vertebrate Neural Stem Cells: Development, Plasticity, and Regeneration. Keio J Med. 65**,** 1-15.

Shin, D., Lin, S. T., Fu, Y. H., Ptacek, L. J., 2013. Very large G protein-coupled receptor 1 regulates myelin-associated glycoprotein via Galphas/Galphaq-mediated protein kinases A/C. Proc Natl Acad Sci U S A. 110**,** 19101-6.

Shine, H. D., Readhead, C., Popko, B., Hood, L., Sidman, R. L., 1992. Morphometric analysis of normal, mutant, and transgenic CNS: correlation of myelin basic protein expression to myelinogenesis. J Neurochem. 58**,** 342-9.

Simon, K., Hennen, S., Merten, N., Blattermann, S., Gillard, M., Kostenis, E., Gomeza, J., 2016. The Orphan G Protein-coupled Receptor GPR17 Negatively Regulates Oligodendrocyte Differentiation via Galphai/o and Its Downstream Effector Molecules. J Biol Chem. 291**,** 705-18.

Skripuletz, T., Gudi, V., Hackstette, D., Stangel, M., 2011. De- and remyelination in the CNS white and grey matter induced by cuprizone: the old, the new, and the unexpected. Histology and histopathology. 26**,** 1585-97.

Skripuletz, T., Hackstette, D., Bauer, K., Gudi, V., Pul, R., Voss, E., Berger, K., Kipp, M., Baumgartner, W., Stangel, M., 2013. Astrocytes regulate myelin clearance through recruitment of microglia during cuprizone-induced demyelination. Brain. 136**,** 147-67.

Skripuletz, T., Lindner, M., Kotsiari, A., Garde, N., Fokuhl, J., Linsmeier, F., Trebst, C., Stangel, M., 2008. Cortical demyelination is prominent in the murine cuprizone model and is strain-dependent. Am J Pathol. 172**,** 1053-61.

Smith, N. J., 2015. Drug Discovery Opportunities at the Endothelin B Receptor-Related Orphan G Protein-Coupled Receptors, GPR37 and GPR37L1. Front Pharmacol. 6**,** 275.

Spiegel, A. M., 1996. Defects in G protein-coupled signal transduction in human disease. Annu Rev Physiol. 58**,** 143-70.

Stadel, J. M., Nambi, P., Shorr, R. G., Sawyer, D. F., Caron, M. G., Lefkowitz, R. J., 1983. Catecholamine-induced desensitization of turkey erythrocyte adenylate cyclase is associated with phosphorylation of the beta-adrenergic receptor. Proc Natl Acad Sci U S A. 80**,** 3173-7.

Stangel, M., Hartung, H. P., 2002. Remyelinating strategies for the treatment of multiple sclerosis. Prog Neurobiol. 68**,** 361-76.

Stangel, M., Trebst, C., 2006. Remyelination strategies: new advancements toward a regenerative treatment in multiple sclerosis. Curr Neurol Neurosci Rep. 6**,** 229-35.

Steinman, L., 1996. Multiple sclerosis: a coordinated immunological attack against myelin in the central nervous system. Cell. 85**,** 299-302.

Stephen, A. G., Esposito, D., Bagni, R. K., McCormick, F., 2014. Dragging ras back in the ring. Cancer Cell. 25**,** 272-81.

Stephenson, J. R., Paavola, K. J., Schaefer, S. A., Kaur, B., Van Meir, E. G., Hall, R. A., 2013. Brain-specific angiogenesis inhibitor-1 signaling, regulation, and enrichment in the postsynaptic density. J Biol Chem. 288**,** 22248-56.

Sternberger, N. H., Quarles, R. H., Itoyama, Y., Webster, H. D., 1979. Myelin-associated glycoprotein demonstrated immunocytochemically in myelin and myelin-forming cells of developing rat. Proc Natl Acad Sci U S A. 76**,** 1510-4.

Stidworthy, M. F., Genoud, S., Suter, U., Mantei, N., Franklin, R. J., 2003. Quantifying the early stages of remyelination following cuprizone-induced demyelination. Brain Pathol. 13**,** 329-39.

Stoveken, H. M., Hajduczok, A. G., Xu, L., Tall, G. G., 2015. Adhesion G protein-coupled receptors are activated by exposure of a cryptic tethered agonist. Proc Natl Acad Sci U S A. 112**,** 6194-9.

Strenge, K., Schauer, R., Bovin, N., Hasegawa, A., Ishida, H., Kiso, M., Kelm, S., 1998. Glycan specificity of myelin-associated glycoprotein and sialoadhesin deduced from interactions with synthetic oligosaccharides. Eur J Biochem. 258**,** 677-85.

Strenge, K., Schauer, R., Kelm, S., 1999. Binding partners for the myelin-associated glycoprotein of N2A neuroblastoma cells. FEBS Lett. 444**,** 59-64.

Syrovatkina, V., Alegre, K. O., Dey, R., Huang, X. Y., 2016. Regulation, Signaling, and Physiological Functions of G-Proteins. J Mol Biol. 428**,** 3850-68.

Tam, J., Rosenberg, L., Maysinger, D., 2004. INGAP peptide improves nerve function and enhances regeneration in streptozotocin-induced diabetic C57BL/6 mice. FASEB J. 18**,** 1767-9.

Tanabe, Y., Fujita-Jimbo, E., Momoi, M. Y., Momoi, T., 2015. CASPR2 forms a complex with GPR37 via MUPP1 but not with GPR37(R558Q), an autism spectrum disorder-related mutation. J Neurochem. 134**,** 783-93.

Tang, S., Qiu, J., Nikulina, E., Filbin, M. T., 2001. Soluble myelin-associated glycoprotein released from damaged white matter inhibits axonal regeneration. Mol Cell Neurosci. 18**,** 259-69.

Tang, S., Shen, Y. J., DeBellard, M. E., Mukhopadhyay, G., Salzer, J. L., Crocker, P. R., Filbin, M. T., 1997. Myelin-associated glycoprotein interacts with neurons via a sialic acid binding site at ARG118 and a distinct neurite inhibition site. J Cell Biol. 138**,** 1355-66.

Tasaki, I., 1939. THE ELECTRO-SALTATORY TRANSMISSION OF THE NERVE IMPULSE AND THE EFFECT OF NARCOSIS UPON THE NERVE FIBER. American Journal of Physiology -- Legacy Content. 127**,** 211-227.

Taylor, C. M., Coetzee, T., Pfeiffer, S. E., 2002. Detergent-insoluble glycosphingolipid/cholesterol microdomains of the myelin membrane. J Neurochem. 81**,** 993-1004.

Tebar, L. A., Geranton, S. M., Parsons-Perez, C., Fisher, A. S., Bayne, R., Smith, A. J., Turmaine, M., Perez-Luz, S., Sheasby, A., De Felipe, C., Ruff, C., Raivich, G., Hunt, S. P., 2008. Deletion of the mouse RegIIIbeta (Reg2) gene disrupts ciliary neurotrophic factor signaling and delays myelination of mouse cranial motor neurons. Proc Natl Acad Sci U S A. 105**,** 11400-5.

Thompson, M. D., Hendy, G. N., Percy, M. E., Bichet, D. G., Cole, D. E., 2014. G protein-coupled receptor mutations and human genetic disease. Methods Mol Biol. 1175**,** 153-87.

Thornton, K. J., Kamanga-Sollo, E., White, M. E., Dayton, W. R., 2016. Active G protein-coupled receptors (GPCR), matrix metalloproteinases 2/9 (MMP2/9), heparin-binding epidermal growth factor (hbEGF), epidermal growth factor receptor (EGFR), erbB2, and insulin-like growth factor 1 receptor (IGF-1R) are necessary for trenbolone acetate-induced alterations in protein turnover rate of fused bovine satellite cell cultures. J Anim Sci. 94**,** 2332-43.

Tobin, A. B., Butcher, A. J., Kong, K. C., 2008. Location, location, location...site-specific GPCR phosphorylation offers a mechanism for cell-type-specific signalling. Trends Pharmacol Sci. 29**,** 413-20.

Traka, M., Podojil, J. R., McCarthy, D. P., Miller, S. D., Popko, B., 2016. Oligodendrocyte death results in immune-mediated CNS demyelination. Nat Neurosci. 19**,** 65-74.

Trandem, K., Anghelina, D., Zhao, J., Perlman, S., 2010. Regulatory T cells inhibit T cell proliferation and decrease demyelination in mice chronically infected with a coronavirus. J Immunol. 184**,** 4391-400.

Trapp, B. D., Andrews, S. B., Cootauco, C., Quarles, R., 1989. The myelin-associated glycoprotein is enriched in multivesicular bodies and periaxonal membranes of actively myelinating oligodendrocytes. J Cell Biol. 109**,** 2417-26.

Trapp, B. D., Quarles, R. H., 1982. Presence of the myelin-associated glycoprotein correlates with alterations in the periodicity of peripheral myelin. J Cell Biol. 92**,** 877-82.

Trapp, B. D., Quarles, R. H., Suzuki, K., 1984. Immunocytochemical studies of quaking mice support a role for the myelin-associated glycoprotein in forming and maintaining the periaxonal space and periaxonal cytoplasmic collar of myelinating Schwann cells. J Cell Biol. 99**,** 594-606.

Tsai, H. H., Niu, J., Munji, R., Davalos, D., Chang, J., Zhang, H., Tien, A. C., Kuo, C. J., Chan, J. R., Daneman, R., Fancy, S. P., 2016. Oligodendrocyte precursors migrate along vasculature in the developing nervous system. Science. 351**,** 379-84.

Tuohy, V. K., Lu, Z., Sobel, R. A., Laursen, R. A., Lees, M. B., 1989. Identification of an encephalitogenic determinant of myelin proteolipid protein for SJL mice. J Immunol. 142**,** 1523-7.

Umemori, H., Sato, S., Yagi, T., Aizawa, S., Yamamoto, T., 1994. Initial events of myelination involve Fyn tyrosine kinase signalling. Nature. 367**,** 572-6.

Vacas, E., Munoz-Moreno, L., Valenzuela, P. L., Prieto, J. C., Schally, A. V., Carmena, M. J., Bajo, A. M., 2016. Growth hormone-releasing hormone induced transactivation of epidermal growth factor receptor in human triple-negative breast cancer cells. Peptides. 86**,** 153-161.

Valdenaire, O., Giller, T., Breu, V., Ardati, A., Schweizer, A., Richards, J. G., 1998. A new family of orphan G protein-coupled receptors predominantly expressed in the brain. FEBS Lett. 424**,** 193-6.

Vetter, I. R., Wittinghofer, A., 2001. The guanine nucleotide-binding switch in three dimensions. Science. 294**,** 1299-304.

Vigil, D., Cherfils, J., Rossman, K. L., Der, C. J., 2010. Ras superfamily GEFs and GAPs: validated and tractable targets for cancer therapy? Nat Rev Cancer. 10**,** 842-57.

Vinson, M., Rausch, O., Maycox, P. R., Prinjha, R. K., Chapman, D., Morrow, R., Harper, A. J., Dingwall, C., Walsh, F. S., Burbidge, S. A., Riddell, D. R., 2003. Lipid rafts mediate the interaction between myelin-associated glycoprotein (MAG) on myelin and MAG-receptors on neurons. Mol Cell Neurosci. 22**,** 344-52.

Violette, S., Festor, E., Pandrea-Vasile, I., Mitchell, V., Adida, C., Dussaulx, E., Lacorte, J. M., Chambaz, J., Lacasa, M., Lesuffleur, T., 2003. Reg IV, a new member of the regenerating gene family, is overexpressed in colorectal carcinomas. Int J Cancer. 103**,** 185-93.

Virlon, B., Firsov, D., Cheval, L., Reiter, E., Troispoux, C., Guillou, F., Elalouf, J. M., 1998. Rat G protein-coupled receptor kinase GRK4: identification, functional expression, and differential tissue distribution of two splice variants. Endocrinology. 139**,** 2784-95.

Vyas, A. A., Schnaar, R. L., 2001. Brain gangliosides: functional ligands for myelin stability and the control of nerve regeneration. Biochimie. 83**,** 677-82.

Wang, H., Hu, L., Zang, M., Zhang, B., Duan, Y., Fan, Z., Li, J., Su, L., Yan, M., Zhu, Z., Liu, B., Yang, Q., 2016. REG4 promotes peritoneal metastasis of gastric cancer through GPR37. Oncotarget. 7**,** 27874-88.

Wang, H. Q., Imai, Y., Inoue, H., Kataoka, A., Iita, S., Nukina, N., Takahashi, R., 2008. Pael-R transgenic mice crossed with parkin deficient mice displayed progressive and selective catecholaminergic neuronal loss. J Neurochem. 107**,** 171-85.

Weiss, E. R., Ducceschi, M. H., Horner, T. J., Li, A., Craft, C. M., Osawa, S., 2001. Species-specific differences in expression of G-protein-coupled receptor kinase (GRK) 7 and GRK1 in mammalian cone photoreceptor cells: implications for cone cell phototransduction. J Neurosci. 21**,** 9175-84.

Weiss, M. D., Hammer, J., Quarles, R. H., 2000. Oligodendrocytes in aging mice lacking myelin-associated glycoprotein are dystrophic but not apoptotic. J Neurosci Res. 62**,** 772-80.

Whistler, J. L., von Zastrow, M., 1998. Morphine-activated opioid receptors elude desensitization by beta-arrestin. Proc Natl Acad Sci U S A. 95**,** 9914-9.

Willard, F. S., Kimple, A. J., Johnston, C. A., Siderovski, D. P., 2005. A direct fluorescence-based assay for RGS domain GTPase accelerating activity. Anal Biochem. 340**,** 341-51.

Willets, J. M., Challiss, R. A., Nahorski, S. R., 2003. Non-visual GRKs: are we seeing the whole picture? Trends Pharmacol Sci. 24**,** 626-33.

Wingerchuk, D. M., Carter, J. L., 2014. Multiple sclerosis: current and emerging disease-modifying therapies and treatment strategies. Mayo Clinic proceedings. 89**,** 225-40.

Yamamura, H. I., Snyder, S. H., 1974. Muscarinic cholinergic binding in rat brain. Proc Natl Acad Sci U S A. 71**,** 1725-9.

Yamashita, T., Higuchi, H., Tohyama, M., 2002. The p75 receptor transduces the signal from myelin-associated glycoprotein to Rho. J Cell Biol. 157**,** 565-70.

Yanagisawa, K., Quarles, R. H., Johnson, D., Brady, R. O., Whitaker, J. N., 1985. A derivative of myelin-associated glycoprotein in cerebrospinal fluid of normal subjects and patients with neurological disease. Ann Neurol. 18**,** 464-9.

Yang, H. J., Vainshtein, A., Maik-Rachline, G., Peles, E., 2016. G protein-coupled receptor 37 is a negative regulator of oligodendrocyte differentiation and myelination. Nat Commun. 7**,** 10884.

Yang, Y., Nishimura, I., Imai, Y., Takahashi, R., Lu, B., 2003. Parkin suppresses dopaminergic neuron-selective neurotoxicity induced by Pael-R in Drosophila. Neuron. 37**,** 911-24.

Yim, S. H., Toda, K., Goda, S., Quarles, R. H., 1995. Comparison of the phosphorylation of myelin-associated glycoprotein in cultured oligodendrocytes and Schwann cells. J Mol Neurosci. 6**,** 63-74.

Yin, X., Crawford, T. O., Griffin, J. W., Tu, P., Lee, V. M., Li, C., Roder, J., Trapp, B. D., 1998. Myelin-associated glycoprotein is a myelin signal that modulates the caliber of myelinated axons. J Neurosci. 18**,** 1953-62.

Yuan, X., Chen, Z., Xiao, S., Zhou, C., Hua, H., 2011. An early Ediacaran assemblage of macroscopic and morphologically differentiated eukaryotes. Nature. 470**,** 390-3.

Zeng, Z., Su, K., Kyaw, H., Li, Y., 1997. A novel endothelin receptor type-B-like gene enriched in the brain. Biochem Biophys Res Commun. 233**,** 559-67.

Zuchero, J. B., Fu, M. M., Sloan, S. A., Ibrahim, A., Olson, A., Zaremba, A., Dugas, J. C., Wienbar, S., Caprariello, A. V., Kantor, C., Leonoudakis, D., Lariosa-Willingham, K., Kronenberg, G., Gertz, K., Soderling, S. H., Miller, R. H., Barres, B. A., 2015. CNS myelin wrapping is driven by actin disassembly. Dev Cell. 34**,** 152-67.